EMERALD
ERASMUS MUNDUS MASTER
IN GEORESOURCES ENGINEERING

LIÈGE université

University of Liège - Faculty of Applied Science

Characterizing and element mapping of internal parts of a smartphone through automated and correlative microscopy

Nathan REINDERS

Masters Thesis submitted in partial fulfillment of the requirements for the triple Degree of

”Master en ingénieur des mines et géologues”, finalité approfondie de l’ Université de Liège

”Master en Geosciences: Planètes, Ressources, Environnement” de l’Ecole Nationale Supérieure de Géologie de Nancy

”Master’s in Geosciences Engineering” of Luleå University of Technology

Supervisor: Prof. Eric Pirard
University of Liège

Mentor: Dr. Hassan Bouzahzah
University of Liège

Academic year 2017-2018

Abstract

This work used correlative and automated microscopy to have a better understanding of the internal components and structures of a smartphones. The objective is to see if there is any potential that these techniques can be of extra value for the recycling of electronic waste.

Parallel slices were made out of one smartphone to study the internal structure and components of the phone. After, the same kind of smartphone was shredded and melted to study the behaviour of the material after these processing steps under the microscope. For this research, the SEM and the attached software Mineralogic by ZEISS were used to provide visual and statistical data. The system proved to be efficient and accessible in treating waste electronic material. That is to say that the components could be easily identified and classified under a specific name. In the case of electronic waste this is either as an alloy or as a pure metal. To have a good understanding of the alloy, detailed analysis by Bruker were often necessary. Precious and critical metals were located and their internal relationships with other components was studied. Shredding showed how these compositions crumbled into smaller fractions or kept together as a whole. This helped for instance to understand how metals are discarded into waste streams during pre-processing steps as being trapped within other metal fraction, ceramics and plastics. The molten phone sections showed how the original composition of the different components completely changed. During crystallization, new compositions are made completely differing from the original ones.

Mineralogic in association with Bruker proved to be a valid system. However, it was suggested to segment the sample in different phases based on optical microscopy and BSE images. These phases could be more rapidly analysed under EDS without analysing all pixel in a pre-determined grid analysis. This suggestion was mainly made to improve the efficiency of automated microscopy on WEEE samples. Another issue to be faced in the future is the sample preparation as it is very hard to generate representative sample for this work. Combination with Ct-scans or other techniques is advised.

Preface

This work is the last chapter in completing the EMerald programme. During two fascinating years I was given the opportunity to learn about all aspects of primary and secondary resources. I had to change to do this in an international atmosphere surrounded by academically institutes and industrial partners spread all over Europe, for which my thanks. As a geologist, the master introduced to me the research field of recycling and its importance in future societies. Captivated by this topic I searched for possibilities to have a better understanding in this field.

At first, I would like to thank my promotor, professor Eric Pirard. He gave me the opportunity to work on a topic combining innovated technology and electronic waste. It helped me to learn more on the possibilities of recycling and the values of electronic waste. This work was done in association with ZEISS company. I would like to thank the company for the chance given. Aside, I would like to express my gratitude to Shaun Graham for mentoring me, during and after my internship at their facilities in Cambridge. Also, special thanks for Dr. Hassan Bouzahzah, who helped in the challenging task of sample preparation. His knowledge on correlative and automated microscopy was of great importance for this work.

Finally, no greater gratitude can be given to the following persons, Rudi and Marijke, my loving parents. They gave me the opportunity and the utmost support to fulfill and experience the last two years. Together with the aid of my classmates, professors and assistants I could complete a fascinating master giving me more than just theory but also life-changing adventures and experiences.

Contents

Chapter 1

Introduction

The study presented to the reader is new and innovated in the world of recycling. A research is conducted using automated and correlative microscopy to characterize e-waste. Although, microscopy and particular electron microscopy has already found its use in mining it has not yet found its ways in the world of recycling. This studies tries to verify to what means microscopy can be used to characterize e-waste. After, the question is asked if there is any interest and application for the use of these techniques in improving the extraction techniques out of e-waste. In the scoop of this research one particular smartphone has been taken as a test case to solve these questions.

Mobile phones and particularly smartphones are highly enriched in precious and critical metals. Precious metals such as gold and silver can hold up to 300 g/t and 3500g/t in a smartphone, respectively. Also, critical metals such as gallium, indium, REE (i.e neodymium), tantalum and cobalt are abundantly present often in much higher concentrations than in ores currently mined. Knowing that the average lifespan of a mobile phone increasingly shortens, averaging at 2-3 years in developed countries (Chancerel et al., 2015a), and that at the moment only 20 % of old mobile phones are recycled, a large quantity of critical and precious metals is still left lost in electronic waste (e-waste).

The extraction of metals out of mobile phones is problematic and in the case of critical metals not always feasible. Bad recovery is often due to design complexity and insufficient liberation of the critical and precious metal bearing components. This lowers the economic potential in e-waste recycling and contributes to greater environmental impact through acidification and leaching of toxic and carcinogenic elements .

In this application, the use of automated and quantitative mineralogy is much the same as with conventional applied mineralogy applications. Akin to conventional ore mineralogy, the focus is to characterize the 'mineralogy', understand the liberation and elemental

deportment in these samples. The goal is to use ZEISS Mineralogic Mining to analyze samples from an old smartphone in order to better understand the distribution of metals within the components. This can be used to quantify metals within mobile phones and indicate target components for metal recycling.
It not only helps to quantify the metals but also to give an idea of the state of the metal. Many of the metals within a phone are present as an alloy, rather than in native form. The study tries to find out how ZEISS Mineralogic Mining makes it able to identify these different zones by creating different classes of metal groups and quantifying the measured abundance of metals in each component.

1.1 Towards a more circular economy

By the end of 2018 more than 50 million tonnes of electronic waste or WEEE will be produced with a value of metals inside of 50 billion euro (Balde et al., 2017). WEEE stands for Waste electronics and electronic equipment. Various definitions for e-waste are available, but to frame e-waste one best has to look at the local legislation. In this case, the European Union is a useful reference (European Commision, 2010, 2012) stating: *'Electronics and electronic equipment or EEE means equipment which is dependent on electric currents or electromagnetic fields in order to work properly and equipment for the generation, transfer and measurement of such currents and fields and designed for use with a voltage rating not exceeding 1 000 volts for alternating current and 1 500 volts for direct current'.* This type of waste has been divided in 5 groups by the European Commission (Balde et al., 2017). They are enlisted here:

1. Temperature exchange equipment for example refrigerators, freezers, air conditioner and heat pumps.

2. Screens, monitors, and equipment containing screens having a surface greater than 100 cm^2 including televisions, monitors, laptops, notebooks and tablets.

3. Lamps going from LED to Fluorescent lamps.

4. Large equipment with an external dimension more than 50 cm^2 varying from household appliances; IT and telecommunication equipment to electrical and electronic tool and toys. Examples are washing machines, electric stoves, coping machines, etc. . .

5. Small equipment with an external dimension not more than 50 cm^2 varying from household appliances; IT and telecommunication equipment to electrical and electronic tool and toys. Examples are toasters, vacuum cleaners, medical devices, microwaves, camera and radio's.

6. Small IT and telecommunication equipment (no external dimension more than 50 cm). These includes mobile phones, GPS, routers, printers, pocket calculators telephones and personal computers.

WEEE refers to the group of these equipment, which are discarded and therefore have no intention by the owner to be re-used. Up to 60 different metals can be found within e-waste (Namias, 2013) changing from base metals as copper and aluminum to precious metals as gold and silver. E-waste is the fastest growing waste stream and has a growth rate of 3-5% (Cucchiella et al., 2015). 50 % of e-waste consists out of large and small equipment defined in categories 4, 5 and 6. The life expectancy of most small e-waste equipment, IT and telecommunication equipment is under 5 years. For smartphones this is even less with an average life-span of 2-3 year (Chancerel et al., 2015a,b). Knowing that by 2015, 12.5 billion smartphones were sold a considerable amount of old smartphones is each year discarded.

Continents	Amounts (mt)	Amount (Kg/inh.)
Africa	1.9	1.7
North and South America	11.7	12.2
Asia	16.0	3.7
Europe	11.6	15.6
Oceania	0.6	15.2

Table 1.1: E-waste generated in 2015 categorized by continents (Kumar and Holuszko, 2016).

The amount of e-waste spread around the globe is shown in table 1.1. It shows how the most developed regions have the highest concentrations of WEEE. Asia has a very irregular distribution where mainly countries as China, India and Japan are the main producers of e-waste mainly due to high population numbers and their recent economic development (Kumar and Holuszko, 2016). Kumar and Holuszko (2016) suggests there is a linear trend with e-waste generated by inhabitants and the gross domestic product.

In developed regions recycling is more and more stimulated by stronger legislation imposed by governmental institutions. There are three reasons brought forward when talking about improving the recycling rate: economic benefits, environmental concerns and public health and safety.
The ongoing manufacturing of EEE puts more and more pressure on the demand of copper, tin, critical metals and precious metals as gold and palladium (Golev et al., 2014). Especially small IT as notebooks, tables and smartphones contain a large concentration of precious and critical metals (Cucchiella et al., 2015). The main concentration of precious metals is to be found within PCB (Cucchiella et al., 2015; Golev et al., 2014; Hagelüken

and Meskers, 2008) but, also in screens, monitors and other parts of small IT equipment (Buchert et al., 2012). To have a better understanding of the quantities it is an interesting exercise to put these values in perspective with traditionally mined ore. Primary ore have shown a decreasing trend in ore grades the last decades. Mines are forced to dive into more complex ore body to coop with the ongoing demand for metals on the global market. Grades in natural ore are becoming so low that there is a significant gap with metal grades in e-waste. Figure 1.1 illustrates these gaps with the average metal grade of smartphones set as an example. It can be seen how the average grade of gold in a mobile phone, which is around 300 g/t, is more than 100 times higher in concentration than gold mines nowadays, averaging 2-5 g/t. Similar gaps can be found for silver, palladium and copper, respectively 40x, 30x and 10x (Buchert et al., 2012). Other critical and precious metals as tantalum, gallium and neodymium show grades close or larger than in natural ore. However, in most of these cases the amount of mines producing these metals are rare or are situated in harsh and war-like regions. This is for example the case for indium and gallium with low production numbers and a complete run-out expected in 20 years (Li et al., 2017). Another situation is tantalum out of Coltan in Central - West Africa, which is mined in a corrupt environment (Ayres, 2013; Perks, 2015).

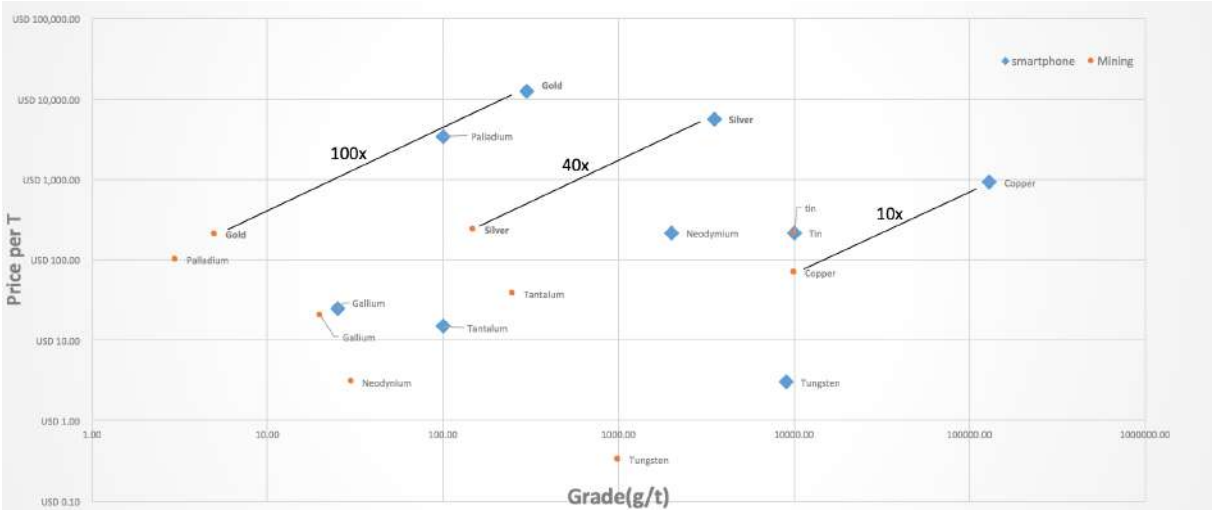

Figure 1.1: The metal grade and price per tonne for average mine grade vs compositional data of a smartphone (average ore grade: USGS, metal prices: London metal exchange, Average grade in smartphone compiled from Holgersson et al. (2016), (Buchert et al., 2012) .

A small calculations can be done to show the value of one million discarded smartphones. Taking an average 110 gram per phone this means that the tonnage of the total amount of 1 000 000 phones is around 110 tonnes. Inside this pile of waste there is 33 kilograms of gold (average grade of 300 g/t), using the average gold price (feb. 2018) this means

a value of 1.4 million €of gold. For the same amount of gold 11 million tonnes of ore needs to be mined. This is without considering all the other metals inside a smartphone. Zeng et al. (2016) showed that only within China recycling of e-waste could result in an additional 30,000 jobs.

Aside economic benefits from recycling e-waste, processing WEEE has a key role in the protection of the environment and human health. Much of the e-waste worldwide is landfilled. Hence, waste is becoming an environmental risk for vegetation, soil and groundwater. Many of hazardous metals can be found within e-waste: mercury, cadmium, lead, chromium and polluting organic material in form of ceramics and plastics (Balde et al., 2017). Once these heavy metals come in contact with groundwater they can spread and contaminate potable water resulting in kidney, liver and hart damage (Suckling and Lee, 2015). It is suggested that a better understanding of e-waste is needed to have a better control on possible polluting chemicals within.
Indirectly, recovering metals out of e-waste can help the reduction of greenhouse gas emission. Recycling of material leads to lower energy consumption in comparison to extraction of new raw natural resources. For example, by recycling aluminum and copper instead of recovering it from earths resources energy consumption is reduced with 95 % and 85 % respectively (Cui and Forssberg, 2003). The costs in energy consumption for acquiring metals from WEEE is only 10-15 % of the cost of mining (ISRI, 2003). Also other problems of mine waste, water consumption and CO_2 gas can be discarded.

These reasons with the ongoing need for metals to support global economy should drive countries more and more to a circular economy. Figure 1.2 shows how e-waste is discarded and the issues faced with it. Aside Japan and the European union no real efforts are done to recycle and recover metals out of e-waste. Attempts are made in North American Countries as Canada and the United States. However only 30 % of e-waste is recycled and the other 70 % is either landfilled or exported. Exporting is mainly done to China or other developing countries as India, Pakistan and Vietnam. The reason for export is mainly unfeasible recovery methods available (Golev et al., 2014). Countries as India and China with an upcoming industry produce a lot electronic waste. However due to lacking structural and legislated motives recycling is not a priority and is often done in a primitive way.

The European union and Japan are doing a better job, mainly driven by a strong legislation. The European union, for example, put goals for it members states to recycle 85 % of it WEEE produced by 2020 (European Commision, 2012). It is an example how strong legislation is needed right now to push economies towards a more circular economy.

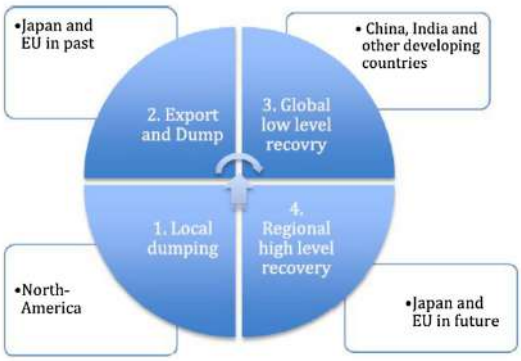

Figure 1.2: E-waste treatment in the different continents (Kumar and Holuszko, 2016).

Although, legislation is pushing countries towards a more circular economy there are still some serious problems that needs to be tackled. Collection of valuable e-waste is a major issue. Within the European Union barely 50 % of e-waste is collected. It is still an big problem to convince people to bring in their e-waste for treatment. Especially for small IT and telecommunication this is a serious problem as often old mobile phones are kept within drawers and closest. The collection rate for mobile phones is at the moment only 20 %, building an unreachable high tonnage of high grade e-waste. Aside collection pre-processing steps before refinery are often lacking the means to recover a large amount of the precious metals inside. In developing countries 70 % of the material is lost during these steps as only automated recycling techniques are feasible. In that way underdeveloped countries are doing a better job as they selectively search for zones of precious metals by hand. A technique unfeasible and considered dangerous in developed countries.

1.2 Goals and research techniques

The goal of this research is to use advanced microscopy in order to map and characterize the different elements within an old smartphone. This research will conduct profound analysis on interior parts of a mobile phone using correlative and automated microscopy. These analysis starts with a light microscopy study to generate overview images. After SEM microscopy (ZEISS Mineralogic mining) is used providing BSE images and chemical data by EDS. The results are overview images giving all components of the phone including statistical data. Bruker was used for detailed spot and map EDS analysis to refine the composition detected using Mineralogic. At last, μ-XRF was as well tested on these samples to verify if metals can be detected which were not found by EDS.
This research procedure is conducted on three different samples all from the same smartphone (Nokia Lumia 925). In the first case the phone was sliced in parallel section to examine the interior parts of the phone. It is examined what the overall content of metal

is in the mobile phones, where the metal is located and in which state it can be found (native or alloy). Second, the phone is crushed in fine particles. The goal in the research is to investigate how the composition and structures detected in the slice are now behaving and if a correlation can be made. Third, the phone is melted. The goal here is to see how these compositions defined in the smarthpone changes during melting and if all metals detected before can be relocated.

The study is done to see if automated microscopy can provide valuable and correct information in the extraction of metals out of secondary resource. Based on this an assessment can be made to determine the ease and reliability of the hardware and software of ZEISS microscopy on e-waste samples. The goal is to validate the microscope for the use in the examination of electronic waste. Based on these findings some suggestion for improvements are made.

1.3 Previous research in e-waste characterization

Little research has been done on characterization of e-waste. The studies that were found were mainly chemical bulk analysis on mobile phones or on the PCB e.g. Chancerel and Rotter (2009); Holgersson et al. (2016); Oguchi et al. (2011b).

End-of-life EEE has been since the beginning of the 20th century receiving more attention as a source of precious and critical metals (Boghe, 2001; Chancerel et al., 2008; Hagelüken and Meskers, 2008; UNEP, 2009). Since the increasing demand of a wide variety of metals the last two decades especially a secured source of these metals has become a critical issue (UNEP, 2009, 2011), in which WEEE is considered to play an important role.

Chapter 2

E-waste characterization and automated microscopy

2.1 Metals within e-waste

WEEE covers a large and varied group of different devices and equipment. All have a specific built and internal composition to achieve its purpose. As a result urban mining suffers from a very heterogeneous 'ore body'. The occurrence of metals, especially in case of precious and critical metals, within the different streams of WEEE can be very divergent. Depending on the type of e-waste, metal content can exceed 100x the traditional grade in primary ore bodies. In the whole WEEE group mobile phones and tablets are the most enriched precious and critical metal carriers. They are part of the 'small IT and telecommunication equipment' specialized in wireless features. The main focus of this work lies on the metal distribution in smartphones.

2.1.1 Metals and there use in smartphones

Mobile phones, part of the WEEE stream of communication technology, is the richest group in e-wast concerning precious metals and critical metals (Chancerel et al., 2015a). A large quantity of different precious metals and critical metals can be found in old smartphones. Critical metals are a group of elements defined by the European Commision based on its rare occurrence as an ore and on the prospect of being soon depleted. European Commission (2017) published the following list of metals as considered critical shown in table 2.1. Included in this table is the amount of these metals getting recycled in Europe and there use in mobile phones.

Element	Input through recycling	Relevance in electronics
Sb	11%	Synergist for flame retardants in plastics
Be	19 %	Electric and electronic connectors
Cr	13 %	Used in stainless steal
Co	16 %	Mainly found in batteries: Lithium-ion, NIMH and nickel-cadmium batteries
F	0 %	
Ga	0 %	Both in LED and as semiconductor in integrated circuits
Ge	0 %	As semiconductor in integrated circuits, used in LED as well
In	0 %	Indium tin oxide (ITO) used as transparent conductive layer in screens, LCD panels and in limited amounts as LESS, solders and semiconductors
Mg	0 %	Casings
Nb	11%	Magnets
P	0 %	Cold Cathode fluorescent lamp (CCFL) and used as magnetic material in LED back lighting systems
PTM	35 %	Platinum and Ruthenium is used in hard disk drivers
REE	0 %	Iridium in LED, Neodymium in a compound of magnets, drivers and loudspeakers, NIMH batteries
Ta	0 %	Used in PCB as capacitors
W	37 %	Vibrating motor in PCB

Table 2.1: Critical metals defined by the European Union, recycling rate and their use in mobile phones. Compiled data from Chancerel et al. (2013); European Commission (2017).

The list shows how little of these element are currently recycled or reused. It is often a problematic case where the choice of recycling of these elements is a pure economical discussion. Hence, it is not feasible and there is little economical interest to recycle these elements out of e-waste. Besides, other precious metals as gold, silver and palladium are more lucrative to mine out of WEEE (Chancerel et al., 2015a). These precious metals are not defined by the European Union as critical however their presence should not be forgotten as already recycling processes for these metals are established (Rotter et al., 2015).

In case of smartphones these metals are spread out over several parts of the smartphone and their use is often limited to certain application within mobile phones. Precious and critical metals are mainly found in IC's or integrated circuits, capacitors and other parts of the printed circuit board. The critical metals as for example REE are used in flat dis-

plays, LEDs or magnets. Cobalt and lithium are a persistent parts of batteries. Especially galium is a crucial element in smartphones. Oguchi et al. (2011b) showed how gallium is used in semiconductor materials of miniaturized integrated circuits for high-frequency powers amplifiers for wireless communication. It is known that smartphones contain ten times more gallium than mobile phones. Indium as part of screens is found mainly in televisions although it can be used in screens of smartphones. If so, they take a miner roll in the consumption of this metal due to smaller display surfaces (Chancerel et al., 2015b).

Tantalum is a newly defined critical metal. Tantalum together with niobium and tin is often related to conflict zones as high concentrations are mined in countries as Rwanda and Congo, linked to conflict and artisanal mining (Ayres, 2013; Perks, 2015). Tin is not defined as critical metal but is often linked with conflict or artisanal mining. Tin is part of the PCB and found in various parts as lead-free solder material for electric circuits or as conductors (Chancerel et al., 2013). Tantalum has the role of capacitor in the PCB.

Gold, copper, silver and palladium are the main metals targeted and are often the only metals valuable for extraction (Hagelüken and Meskers, 2008). Gold and silver are used as contact material in electronic systems, respectively as bonds and solders in printed circuit boards. Palladium is present in capacitors within PCB (Chancerel et al., 2013).

2.1.2 Chemical data and characterization

The amount of research on bulk chemical composition of a smartphone is limited and restricted to the printed circuit boards (PCB) within. This narrow the discussion of the chemical composition to only a few article. Taking into account that there is a difference in time of manufacturing only a few relevant sources are left.

An overview on the general composition of a mobile phone and smartphone is given in table 2.2 based on data from (Holgersson et al., 2016). These values are an average from 30 different mobile phones and 30 different smartphones.

Type of phone	PCB	Plastic casings	Metal casings	Battery	Screens	magnetic	other
Mobile phones	21.3 %	41.0 %	3.7 %	20.5 %	8.1 %	3.1 %	2.3 %
Smartphones	20.1 %	32.9 %	3.3 %	13.3 %	26.2 %	2.5 %	1.6 %

Table 2.2: Compiled data on average mobile and smartphone composition from Holgersson et al. (2016).

Other data on this matter is given by Oguchi et al. (2011b). Oguchi et al. (2011b) estimated the average content based on 16 mobile phones to be 0.8 % ferrous material, 0.3 % copper cables and material, 37.6 % plastic, 30.3 % printed circuit board and 20.4 % battery. These findings are more or less in line with those of Holgersson et al. (2016), but it already indicates how results can fluctuate when examining different phones.
In Yamane et al. (2011) the PCB of mobile phones were characterized as 63 wt. % metals; 24 wt. % ceramics and 13 wt. % polymers. The metal content in PCB was estimated to be about 34 % copper. Batteries in standard mobile phone are around 20 wt % of which more or less 3.8 g consists out of cobalt. In the case of smartphones batteries might have a weight % up to 33 consisting for 6.3 g of cobalt (Buchert et al., 2012). Magnets which are in all these studies removed by manual separation or by a magnetic separator are common in loudspeakers. They can contain up to 0.050 g neodymium and 0.010 g praseodymium (Buchert et al., 2012) .

Holgersson et al. (2016) analyzed a mixture of 30 different printed circuit boards of mobile phones and smartphones. This was done simply for the same reason as described above that PCB contains most of the critical and precious metals. The author makes a clear separation between smartphones and mobile phones. A difference that is based on the lack of internet connectivity in mobile phones. The phones were dissembled in PCB, plastic casings, metal casings and screens (weight % data in table 2.2). After removal of the battery all the material was milled to a 2-3 mm fraction and homogenized. Three samples were taken and each one was milled further with a cyro centrifugal milling device. The samples were analyzed for their metal content using aqua regia as leaching reagent (Holgersson et al., 2016).

The results of all the elements targeted within the PCB by Holgersson et al. (2016) are shown in table 2.3. Added to this table are the results from other researches on PCB of mobile phones (not smartphones) (Ernst et al., 2003; Oguchi et al., 2011b; Ogunniyi et al., 2009; Tan et al., 2017).

Element	Smartphone - Holgersson et all.201	Mobile phone - Holgersson et all.2016	Mobile phone - Oguchi et al., 2011	Mobile phone - ernst et all., 2006 -	Mobile phone - Q. Tan 2017	Mobile phone - Ogunniyi 2009
Ag	2773	2640	3800	5000	2000	3301
Al	17800	19068	15000			
As	141	93.3				
Au	1083	1051	1500	1100	1200	570
Ba			19000			
Be	115	98.7				
Bi	60.6	39.6	440			
Cd	<0.2	<0.2		45		
Co			280			
Cr	1219	865		4000	2000	
Cu	395000	342667	330000	120000	418000	234700
Fe	8793	6810	18000		6600	
Ga			140			
Hg	0.3	0.6				
Ni	15433	11600		30000	19300	23500
Pb	260	3747	13000	11000	1900	9900
Pd	55.4	119	300	<3		294
Pt	0.8	4.3				30
Rh	8.5	5.7				
Sb	30.4	543		2500		
Sn	32220	19267	35000		45700	
Sr			430			
Ta			2600			
Ti					6500	
Zn	6667	5483	5000			

Table 2.3: Chemical composition (in PPM) of PCB in smartphones and mobile phones. Data is compiled from various authors: Ernst et al. (2003); Holgersson et al. (2016); Oguchi et al. (2011b); Ogunniyi et al. (2009); Tan et al. (2017).

The first things that strikes out from the table is that data is inconsistent for the different studies. It shows how each researches has only information for a limited set of elements. For example Ta, which is active component in the manufacturing of mobile phones (Cucchiella et al., 2016), can only be noticed in the research of Oguchi et al. (2011b). As a result valuable information is often lacking. This makes it hard to compare different studies.
The only data on real bulk chemical data on PCB of smartphones was given by Holgersson et al. (2016). There is more data available on mobile phones as results of the larger time spans of their existence. Similar observation were already expressed in Buchert et al. (2012) and the author reports the need for more grounded and complete studies on this matter. Buchert et al. (2012) recognizes in a review studies the existence of several metals within a smartphones. However only four elements were reported with quantitative data for one smartphone (Buchert et al., 2012):

- Gold 24 mg or 340 ppm
- Silver 250 mg or 3500 ppm
- Palladium 9 mg or 130 ppm
- Copper 9000 mg or 13 %

The results (table 2.3) report over a wide time period and are used by Holgersson et al. (2016) to see trends how metal content changes over time of manufacturing. With the main difference in the data set between the metal content of a mobile phone and a smartphone. This reasoning is questionable, and to show this Ag is taken as an example. The data from Holgersson et al. (2016) shows that there is little difference in concentration between the use of Ag in smartphones and in mobile phones. However the study of Tan et al. (2017), published after Holgersson 2016, reports other-ways. Based on samples from mobile phones manufactured between 2006 and 2011 Ag values are lower than the analysis of Holgersson et al. (2016). Tan et al. (2017) speaks of a standard deviation of 50 % of the measured data. It is therefore more assumable to define this difference not by time but rather by a larger set of variables (metal prices, manufacturing, model, application of the mobile phone, error in chemical analysis, amount of mobile phones used in research . . .). Hence it expresses the difficulty of treating mobile phones as a homogeneous source and to correlate data. Another reason could be the heterogeneity in the sample itself. The main problem with e-waste is that most of the metals are find in certain zones (e.g Ta in capacitors, Au in specific parts for conduction, . . .) creating a sort of nugget effect. If the concentrations of Ag is very larger in certain parts crushing to 1-3 mm might not be enough to guarantee a homogeneous mixture giving a biased result. Hence, The

representative of samples used in this article is arguable for such heterogeneous material. The problem becomes visible in the data discussed. Ag was measured in three different samples with values of 1219, 2540 and 2773 ppm and gold with values 199, 1051 and 1083 ppm. In the article only the highest amount detected was used in the discussion for all the elements analyzed.
Aside, During chemical analysis as leaching with aqua Regina certain elements needs to be target. This creates the effect that certain elements of importance are forgotten and left out of the discussion. Ta and W for example were not discussed in Holgersson et al. (2016) but are discussed in other articles. Some of these metals as Ta an Ga are found to be present in relatively high abundance. Hence, they can be an important factor in the recycling of mobile phones. It is unclear why these metals were not investigated in the research of Holgersson et al. (2016).

Values for Au are around 1100 ppm with a standard deviation of 210 ppm in Holgersson et al. (2016). This is quite close to the 340 ppm considered for the whole mobile phone by Buchert et al. (2012), knowning that around 20-30 % of a mobile phones exists out of PCB. Even the highest value of 5000 ppm measured of Ag in PCB by Ernst et al. (2003) can not be correlated with the 3500 ppm of (Buchert et al., 2012) for a whole mobile phone. It might be an indication that silver is present in other parts of the phone aside the printed circuit boards. Or one of the two data is an over or under estimation.
The occurrence of Ba was only described in Oguchi et al. (2011b) with concentration exceeding values of Al. Oguchi et al. (2011b) is also the only author describing the presence of Ta, Sr, Ga and Co within PCB. Oguchi et al. (2011b) data is based on 19 different samples coming from own research as well from literature. It is unclear which types of mobile phones were used in this article, but all data was generated from mobile phones not from smartphones.

Cr, known as a polluting element, is relatively abundant (as said before in stainless steel). Values change between 1000 till 4000 ppm. No real patron could be observed from these data and are present in older and newer models. Cu data is the most abundant metal taking up to 40 % of the content of PCB. There seems to be a trend showing more Cu in smartphones but these values fall within the standard deviation when compared to other data. Ni is the second most abundant metal in PCB of mobile phones. Sn is another highly concentrated metal in mobile phones and smartphones. Values are between 20000 ppm and 45000 ppm and no difference between smartphone and mobile phones can be inferred.

The small amount of Pb in comparison to mobile phones is remarkable. Holgersson et al. (2016) explains this by a stronger legislation, especially in Europe (European Commision,

2010). Where the use of lead, as a toxic metal, is been reduced in the manufacturing of newer and more recent phones (e.g smartphones). A similar trend can be observed for Pd with higher values in mobile phones. Interesting is the presence of elements as Pt and Rh, although in very small amounts but not neglectable. Holgersson et al. (2016) indicates a large difference between the use of Sb in mobile phones to smartphones (18 x) and 80x in comparison with the study of Ernst et al. (2003).

Only (Oguchi et al., 2011b) examined the presence of Ta and Sr. Sr is present in relatively small amounts but Ta has values exceeding Au, coming close to the quantities of Ag. Same can be said for Ti mentioned by Tan et al. (2017). Zn is present in similar concentrations for both smartphones and mobile phones. Ga is reported with a value of 140 ppm. Ar is is present in PCB with more or less the same value as Ga.

Although, most of the elements enlisted in table 2.3 are described in literature some elements are still missing quantitative reporting in literature. The missing elements includes Dy, Ge, Pr, Ir, La, Ce, Mn, Y, Sc, Tb, Eu and Gd (Buchert et al., 2012). Most of these elements are found within screens. Also, it doesn't always mean that all the metals should be present. It depends on the type of phone and the manufacturer.

2.2 Recycling steps and problems

In mining all steps from geology to processing to smelting are in detail analysed and are after combined to make an overall assessment to declare the mine feasible or not. In terms of secondary resources equal to mining all steps should be included in the overall analysis. This includes: collection (transportation), sorting, dismantling and mechanical separation, smelting and/or refining. Similar to mining, where prospecting, exploration and feasibility studies are required, same research steps should be undertaken on collection and processing steps to define feasible economically targets (Chancerel et al., 2008; Hagelüken and Meskers, 2008; Oguchi et al., 2011b; UNEP, 2011). A visible representation is given by (Oguchi et al., 2011b) in figure 2.1, comparing mining of primary and secondary resources. From this view EEE with a high metal content and a relatively ease in collection will be chosen as a feasible target. For example, Oguchi et al. (2011a) states how mobile phones and portable audio players received more attention in Japan as potential source of precious and critical metals. The scheme by Oguchi et al. (2011b) (figure 2.1) helps to understand how not only metal grades are important but also the collection rate and amount of WEEE available.

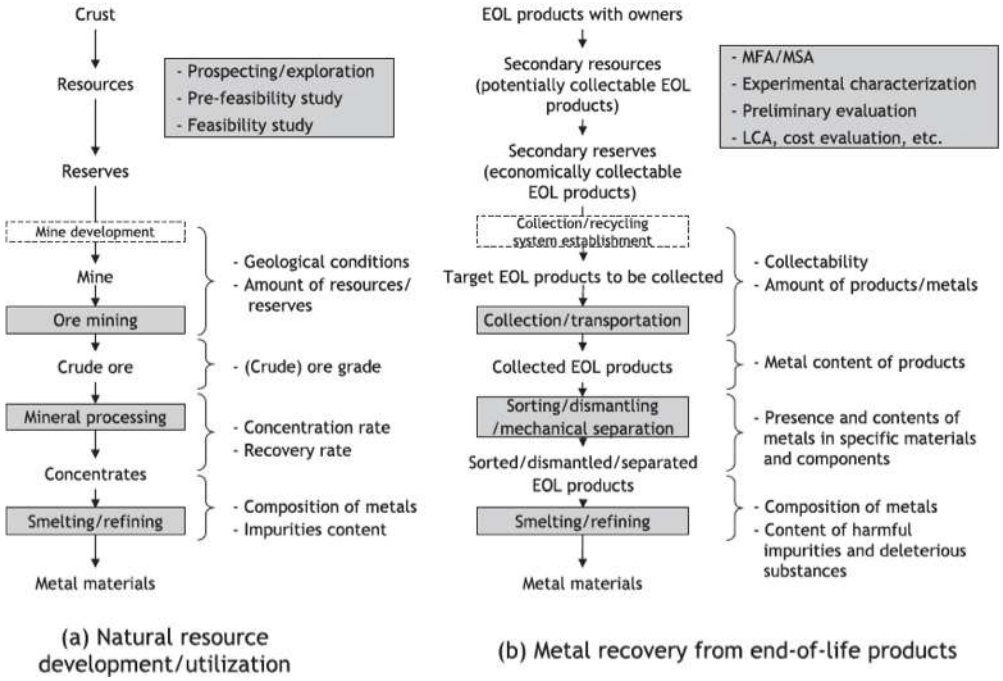

Figure 2.1: (Pre-)processing steps for e-waste and traditional primary ore (Oguchi et al., 2011b).

It is therefor critical in the overall assessment to understand which metals and in what state they can be found within certain types of WEEE. This especially important information in the next step: dismantling and separation processes. More over, understanding all metals and their phase within can be important information to see impurities and deleterious substances that can influences smelting and refining processes. This overall assessment of collecting and analyzing data from all different steps in the processing circuit is known in mining as geometallurgy (Rosenkranz and Lamberg, 2014).

Pre-processing of e-waste is focused in two domains. First is the collection of e-waste, which is the ratio of generated WEEE and collected WEEE for recycling. Second is a mechanical step where e-waste is sorted and dismantled in different fractions. In both steps a lot of materials with precious metals as gold is lost. In most cases the recovery of gold is dropped below 20 % during these steps (Hageluken C, 2006). And although refinery steps as smelting or acid treatment have a high recovery the overall recovery is low due to very low efficiency in pre-processing (Hagelüken and Meskers, 2008). The efficiency of recycling can be defined through the recycling rate which is the quotient of the recycled metals and the total amount of metals generated in the material recycled (UNEP, 2011).

2.2.1 Collection of electronic waste

One of the most difficult challenges to overcome in recycling is the collection of WEEE. Whereas in mining the targeted resource is neatly mapped in geological studies this is rarely the case in recycling. Here, the resource is spread over landfills, waste belts or ends up as dead storage in drawers or other small storage rooms at home. The latter is especially the case for mobile phones and other small electronic equipment. Another issue with this waste stream is that it easily gets mixed with other waste because of its size. All this makes it very difficult for a recycling company to maintain a steady stream of WEEE (Murakami and Murakami-suzuki, 2008; Sarath et al., 2015; Yin et al., 2014). Globally the collection rate of mobile phones lies under 10 % (Welfens et al., 2016).

A study by Yin et al. (2014) illustrated that in China the life cyclus of mobile phones is less than 3 years. This is less than the designed service life but a result of the increasing demand for new functions and styles. This increase in quantities of old mobile phones are for 41.7 % stored at home. Similar conclusions are stated in Sarath et al. (2015), with life time of 2 years in developed countries and 3 years in developing countries. Improving the recovery of old smartphones strongly depends on creating awareness under the public and governmental decision making. Something which is in more detailed explained by Baxter and Gram-hanssen (2016). A series of suggestion on creating succesfull collection campaigns has be provided in Welfens et al. (2016) and in Victoria et al. (2017) but have so far never found full effectiveness.

2.2.2 Sorting and dismantling

When it comes to recycling itself the whole process chain must be analyzed when discussing recovery rates (Reuters and van Schaik, 2015; van Schaik and Reuters, 2010). A regular problem in this matter is design-related resulting in losses due to insufficient liberation (Reuters and van Schaik, 2015; van Schaik and Reuters, 2010). Therefore, the complexity of the WEEE lies in liberation and separation. Decent and efficient pre-processing steps are often difficult and not feasible to establish. Consequently, the materials set up in end refining process are limited to only recover a particular set of metals (Khaliq et al., 2014). A typical example is an end-off life smelter capable of recovering copper, precious metals and some additional elements (Hagelüken, 2006; Hagelüken and Meskers, 2008). Unfortunately, other metals and materials end up diluted in slag and scrap metals and are unrecoverable. This especially true for critical raw materials (CRM) as REEE and tantalum. For critical metals as indium cobalt, REE, etc. mainly found in complex WEEE products no recycling strategies are implemented yet as there recovery process is too sophisticated and price demanding (Kumar and Holuszko, 2016; Li et al., 2017; Zeng

et al., 2016; Zeng and Li, 2016).

Pre-processing steps are often very limited due to the high operational costs in contrast with the value of metals to recover. In an ideal scenario e-waste streams would first be sorted into different e-waste groups (small IT, Large IT, . . .). Secondly, a specific separation process would target the metals of interests. It has been pointed out by Oguchi et al. (2008) that for an effective reuse of metals from different types of end-of-life EEE it is important to define which metals in what types of equipment should be given priority. It is desired to reconstruct the systems for collection, sorting and pre-processing taking into account each type of equipment's specific characteristics. However, the hard truth is that in most cases all kind of e-waste are randomly collected, mixed and finally shredded for further processing (Chancerel et al., 2009).

To find the most efficient way of recycling it is important to establish a material flow and a stock analysis/accounting to understand better the effects of sorting and dismantling techniques. During recycling a lot of material gets lost before reaching the smelter. Trying to find out where all the material is lost, batch analysis are made in each step of the processing route determining the current state of the metals. In the end a material balance can be made showing how the metal is distributed over the different product and tailing streams. Such study is done by Ueberschaar et al. (2017) using batch analyses (physical and chemical treatment) of pre-processing products of waste electronics. Batch analyses can be done with standards including fire assaying and re-melting with recuperation of target elements. X-ray fluorescence analysis and acid based digestion are done prior to determination with inductively coupled plasma mass spectrometry (ICP-MS) and atomic emission spectroscopy (ICP-AES) (Ueberschaar et al., 2017).

The outcome of the study of Ueberschaar et al. (2017) is given in figure 2.2 showing results for Cu, precious metals and critical metals. The figure demonstrates how precious metals and copper are not efficiently separated but rather distributed along various output fractions. The critical metals as REE and cobalt were as well badly recovered and resulted in significant losses. The batch tests with fractional chemical analysis give valuable information on the evolution of the metal during processing, but the author expresses that there are still difficulties to provide a critical evaluation. Chemical analysis of precious metals and critical metals are very sensitive to matrix effects as result of accompanying elements that can lead to an over- or underestimate. Therefor, the analytic method must be adapted to the matrix, which is often not feasible resulting in a large error on the analysis (Ueberschaar et al., 2017).

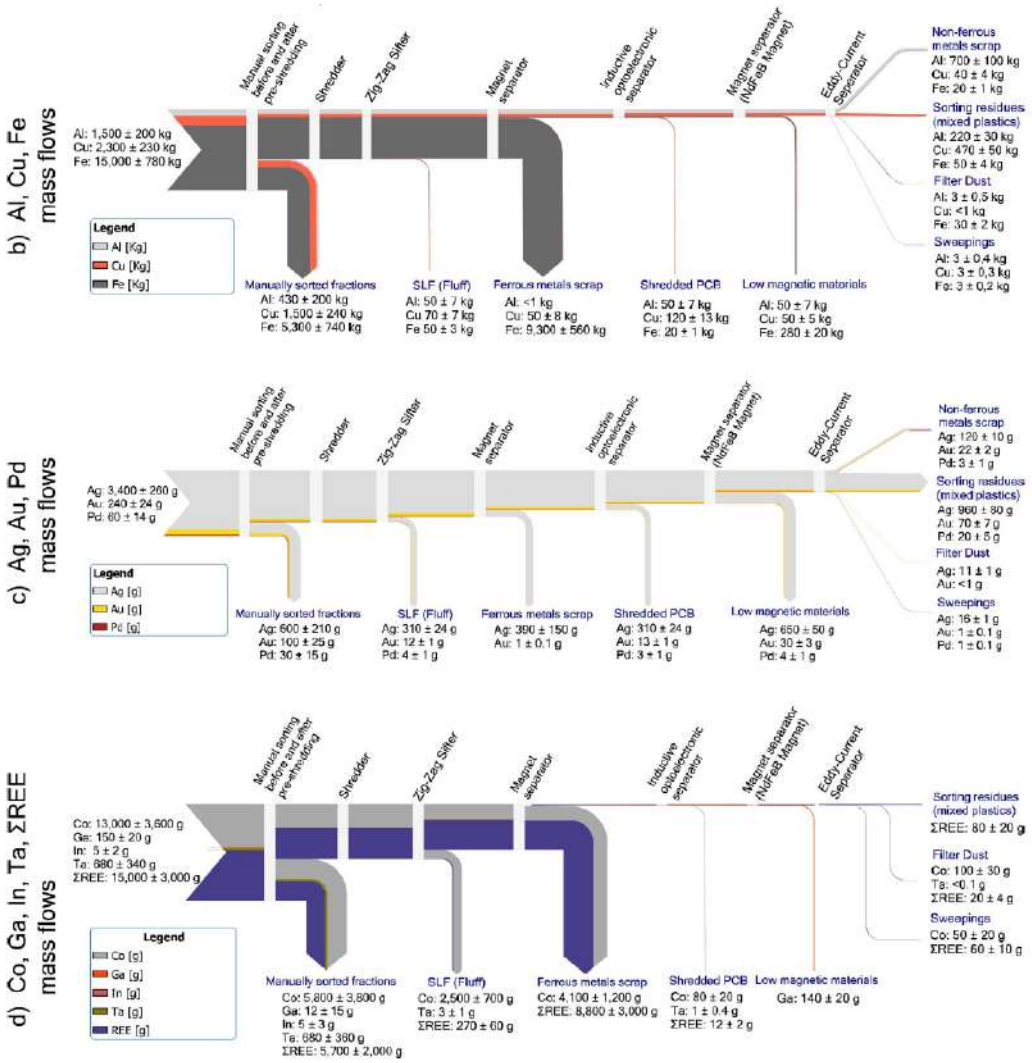

Figure 2.2: Schematic overview of the mass balance of the different metals in a pre-processing plant treating e-waste by Ueberschaar et al. (2017).

A large part of the valuable metals is directly distributed in a first product stream after manual sorting. That is to say that PCB, copper wires and other valuable zones highly enriched in these metals are picked out. For gold almost 50 % from the original batch ends up in a manual sorted fraction. This could be explained by the fact that gold is mainly present within the PCB. The remaining gold is distributed along the different product streams of magnetic separator, optical sorting, magnetic sorting and eddy-current separator with no specific high concentration of gold within one of these different fractions.

PCB that is not hand-picked during manual sorting is shredded with the rest of the waste. The losses of metals in this process are large. 25 % of Ag, 30 % of Au and 60 % of Pd are lost in this process. In the studie of Reuters and van Schaik (2015) it was even concluded that shredding and mechanical separation can lead to a complete loss of

Au. An explanation needs to be sought in the complex nature of PCB, the location of the metals and the form in which gold is present. In case of gold as it is used for plating, small contacts and its present in ceramics and inter-board layers of the PCB, the impact of smashing and shredding results in breaking of contacts and damaging the coating. In the end gold gets mixed with dust and ferrous particles unable to recover in later stages. Pd is lost in a similar pattern as it is in in close presence of ceramic compounds, ending in a dust fractions, lost or sticking to other metal fractions (Chancerel et al., 2009; Reuters and van Schaik, 2015; Ueberschaar et al., 2017).
For REEE and critical metals the problems gets even worse. REEE is transported together with dust, due to their small fractions, ending up in the fluff fraction after a zig-zag shifter. Another fraction joins the ferrous metal scrap due their magnetic characteristics (f.e. Pr & Nd). In the same scenario as Au a large part of REE is recovered through manual sorting (e.g cobalt through battery removal) (Chancerel et al., 2009; Reuters and van Schaik, 2015; Ueberschaar et al., 2017).

In an earlier study by Chancerel et al. (2009) the problems of recycling were also pinpointed. The study is based on a German recycling plant treating a mixture of IT, telecommunication and consumer equipment but also wrongly sorted non-electronic waste. In the first stage manual sorting results in the removal of hazardous and problematic components as batteries, chunks of metal and motors. PCB, when easy to separate are also removed during this process. The plant relies on a coarse shredding, after which a second manual sorting takes place aiming for PCB or hazardous components. In later phases the material is sorted automatically. Every section was analyzed for its gold, silver, palladium and copper content. PCB and metal fractions concentrated in precious metals and copper were send to refineries for metal extraction. Chancerel et al. (2009) found that only 11.5 % of Ag is recovered. The rest of Ag was distributed in plastics and ferrous metals. Also Au is for 40 % present in ferrous metal section. In comparison to silver the overall recovery is higher (26 %). This is still low knowing that up to 74 % is spread over the different fractions. The total distribution is given in figure 2.3.

Losses of precious metals during the different steps after shredding are significant. Between the coarse shredding and final shredding the material is downsized from < 8 mm to < 2.5 mm. In both cases PCB is sorted either through manual or automated sorting. In the first case when PCB are barely broken due to their easy access there is a poor loss of material 7 % while for in the second stage of shredding this loss is 62 %. Easily liberated PCB are found in personal computers and mobile phones which have a higher concentration of precious metals in comparison with more difficult to liberate PCB in printers and radio's. Also, once the PCB is shredded into fine particles it gets

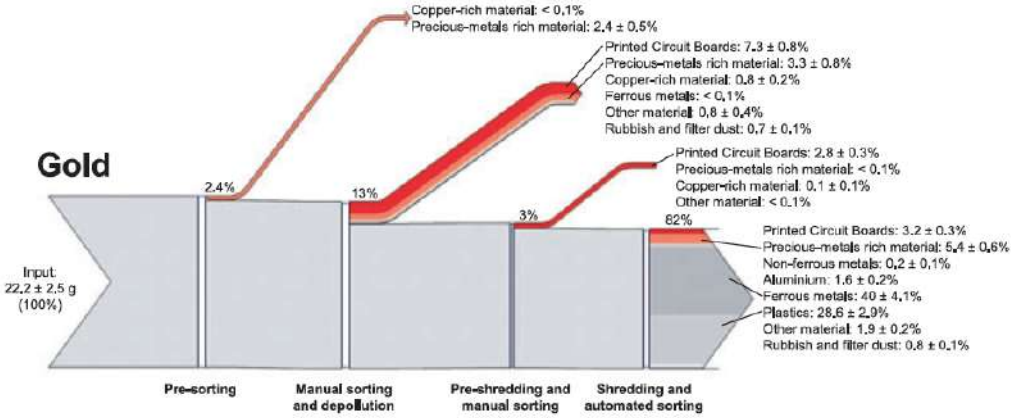

Figure 2.3: Distribution of gold through the different fractions after dismanteling and (pre-) processing (Chancerel et al., 2009).

easily mixed with with other outputs (Hagelüken, 2006; Hageluken C, 2006). The reason therefor is that the (precious) metals in PCB are embedded in a complex material mixture with ceramics (Multilayer capacitors (MLCC), integrated circuits, plastics and inter board layers (Hageluken C, 2006). Often these metals are coated on layered materials making their liberation process hard and often not possible to isolate (Castro et al., 2005).

Improving the recovery of precious metals out of PCB would require to avoid shredding. Reuter et al. (2006) discusses the grade and recovery of e-waste and implies that complex products high in precious metals should be avoided to be shredded. It would mean to adjust the manual sorting step at the beginning of the process aiming for precious metal-rich materials (Chancerel et al., 2009). According to Chancerel and Rotter (2009) it would be necessary to have knowledge on the location and the state of precious metals in WEEE. This information is currently missing for a part and is lacking in literature. Also, little is known on the quantity of precious metals in other parts of e-wast than PCB. One possibility is to have better communication flow with manufacturers providing the missing information. Another solution would be to apply a geometallurgical approach to discuss the liberation process. A useful tool within this field is microscopy.

2.2.3 Refinery: smelting

After a dominantly mechanical separation the remaining fractions are further refined for the extraction of precious metal. A well known method is smelting. From electronic waste typical materials are printed circuit boards, cut-off parts relatively rich in precious metals as metallic granules (mostly copper based), mixed plastics fractions with residual metals, and (precious) metals containing dusts (Hagelüken, 2006). In contrast to ores the combination of metals found in WEEE is different. Therefore the smelting techniques used for ores do not guarantees similar high recoveries. Still, pyro-metallurgical methods are a dominated processing technique nowadays for the reprocessing of WEEE. It is an ongoing trend to incorporate this feed material into copper smelting process. Examples are found in Noranda in Canada, Boliden AB in Sweden, Aurubis (Lunen) in Germany, Umicore in Belgium and Brixlegg in Austria. Of these, Umicores Hoboken plant is considered the globally most advanced full-scale processor, various precious metals are recoverd directly coming from electronic scrap (Anindya et al., 2011). The scrap material is burned in a

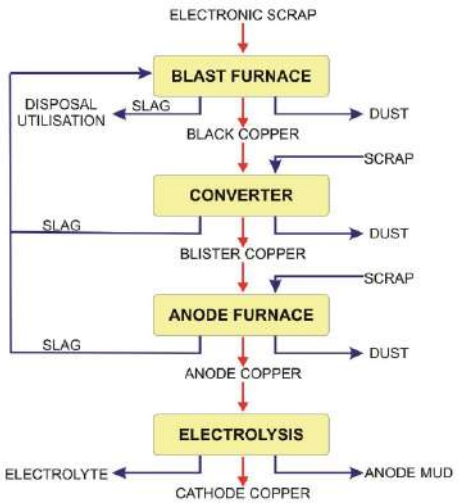

Figure 2.4: Thermal treatment of WEEE focussing on Copper and precious metals. (Gramatyka et al., 2015)

furnace or a molten bath to remove plastics and organics. Hereby further concentrating the metals to a molten metallic residue. The burned plastics and refractory oxides become the slag phases (Gramatyka et al., 2015). In an integrated smelter as Umicore plastic serve as an energy source and reducing agent (Brusselaers et al., 2006). In smelting reactions a collector metal, which is in most cases Cu, collects other metals as Au, Ag and Pd. However, also impure alloys can be formed by smelting the crude metal concentrates. Precious metals in scrap as Ag and Au can be treated in a copper smelter. Final refining steps includes reduction and smelting, raw copper production in the converter, fire fining, electrolytic refining and processing of the anode mud. In modern secondary smelters as

in Umicore many different kinds of secondary Cu can be treated. In Figure 2.4 a typical recycling process is illustrated dealing with waste electronics consisting out of Cu and other materials as Ni, Pb, Sn, Zn, Fe, Ar, Sb and precious metals among many others. The precious metal are concentrated together with Cu and are later during electrolysis recovered from Cu anodes (Gramatyka et al., 2015).

In integrated smelter-refineries as in Umicore high graded PCB do not necessarily have to be shredded. Other than smelting hydrometallurgical steps are still used to receive pure metal concentrates (Hageluken C, 2006). Recoveries during smelting reach values of 95 % with overall efficiency of more than 90 % (Hageluken C, 2006).

2.3 Automated mineralogy

Automated mineralogy (AM) has been used for several decades in the mining industry worldwide. And is a sort of 'smart' alternative on the traditional optical and light microscopy and XRF analysis. Automated mineralogy systems became available during the seventies (Sandmann, 2015). Linking mineralogy with plant performances started in the 70 and 80 (Petruk, 1976, 1988) and became more and more important with the rise of more developed systems as QUEMSCAM, QEM*SEM, MLA and EPMA. At the turn of the millennium the two dominant systems MLA (Mineral Liberation Analyser) and Quemscan (Quantitative Evaluation Of Minerals By Scanning Electron Microscopy) started to have their full growth on the market. By the end of 2014 the market was dominated by systems of FEI (MLA and QUEMSCAN) with 240-250 systems (Sandmann, 2015). In 2014 ZEISS launched their own Automated Mineralogy system named 'Mineralogic' (Carl Zeiss AG, 2014).

The upcoming use of AM systems can be explained by a decrease in purchasing costs, being more user friendly and being less time consuming (Graham et al., 2015; Gu, 2003). These instruments provide visual and statistical data on elemental composition, liberation, size distribution and interaction of the different components. These data has become vital in ore characterization, optimizing the process design and has become a key component in geometallurgy. Recent studies showed how automated mineralogy helped to optimize processes like grinding and flotation, increasing significantly the overall recovery (Baum, 2014; Evans et al., 2011; Goodall and Scales, 2007; Lotter et al., 2011; Mermillod-Blondin et al., 2011; Rule and Schouwstra, 2011).

2.3.1 QUEMSCAN and MLA

QUEMSCAN is used to collect mineralogical data through an automated system. With (or without) the use of backscattering electron images (BSE) of the sample under the microscope, energy dispersive X-rays (EDS) are deployed to rapidly identify different composition in order to produce mineral maps. Hereby a color code used to indicate certain minerals, making them visible after analysis. During the analysis not only minerals of economic interest but also different gangue minerals can be targeted and quantified. These maps are able to describe a set of different characterization of the samples analyzed: textures, mineral association, modal mineralogy, mineral grain size, mineral liberation and element deportment by mineral (Lotter, 2011).

A key aspect of QUEMSCAM is that compositional information for every mineral is necessary to gain the right data as elemental deportment calculations. Composition in-

formation can be found in textbooks and literature and form a solid basis in these analysis. However, solid solution or variations in composition in same mineral type but different deposit, small analytic errors can make it happen that measurements do not fall within these pre-defined ranges. Detailed analysis through EDS or with more detailed electron microprobe analysis of individual grains and textures a more accurate result can be made of the composition. These newly obtained compositional data is after added into the QUEMSCAN software to adjust the elemental deportment calculations. Here fore, the original classification saved in SIP files must be adjusted and re-implemented in the system (Pownceby et al., 2007).

A MLA measurement focus on particles their mineral composition and gives information on liberation, locking and grain size. At first a BSE image is acquired followed by particulation and segmentation on this images. Particulation exists out of three steps: de-agglomeration, background removal and clean-up. This is only necessary if the material exists out of granular material. Segmentation is done to remove artifacts such as holes, relief and cracks on the sample. Hereafter, X-ray analysis are done based on the chosen measurement method. Two methods are possible: the entire phase is mapped through a dense grid of X-ray points or a single x-ray acquisition is done for each phase identified in the BSE (centroid method) (Gu, 2003; Sandmann, 2015). The two methods are illustrated in figure 2.5.

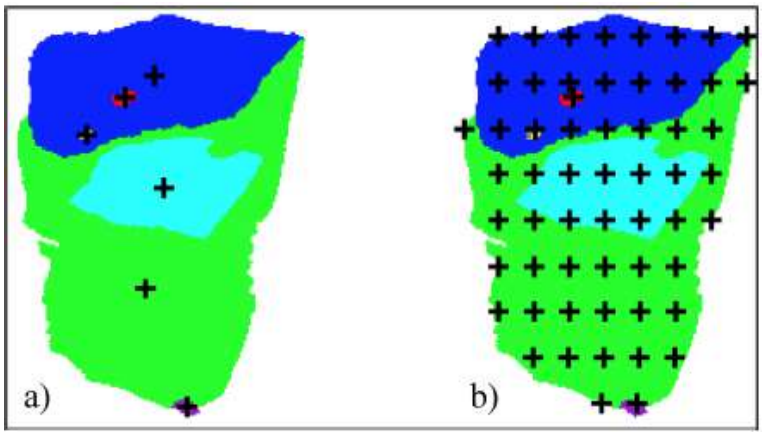

Figure 2.5: Schematic overview of the x-ray acquisition methods: a) centroid method, b) grid method (Sandmann, 2015).

2.3.2 Mineralogic by ZEISS

The ZEISS Mineralogic Mining is one of the latest achievements in automated mineralogy (AM). The new technology combines full quantitative energy dispersive spectroscopy (EDS) mineral classification system and advanced image analysis capabilities. Classification of minerals is based in the wt% contribution of the elements detected and therefore uses the minerals stoichiometry. The company was able to correlate Light microscope (LM), Scanning Electron Microscope (SEM) and Automated Mineralogy (AM) colored mineral maps in order to make flawless and efficient information to make the most of the information each technique provides (Graham et al., 2015).

So far, technique as LM, SEM and AM are most often treated separately and little is known and developed on the correlation and application between these techniques in process mineralogy. ZEISS claims to solve these optimization problems as (Graham et al., 2015):

- "Correlating stage coordinates and areas of interest between instruments"
- "Correlate images into data layers to benefit from the unique data available from each and to"
- "Have an optimized workflow for data collection and analysis"

ZEISS Mineralogic Mining machines has been able to coop with these issues. They achieve this goal by using LM to efficiently identify areas of interest before a more detailed characterization using SEM and Mineralogic. By achieving an efficient workflow the sample throughput is increased. This could be of certain interest to target metals within the WEEE fast and cost efficient.

In comparison to older automated mineralogy analysers as QUEMSCAN ZEISS Mineralogic mining provides an advanced image processing capability and fully quantified EDS classification methodology. The system is based on a Recipes-based protocol. Here, once the first analysis is done and the defined parameters for this analysis are saved for a certain sample or application they can be easily recalled, edited, copied and reassigned to other applications and samples. These parameters include: SEM, operating conditions, calibrations, mineral classifications, assay and target mineral phases. This creates the possibility of a routine analysis without the need of a skilled mineralogist. All these data files can be transferred and shared with other Mineralogic Mining systems. This can for example be interesting to have the software on a PC not linked to a microscope but which can be used to optimize the classification system (Graham et al., 2015).

ZEISS presents five analysis modes, configurable and user friendly dependent on the information required from a sample and the time available: mapping, spot centroid, feature scan, line scan and Back Scatter Electron (BSE).

- Mapping: Based on a self- determined EDS pixel size and magnification an analysis grid is drawn over the sample. Depending on the step size, EDS dwell time, number of analysis point and the sample surface area a full analysis is done within a certain time frame.

- Spot centroid analysis segments focuses on individual mineral grains found by the BSE image. These grains are analyzed by a single EDS measurement. This specific amount of EDS analysis makes it a fast mode but due that only one single EDS analysis is done on the grain no changes in elemental deportment will be reported.

- Feature scan is using the BSE function to find the mineral grains of interests. Here the total grain is analyzed by X-rays and an average composition will be given. The technique is faster than mapping but slower then spot centroid.

- Line scan is a fast and statistically based mode to determine the bulk mineralogy of the sample. The technique uses pre-determined points across a single line through the center of each particle for EDS analysis. It is a fast measurement applied mainly for non-unique BSE Values for minerals. It gives an indications of relative texture e.g. size, liberation and association.

- The BSE use the electron scale ranging from 0 to 255 in grey scales to classify mineral phases. No EDS measurements are done during this analysis making the technique the fastest mode.

The Back Scatter Electron (BSE) is the fastest mode available creating map in grey scale classifying mineral phases uniquely based on BSE value. Interesting for this system is that by adjusting the dwell time of the EDS the counts per pixel are altered. For the classification and accurate detection of elements and minerals 2500 counts is advised (Graham et al., 2015).

Mineral classification is done by quantification of the (in wt %) elements after full quantitative EDS. Here the spectrum, resulting from the EDS analysis, gives the wt % contribution of the elements. Bases on these results and the optimal stoichiometric composition of the minerals, a classification can be done. It is however necessary that the mineral classification is set containing the minimum and maximum percentages of the elements within the stoichiometry of the mineral. If the EDS data is found within this range the

particle or pixel analyses can be defined as a certain mineral. In the case of the WEEE analysis it would be interested to try to group certain type of alloy types. This could help in determining the different alloy types within the WEEE. For each mineral determined a specific gravity is defined to specify the modal mineralogy and the assay value for the sample. Similar to this idea this could help to make up the average alloy and metals composition, liberation and elemental deportment data of the WEEE.

With all analysis by the ZEISS MINING device comes along BSE images in high resolution. The area, elongation, etc. . . must be defined before making the BSE image. After, image processing functions and techniques can be used to adjust the images as desired. The system makes sure physical measurements of the particle, improved touching particle separation and other additional visual data are stored with the BSE image (Graham et al., 2015).

2.3.3 Value of automated Mineralogy

The gain from automated mineralogy is indirect and rather hard to express in numbers. According to Yin et al. (2014) the value of automated mineralogy can be divided in three steps. First, the investments costs for gaining automated mineralogy information depends on a proper valuation of the systems, the information needed and the size of operation. The mineralogic data is often used to mark problematic areas of phases in the process plants. Second, the value of these techniques increases with the expertise of the user. Third, these techniques encourage to maintain a critical evaluation procedure reducing the risk and maximizing investment costs. In general, it is hard to quantify the value of data microscopy as it is a rather abstract content to numerical value an information flow. To do so Hubbard (2010) provides a good framework to characterize and solve this problem by reducing uncertainties based on one or more observations. The study indicates how much money needs to be spent to obtain information to reduce the risks in making decision leading to higher costs. The expected value out of information is defined as the expected opportunity loss after information subtracted with the expected opportunity loss before information.

In case of automated mineralogy several examples can be given. Yin et al. (2014) showed that the information gain with automated mineralogy in a platinum mine reduces the risk in a fine grinding project. Therefore, determining the investment costs in improving the grinding units and optimizing the circuit design. It showed how with automated mineralogy the investment risk decreased from 45 % to 20 %.

2.3.4 AM in other fields and recycling

Automated mineralogy has also found application in other fields as mining. Berk (2009) used these techniques together with SEM/EDS to identify metal residues in airbag used as forensic material in criminal investigation. A similar study was done on gunshot residues (Martiny et al., 2008). Here gunshot residues were examined to determine their origin and their composition. But also in archaeology these techniques are used (Ward et al., 2017). It is of importance to speak of automated microscopy instead automated mineralogy when dealing with man made material. After all, no minerals but metals and alloys are studied.

Chapter 3

Methodology

3.1 Sample preparation

In this research all analysis were conducted on parts of the smartphone Nokia Lumia 925 (figure 3.1). In total of three phones were collected in order to prepare samples for three different kind of analysis under the microscope. The first phone was sliced in parallel sections to study the interior structures and components. The second phone was shredded, sorted in different fractions and prepared as polished sections. The different components and structures were studied and compared with the sliced sections. The last phone was melted to examine how the chemical compositions changes during a melting process.

3.1.1 Parallel slices

At first, the battery of the sample was removed. This was done to conduct further experiments in safe conditions, e.g. avoid leaking of acids or causing small explosions during sawing. The battery was carefully displaced in order to maintain the same internal configuration. Two portions of 82g of epoFix Resin material were heated in an oven at around 65C, added with 10 ml of EpoFix Hardener and stirred. Silicone oil was applied on the edges of a mold to ease the removal later of the hardened material. Next, the phone was placed within the mold and embedded in the prepared Epoxy. The material was placed under vacuum conditions in order to remove all air out of the sample to fill all voids with the epoxy liquid. The hardening time for the epoxy is 8 hours. Hence, the sample was put to rest for the night.

Once the epoxy got stiff the phone was carefully sliced in 10 parallel sections without breaking up the internal structures. Slicing was done by an automated saw. The use of an automated saw made it possible to slice at an exact positions, creating a clean cut

Figure 3.1: Picture of the Nokia Lumia 925 after the removal of the battery.

without vibration. The latter is of essential importance when it comes to polishing the section, where an ultimate flat surface is required. Also, as the goal of the research is to study the changes of elemental deportment through the whole phone it is important that all slice are parallel to each other. Something, that is guaranteed by an automated saw. The major downside of using the saw is that the thickness of the blade was 3 mm, causing loss of material. Nevertheless, it was the best option found with the equipment available for this research.

The sample has been divided in eleven sections (figure 3.2). Of which, nine sections were further treated. Each section was placed in a mold and another 66g of epoxy, mixed and stirred with 8 ml of epoFix hardener, were added to the mold. First 1/3 of the epoxy was added after which again the sliced samples were placed under vacuum condition. After two weights were placed on top of the sample (in this case two big screws) to firmly press the sample against the bottom of the mold to ensure the sample was not tilted by resin slipping under the sample. After the rest of the epoxy was added together with a QR code for easy sample recognition. Again, the samples were put to rest for 8 hours.

A polish device, Tegramin-30 Struers, was used to flatten the surface till 1 um. This was done in 8 stages: 500, 1200, 2000, 4000, 9, 3 and 1 μm. Between the final two stages the

samples were cleaned in an ultra sonic bath. The final result is shown in figure 3.2. It shows a polish section of 6 cm in length and approximately 3 cm in width and depth. The samples are now ready to be used for optical microscopy. For analysis with the SEM the samples were coated by carbon with an Quorum Q150T ES high resolution and vacuum sputter coater. Copper or silver tape was attached to the sample to ensure a good conduction of the electrons. Samples have to be treated with care to avoid that they become greasy.

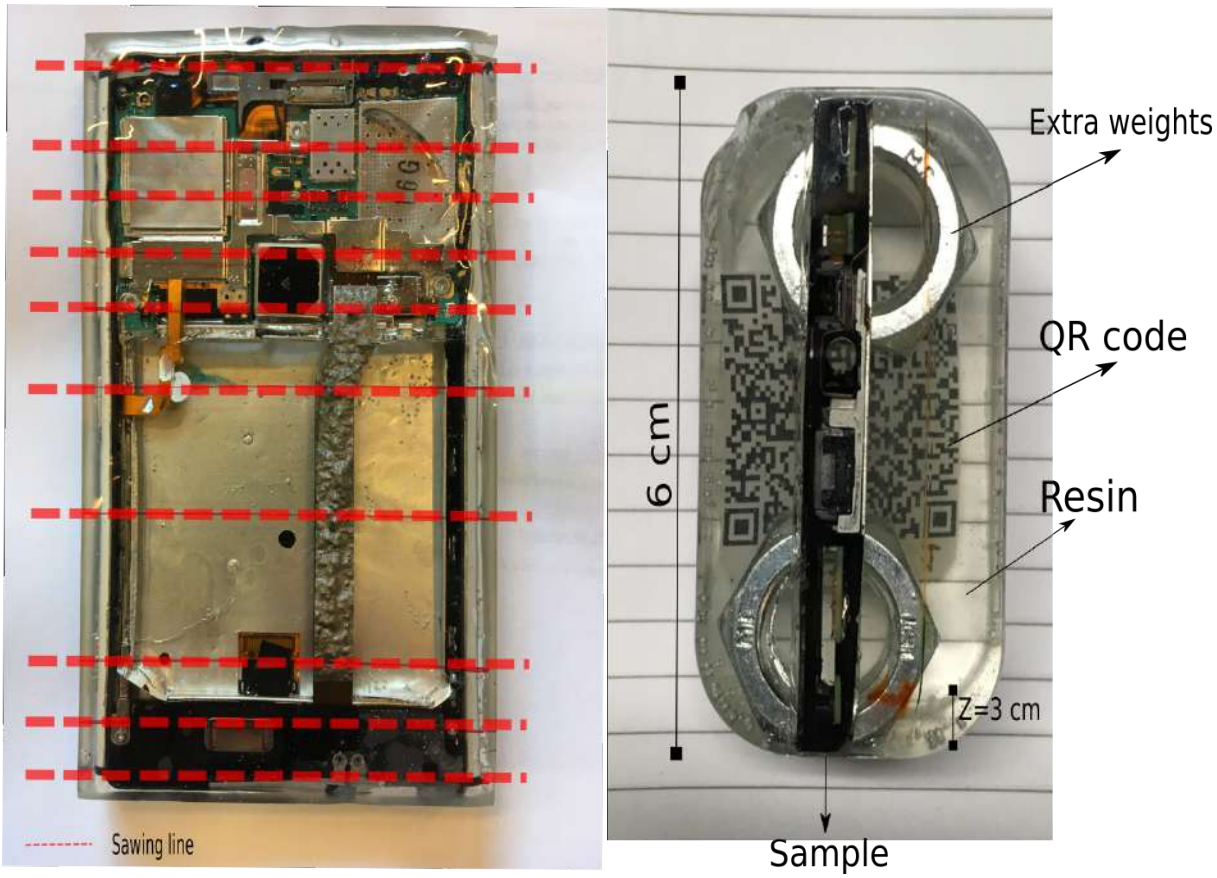

Figure 3.2: Left: Marking of the sawing line on the smartphone in hardened resin. Right: The final result of a parellel section after sample preparation.

3.1.2 Shredded smartphone sections

The second phone was shredded in a small shredding device at the university of Liège. The shredding machine combines the force of a hammer mill and crushing through rotation, with a RPM of 546. The resulted fraction existed out of broken glass, plastics, aluminum, PCB and other metal rich parts. The size of the end product changes from just a few mm up to 10 cm (mainly soft plastic parts). A magnifying microscope was used to separate

carefully large parts of plastics, aluminum and glass from the PCB and other metal enriched parts. It is this final fraction that is carefully sampled to have a representative mix of different fractions. However, due to the complexity, heterogeneity of the sample and losses during shredding (dust, fine particles) it is hard to avoid being biased. The parts are being put in resin and polished as described above. A total of 6 different polish sections were made, each with a diameter of 3 cm.

3.1.3 Molten smartphone sections

The last phone was first shredded. After all parts were placed in a ceramic bowl. The bowl was placed in an experimental oven at the university of Liège. The temperatures in the oven built up to 1200 °C. These were kept stable for 4 hours after which the system cooled down. The whole process took around 24 hours.

From large clumps of molten material sections were saw to create a clean flat surface which can be polished, resulting in vertical section through molten clumps. Small lose particles were crushed with a mortar. The resulting material was put in resin and polished as described above. To avoid floating of these particles in the resin the material was mixed with carbon.

3.2 Light microscopy

The first analysis done were made with light microscopy. Here for a microscope at the university of Liège was used manufactured by ZEISS microscopy. The light microscope analysis was carried out in reflected light, using a ZEISS Axio Imager. Z2m equipped with transmitted and reflected light capability. The light microscope is equipped with a halogen light source and a scanning stage 130x85 STEP (D) allowing automated image collection. Images were acquired using a high resolution AxioCamMR3, 24 bit RGB color with the EC Epiplan-Neofluar 10x/0.25 HD DIC M27 objective providing a 100x magnification (1.36 μm pixel size).

A magnification of 5x and 10x was used to examine internal structures and to differentiate phases. Overview images of all the samples were made with an implemented stitching tool. By defining the corners of the sample, the software set up a grid covering the area between these corners. The grid consists out of cells, adjusted in size by the magnification set, which was in this case 5x. For each cell a picture is taken with a certain overlap with the previous cell. Once all the pictures are made a stitching tool combines all pictures into one overall image. The time for obtaining these pictures is around 15-20 min.

3.3 Automated Microscopy

Analysis using the technique and instruments of automated mineralogy were done on The ZEISS Mineralogic Mining system at Cambridge and the university of Liège . A short training was given at the ZEISS Natural Resource Laboratory in Cambridge, UK. Where after a four week internship period started. During the internship the microscope was used to analyses a first set of sliced samples in detail. The same system and set-up is emplaced at the university of Liège. Here data generation was continued and voids in the data were filled. In contrast with the system in Cambridge the microscope at ULg is equipped with a Micro-XRF (x-ray fluorescence).

Figure 3.3: Image showing the Axio Imager. Z2M and the Mineralogic SIGMA VP at the ZEISS Natural Resources Laboratory, Cambridge.

3.3.1 Scanning electron microscopy (SEM)

Samples were mounted on ZEISS SEM sample holder and placed within the Mineralogic Mining SIGMA VP. The BSE detectors are emplaced above the sample. The SEM is equipped with two Bruker 6—30 detectors. Energy dispersive X-ray spectroscopy analysis was conducted with a field emission gun provided with a zircon tip shooting a Li-B beam. Light elements as below N can not be detected using the Li (B) detector. Figure 3.3 shows both the SIGMA and the light microscopy with Axio imager.

Back scattering images

Back scattering electron imaging is the result of a variety of elastic and inelastic collisions between electrons and atoms. When an electron beam interacts with atoms the trajectory is changed due to elastic scattering. The chance of electrons having an elastic collision with atom increase with its size. This means there is a higher probability that back scattered electrons reaches the BSE detector when interacting with a greater atomic number Z. An element with greater average Z, as for example gold, will correlate with a higher BSE intensity and a brighter display of phases, in contrast with for example silica with lower atomic number, showing a more dark area.
BSE images provide high-resolution composition maps displaying different phases. Depending on the scan rate and the magnification these images are mostly obtained instantly. It is used as a first analysis for phases differentiation and textural relationships. BSE images serves as a sample map for spot analysis. BSE images are based on only one variable, average Z, and so limited to a gray scale range. The brightness and contrast parameters of the detector can be changed to maximize the contrast between different phases (Egerton, 2005; Goldstein, 2003).

BSE images are used to create elemental composition maps using Energy-dispersive (EDS) detectors. Here a beam of electrons interacts with the different elements present resulting in a series of X-rays. The EDS detector separates the characteristic x-rays into an energy spectrum. By using a specific software, in this case Mineralogic or Bruker, the energy spectrum is analyzed and transferred in quantitative data. An EDS spot analysis provides the chemical composition of material for a specific spot the size of a few microns. Elemental composition maps can be made with EDS over a broader area giving the chemical composition for all the different pixels, with a per-determined size, in that area (Egerton, 2005; Goldstein, 2003).

Energy dispersive detector

An EDS detector exists out of a crystal that absorbs the energy of incoming x-rays by ionization. As a results free electrons in the crystals become conductive producing an electrical charge. The electrical voltage from this energy conversion is proportional to the energy of the x-ray and thus correspond to the characteristics x-rays of the element. The x-ray absorption then converts the energy of individual x-rays into electrical voltages of proportional size. Hence, the electrical pulses correspond to the characteristic x-rays of the element.

During a spot analysis this data is converted using a supporting software, in this case Bruker or Mineralogic, in a full elemental spectrum. An EDS spectrum is displayed as a plot of x-ray counts vs. energy (in keV). The energy peaks in this spectrum corresponds to the Kα or Lα keV values of the different elements. The software already makes an analysis defining the different peaks to certain elements. Manual adjustments can be done in Mineralogic and Bruker to add or remove elements. When all the right elements are found, the software will make automatically do a calculation based on the peak-height ratio relative to a standard to determine quantitative the chemical composition. This analysis can be done in only a few seconds. Bruker software makes it possible to maps entire images acquired with BSE through EDS. It can focus during analysis on specific elements and determine where these elements can be found in the image (Goldstein, 2003; Severin, 2004).

The energy peaks in the spectra are the result of X-rays generated by the emission

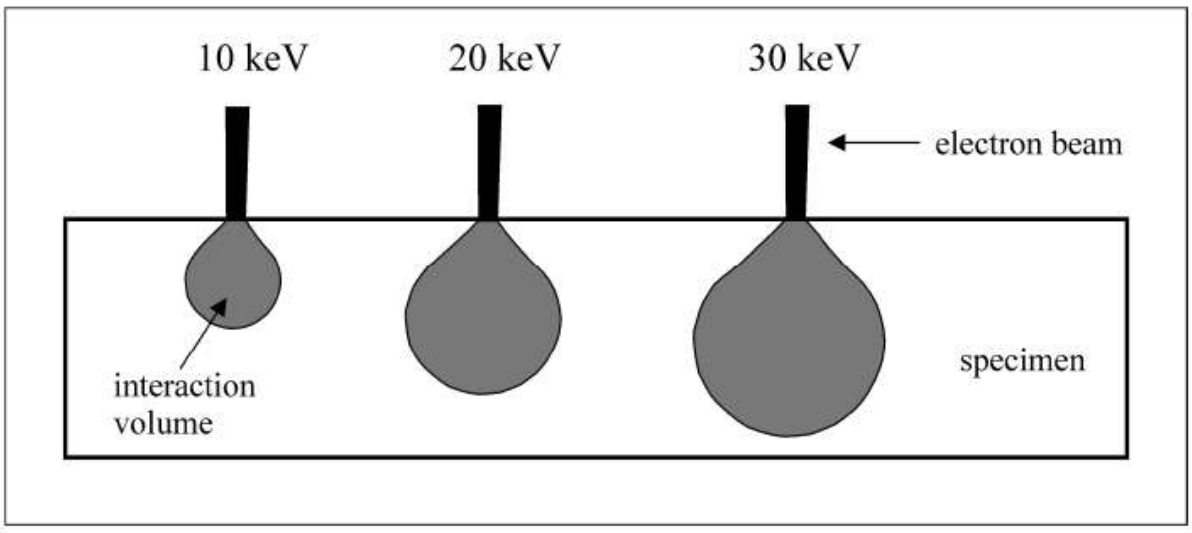

Figure 3.4: Interaction volume of the electron beam with different intensities after (Sandmann, 2015).

from electron moving to different energy-level shells (K,L and M). For some elements the energy values are very similar or there is a close overlap between Lα and Kα values resulting in a wrong designation of elements by the software. Therefore it is strongly advisable to control the existence of certain elements by controlling the spectra for second peaks (Kα, Kβ, Lα, . . .) or by checking continuation of the elements in a group of pixels.
The energy level used in shooting the electrons to the sample is of importance in the detection of the elements. These energy levels changes normally between 10 to 30 KeV. High Kev values results in a large range of X-rays emissions from the interaction with one of the electrons. This can be of importance in detecting elements with very large atomic numbers as for example Mo, which is only detectable when interacting with a high energy beam. On the other hand increasing the energy level also enlarges the interaction area with the sample. This could imply more noise or unwanted interaction with other elements as shown in figure 3.4. This may lead to hidden x-ray peaks for certain elements not resolvable from the background radiation (Goldstein, 2003; Severin, 2004).

3.3.2 Workflow

After polishing and light microscopy analysis, the samples were carbon coated for the electron microscope. The chamber of the microscope was first vented to lose it vacuum condition. The sample is placed in the mean time on a sample holder, which was a square-shaped metal plate. Once on top of the sample holder a silver or copper tape was attached on the sample to assure a good conductivity of the sample surface when interacting with the fired electrons. With the sample inside, the microscope chamber was pumped to achieve pure vacuum conditions. Once these conditions were reached BSE image can be acquired. By adjusting the brightness and contrast the most optimal scenario was found for displaying the different phases in the BSE images. The optimal resolution was found by adjusting the height of the sample while leaving the distance between the surface and the EDS detector constant at 8.5 mm.

Images from optical microscopy were used as a reference to easily locate certain zones brought in images with the BSE. Something mainly done on sight. It is possible to do this automatically. ZEISS has an implemented tool to transfer optical microscopical images and markings on it to the SEM. Based on a coordination system pin pointed locations are automatically brought in image under BSE. Point analysis were done with the eds detector to quickly analyze the chemical composition of specific areas. Based on images form the BSE quick scans could be made using the EDS detector from Mineralogic to map the different compositions in that images. These primary analysis by EDS made it possible to have an idea of the different compositions in the smartphone rapidly and are

used to built a preliminary classification system.

Classification list are defined by the different compositions analyzed and named accordingly. Each pixel analyzed is given an elemental composition with the EDS. This can be a pure mental, e.g Cu or a mixture of different elements, e.g Cu-Zn-Ni. Based on a set of criteria a group of pixels is defined under one name.The classified group is given a color. These criteria mainly exists out of a set of ranges for certain elements or can also exist out of the ratio of elements present in this defined group. For example, all pixels having a Cu % over 95 are defined in the group 'Cu'.

Once this preliminary classification system was built a macro was set up in Mineralogic. This macro saves the optimal bright and contrast levels, the classification systems built and the threshold defining to which extent pixel should be analyzed based on the brightness of the BSE image. After an area of the sample is selected to be analyzed and grid is set up to divide the image into tiles. Each tile is individually analyzed. All tiles are later compiled into one image. The pixel size for the EDS analysis is chosen depending on the time available for the analysis. In cases of 5 μm, preferably used to obtain more detailed, a sliced mobile phone sample could take 50 hours to be fully analyzed. This time was reduced by more than 50 % when assigning a pixel size of 10 μm. Therefor depending on the details in the samples a choice was made to either run the analysis for 5 or 10 μm.

Once the macro is finished, the classification could be adjusted and optimized using an offline system of Mineralogic. The goal when making the classification is to assign $>$ 95 % of the pixels analyses to a group. Each group was assigned a specific gravity constant. In case a group represents a pure metal this was fairly easy. However, in case of an alloy the situation proved not be ideal. In order to have a representative value for this constant the following formula was used:

$$\frac{a}{D_{alloy}} = \frac{Massfractionmetal1}{D_{metal1}} + \frac{Massfractionmetal2}{D_{metal2}} \ . \ . \ .$$

An schematic overview of the workflow is presented in figure 3.5.

Additionally to Mineralogic the Bruker Software was used to better understand more difficult and specific composition. Using Bruker Software analyses were done both in spot as map EDS analysis. Before using the Bruker software a standard is examined to calibrate the software. Micro-XRF is an additional spot analysis with a larger intensity than EDS. μ-XRF proved to be more accurate of examining trace elements as REEE. The diameter of the spot analysis is larger (+/- 40 μm) and has a penetration depth above

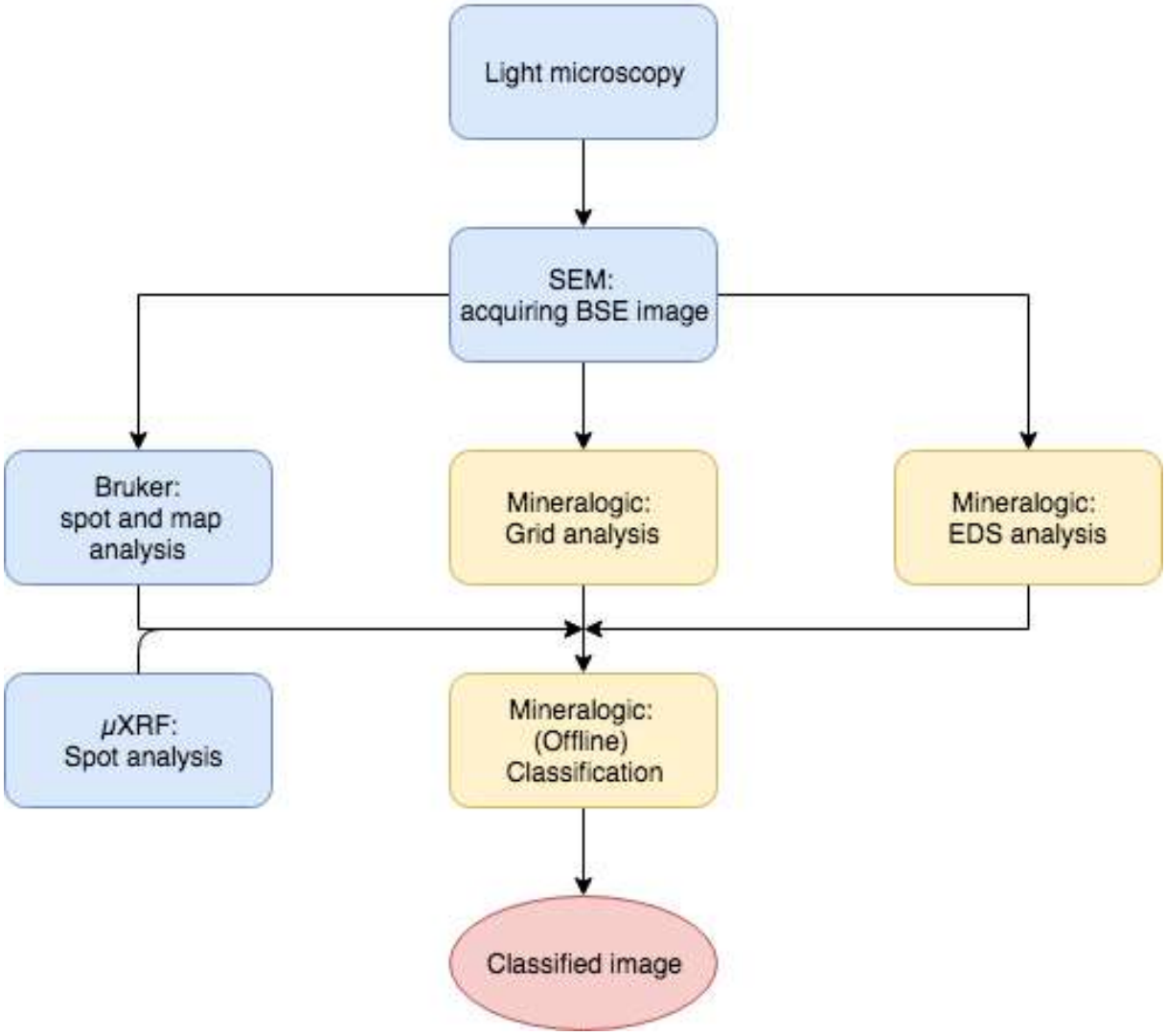

Figure 3.5: Schematic overview of the workflow.

80 μm. Information from both methods is used to improve the classification and adjust information acquired by Mineralogic.

Chapter 4

The inside of a smartphone

4.1 Sample generation

FROM of the parallel slices prepared, 9 surfaces were selected for polishing. The polishing surfaces are indicated in figure 4.1 where the arrow points towards the surface of the slice. The first slice is on top of the smarthpone cross-cutting just above the PCB and through the 3.5 mm headphone jack. Slice 2, 3 and 4 are intersecting right through the PCB. Most the PCB is capsuled by a metal frame. The surfaces of slice 2 and 3 are both located at the same cutting line. During sawing 3 mm of material is lost. To ensure the most interesting zone are analyzed it was decided that over 3 mm in the PCB the alterations are worth capturing. Hence, the selection is made to guarantee more or less a representative study of all aspects of the PCB.

Slice 5 is still cutting through the PCB but also through the middle of the main camera. Slice 6 is a section just aside the PCB. Between slice 6 and 7 there is relatively wide open space, for the battery holder, and is left out of this research. This area exists solely out of aluminum as a framework to hold the battery. It was therefore decided that examining one slice (7) is enough to understand these features in order to reduce costs and time. Slice 8, is slicing through the speaker at the bottom of the mobile phone. The last slice (9), is at the upper bottom of the smartphone and does not cross cut any particular features at first site.

The description of the results is divided in four parts. In the first part the PCB is discussed using slice 2,3 and 4. In the second part, the transition from PCB to the battery holder through the camera is described using slice 5 and 6. The third part describes the bottom of the phone holding the speaker and the internal features between the battery holder and the bottom of the phone is discussed. Slice 8 and 7 are used to capture and

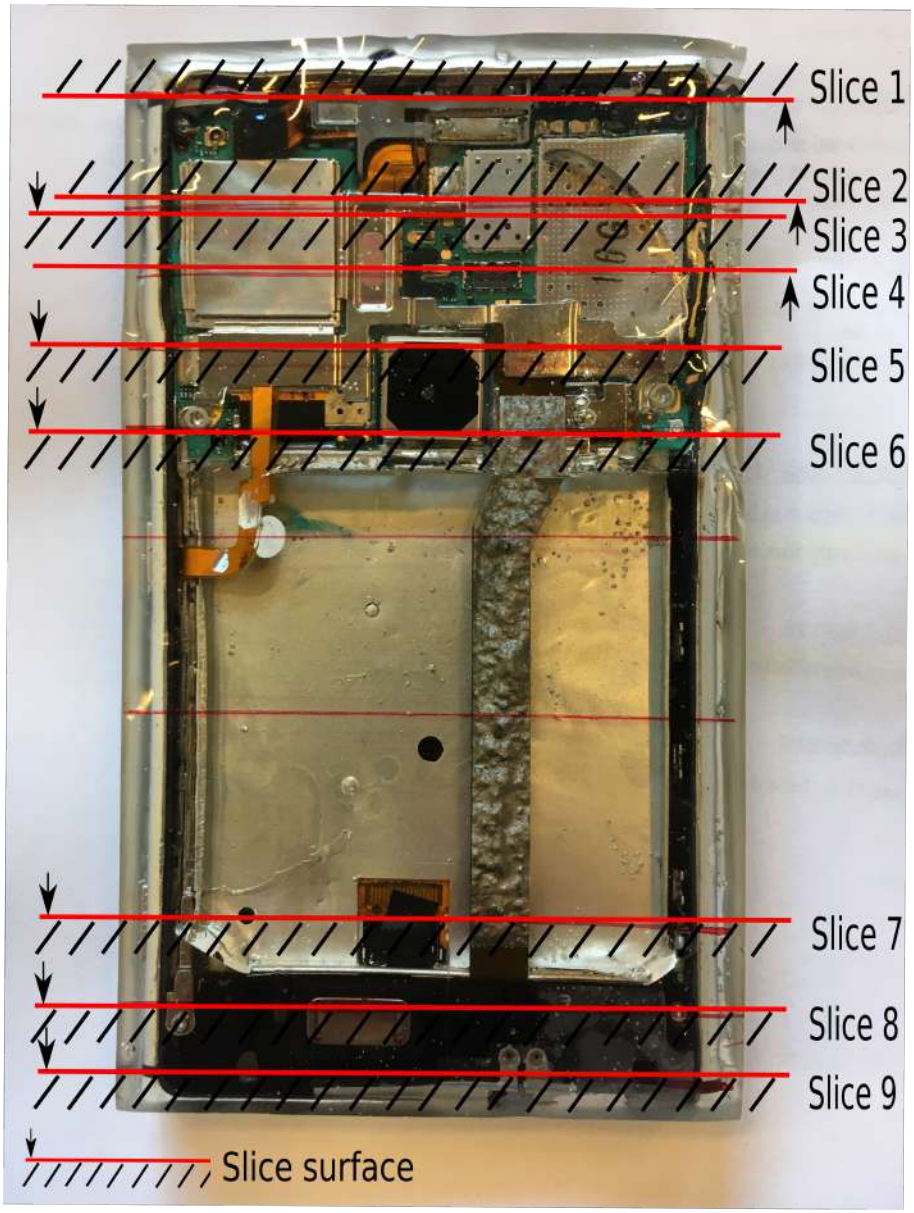

Figure 4.1: Marking of all location surfaces examined, the arrow marks the surface that was polished

examine this area. The final part discusses the edges of the phones at the bottom and top. At first sight they do not capture any interesting feature, but are considered worth looking at to make an overall overview of the phone. This will be done by approaching slice 1 and 9.

4.2 Printed circuit boards (PCB)

4.2.1 Optical microscopy results

In the first stages of the research light microscopical images were taken. Using a stitching tool detailed images of the whole slice were made. Figure 4.2 shows the light microscopy analysis of slice 4 using a magnification of 5x. Two detailed images from the left and right side of the slice were made with a magnification of 10x. The orientation of the image is in that way that the screen and touch panels are placed at the bottom of the images. They have a more darker color. The image shows how the PCB is enriched in a diversity of metals encapsuled by two yellow/white frames. A bunch of parallel plates are at the center of the PCB. On top or attached at the bottom of these plates several different structures are presents. They exist out of boxes containing different components. These containers have often a similar built but contain different components based on shape and color. These attached containers can become very detailed as can be found in figure 4.2 B. The figure demonstrate how at 1 mm several different components are waved within each other in 6 different colors, possibly implying 6 different metals or alloy types.

A trained mineralogist, could based on some typical colors identify some metals. A good example is copper that is highly present in these slices. The clear whitish yellow color makes it almost indistinguishable that all the parallel plates implicate the presence of copper. These analysis just give an idea but do not provide certainty as these copper could be in alloy with an other metal not able to detect solely based on color. Another example is gold typical for its bright intense yellow color. An example is given in figure 4.3. The figure is a detailed image from slice 3. The full results from slices 3 can be found in appendix.

4.2.2 SEM results

For each slice, BSE and EDS maps were produced using Mineralogic. Through the printed circuit board three slices were prepared and examined under the microscope: 2, 3 and 4. The result of such a slice can be seen in figure 4.5. Here both the BSE and EDS maps are shown. As can be noticed parts of the screens are not displayed in the EDS maps as these were not analyzed to reduce the analysis time. In case of the illustrated slice 3, the eds map was produced with a 5 μm resolution resulting in a analysis time of 50 hours. Slice 2 and 4 were mapped with a resolution of 10 μm and can be found in the appendix.

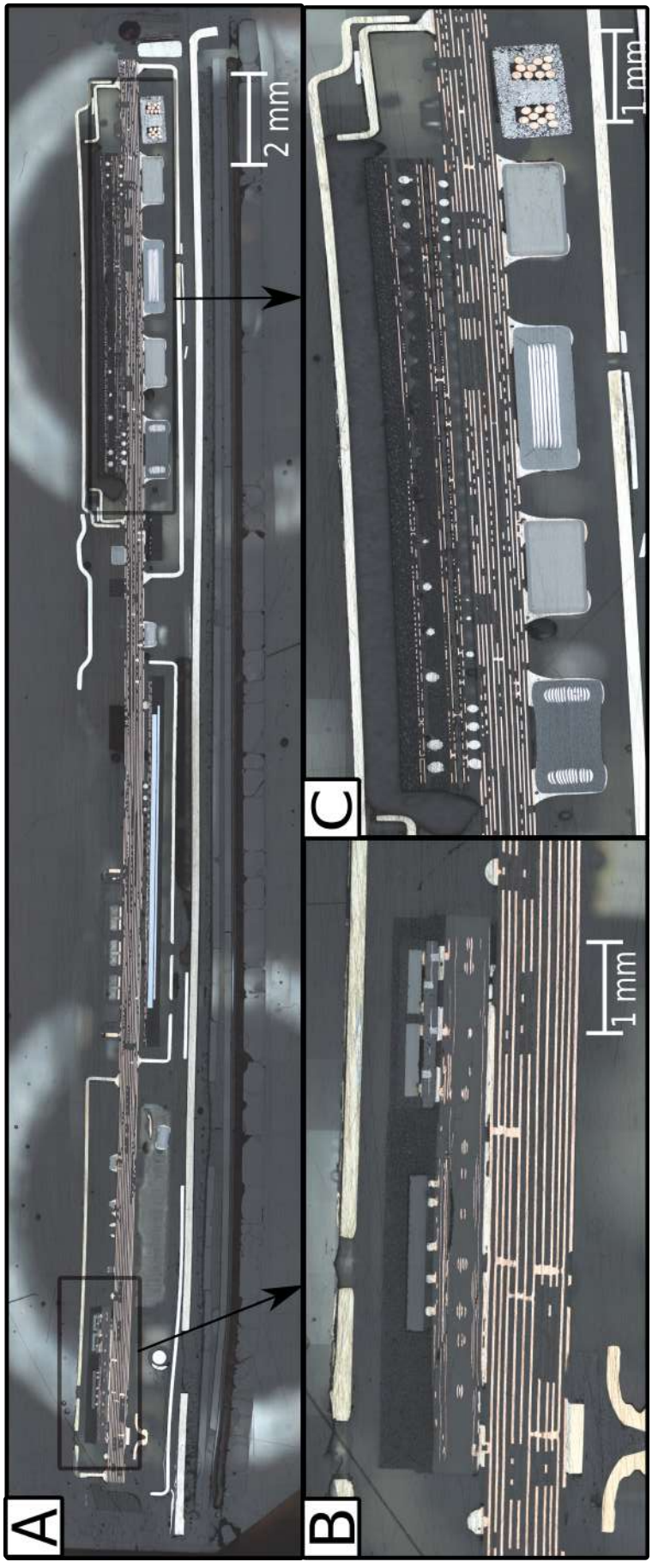

Figure 4.2: Optical microscopy image of slice 4. A: Overview pictures with 5x magnification, B: Detailed image of the left corner with 10x magnification, C: Detailed image of the right corner with 10x magnification.

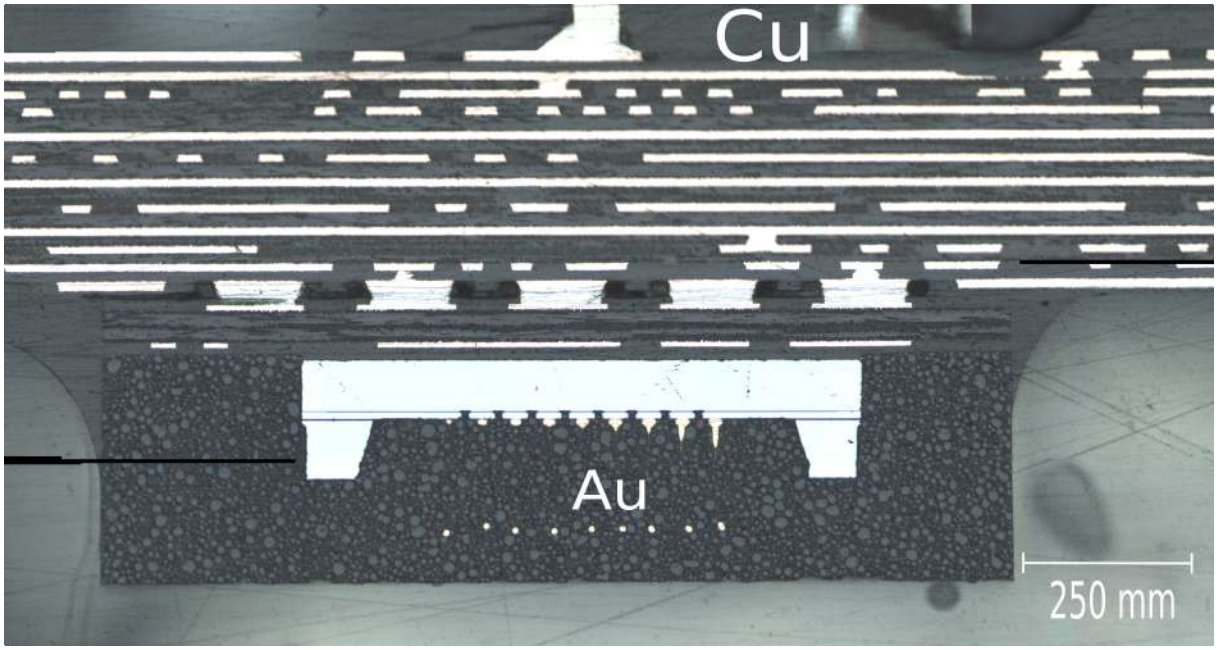

Figure 4.3: Detailed optical microscopy image from slice 3. It shows copper coloured plates but also pins and round shapes with a goldish colour. The full optical microscopical image can be found in appendix.

4.2.3 Components of the PCB

In the PCB seven different component groups were identified and are carefully described. First are the Cu plates and soldering. These exist out of several parallel plates, which are visible in orange in figure 4.5. On top or between these plates are round shaped components in a blue color. These are defined by the EDS as pure Sn. Additionally, often, although not as present as Sn, Ni is found as thin plates on top of the copper plates, often the Ni plates are lying at the upper top or bottom.

The second group contains the precious metals Au and Ag. These metals are found in a pure state. Au, marked in yellow, is mainly found quite isolated from other metals in ceramics while Ag, marked in dark blue, is often occurring in close contact with other metals and alloys. Au is not always visible in the overview images as the Au components are relatively small compared to the other components.

The third groups refers to boxes (or containers to put a name on the rectangle shaped components) found on top or below the copper plates containing a complex mixture of Ni and Ba-Ti alloy. They are characterized by a detailed whirling structures changing between Ni, dark brown and Ba-Ti, light brown. These boxes are surrounded by Ni, Sn and Cu.
The fourth group combines a set of different Fe based alloys. These alloys change in com-

position from Fe-Zn to Fe-Ni-Co. They are all marked with a darker blue or purple color. Hence, Fe is omnipresent but often as part of an alloy e.g. Fe-Zn-Ni. The fifth group are small boxes of around 250 μm containing the rare earth element Nd. Nd is present in the alloy Nd-Ti-Ba-O. Inside there are small wires shaped components of less than 2-3 μm consisting out of Pd. They are made visible in an intense red color with Pd as dark Blue, close to the color of Ag.

The sixth groups contains the critical elements Ta, Mo and W. They all occur in a pure state and often are found close to each other. The last group consists out of larger components visible in the overview image as capsules, ceramics and aluminum. Capsules are made out of an alloy existing out of Cu-Zn-Ni or aluminum. The latter is in general omnipresent often close to the margins of the slice. Ceramics, marked with a whitish color, is present all over the slice. Its composition changes but is mainly built around the elements Si, Al and O. The screens is also part of this group as it main compositions are the same as the ceramics.

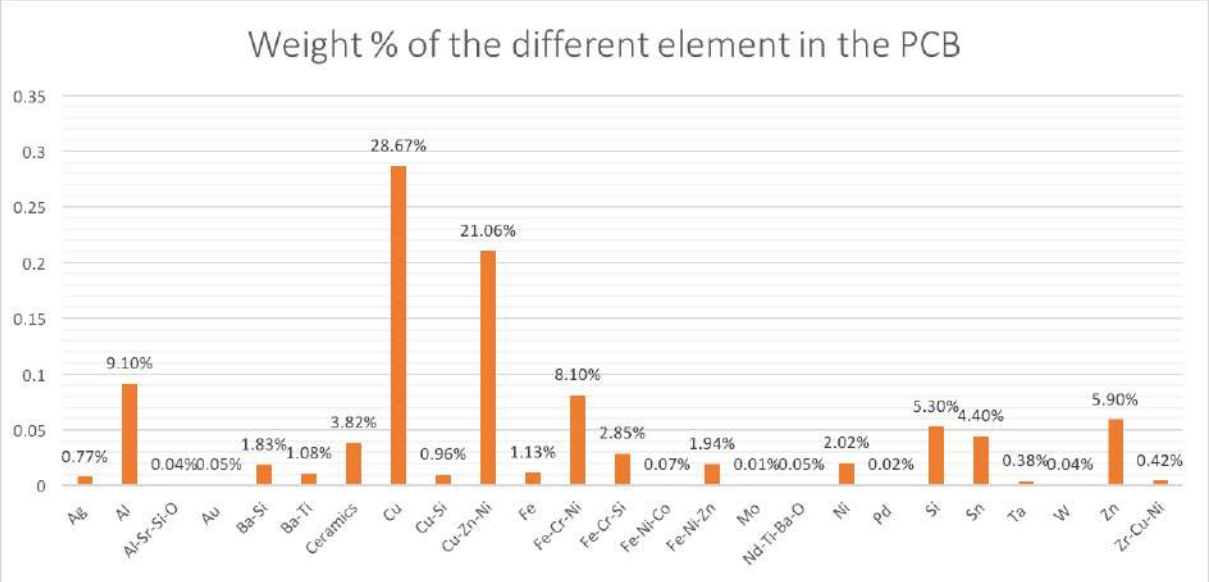

Figure 4.4: Average chemical composition in weight % of the sections crossing-cutting the PCB.

The average chemical composition in weight % in the PCB is given in figure 4.4. It solely gives an impression of the ratio between the different metals present in the PCB. It does not give any concrete notion on the quantities of the different metals present PCB. In no way these data can be compared with the other parts of the mobile phone.

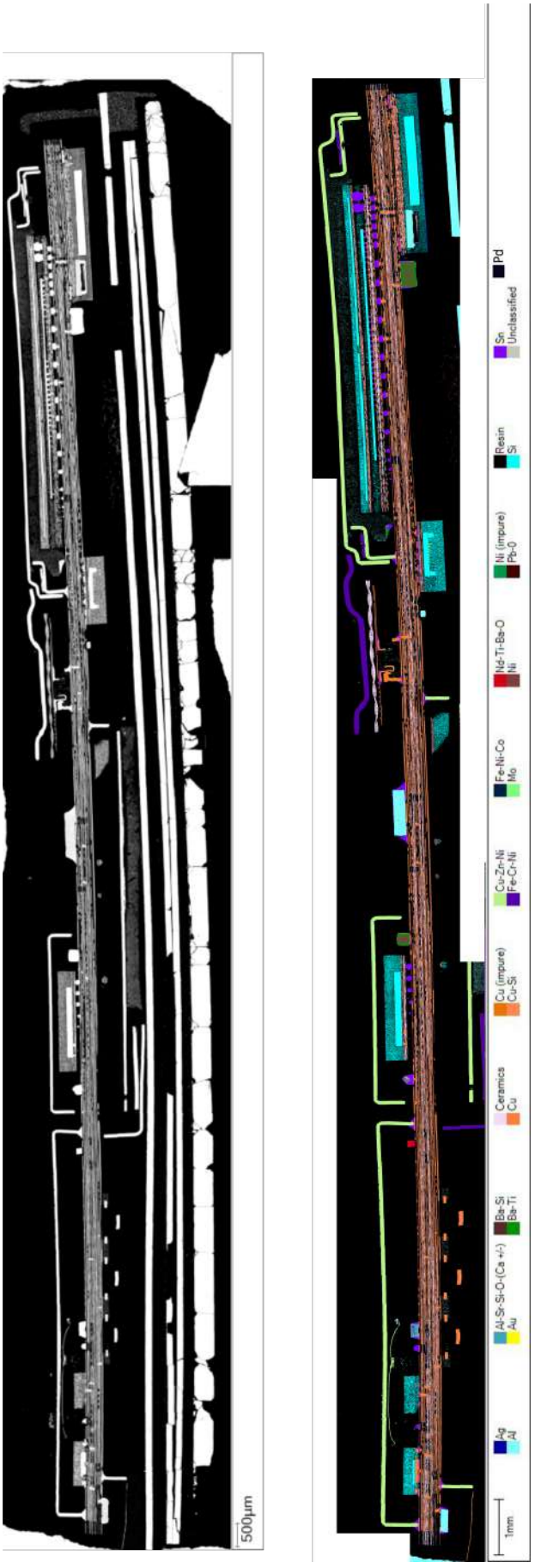

Figure 4.5: BSE and EDS map of slice 3

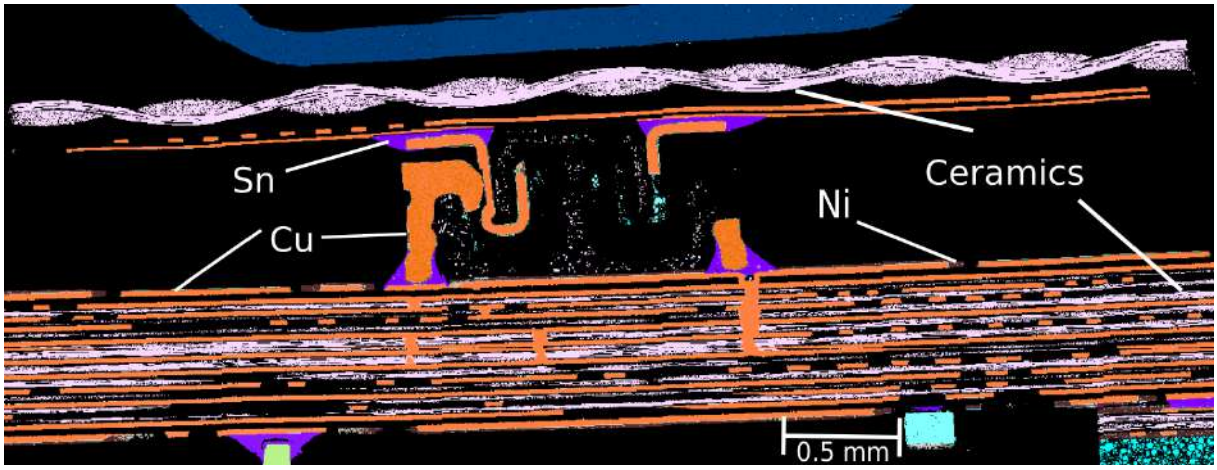

Figure 4.6: Detailed section of the PCB analyzed by EDS of slice 3

Copper plates

A detailed pictures of the copper plates is shown in figure 4.6. The plates are visible as parallel lines with in some places more than 10 plates on top of each other. The copper within these plates is defined as a pure metal. In Mineralogic this means all pixels existing for 90% or more out of copper. Statistical data from Mineralogic shows that between 65 to 70 % of the copper in PCB is found in a pure state (the remaining fraction is found in alloy). Sn and Ni are often attached to the surface of the copper plates. The first mainly as round shaped bulbs or types of soldering between the plates or other attachments on top of of below the copper plates. Sn is always present in a pure form, never in alloy with other elements. The second element, Ni is present in mainly in horizontal thin and short layers. They are found sticking to the copper plates and often marks together with Sn the transition from copper plates to other components attached to the copper plates.

In some cases pixels are classified as 'impure'. This means that there is unclear zone which can not for sure be defined as one of the three metals. For instance when a Ni plate or a Sn bulb are placed next to a copper plates the border between is often defined as 'impure'. The Cu, Sn and Ni in these pixels represents less than 0.5 % of all Cu, Sn and Ni detected.

Precious metals Au and Ag

The precious metals Au and Ag were both often detected. Mainly, Ag has been found in larger quantities. Of a whole slice the weight percentage of Ag was determined to change between 0.5 and 2 %, while Au varies between 0.1 to 0.05 %. Same as in case of Cu

and Sn both precious metals were found in native form. Au is mainly found a bit more isolated from other metals. Au is in most cases trapped in a Si rich matrix. An example is shown in figure 4.7. In the figure Pb was found close to gold and the silica. It was also the only place in the whole smartphone where Pb was detected. Pb has black color in the image. In case of slice 4, there is a detailed and complex area where Au was shown to be in close association with Ta, Mo and W (figure 4.10). Here Au was shown to be for 12 and 14 % attached to respectively the metals W and Ta.

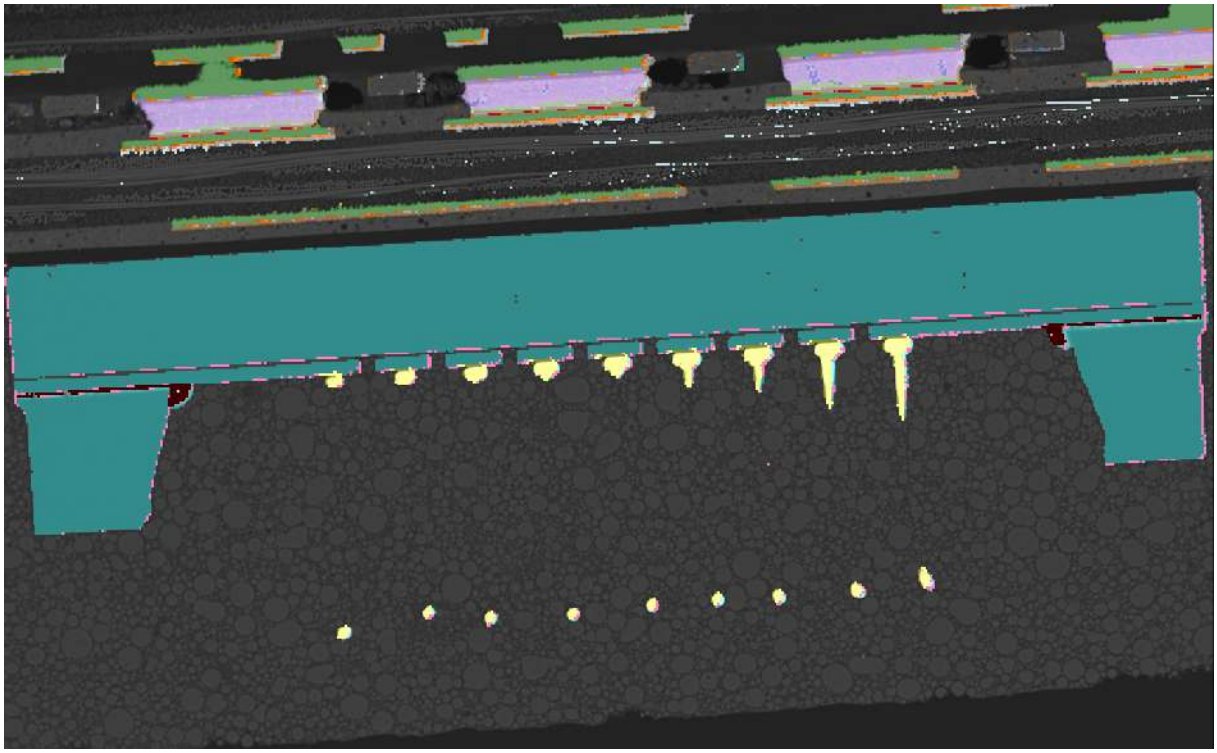

Figure 4.7: Detailed section with EDS of slice 3 focussing on an Au rich zone. The granualar background exists out of Si. This is the EDS maped version of figure 4.3.

The occurrence of Ag is more complex and closely linked to other metals. In case of slice 4, Ag is found in the presence of the alloys Fe-Ni-Zn and Fe-Zn. The container in which these two alloy types occur are surrounded by a thin line of Ag. As most of these rectangle shaped structures are surrounded by Ni and Sn, also these elements are in contact with Ag. In case of slice 2 Ag behaves much the same as gold by being isolated from other metals but is rather trapped within ceramics or a Si rich matrix. In Slice 3, Ag is in association with Al, the alloy Al-Sr-Si-O, Ba-Si, Ni or is present only within plastics or ceramics.

Nd-Ti-Ba-O alloy with Pd wires

Nd-Ti-Ba-O is an alloy detected in two places within the PCB (slice 3 and 2). It occurs in square shaped boxes quite isolated from other parts of the PCB on top or at the bottem of the copper plates. They are quite small with a average size of 250 μm. There existence was in first instance detected by normal EDS mapping using Mineralogic giving Nd-Ti as result. A detailed study with Bruker software using both detailed EDS mapping as spot analysis concealed the elements Ba and O. An overview of this detailed approach and results are given in figure 4.9. The Composition of the alloy is around 50 % Nd, 25 % Ti, 23 % O and 12 % Ba.

Within this alloy small wires of barely 2-3 μm wide are present. In the BSE they have a very bright color and are identified by the EDS as Pd.

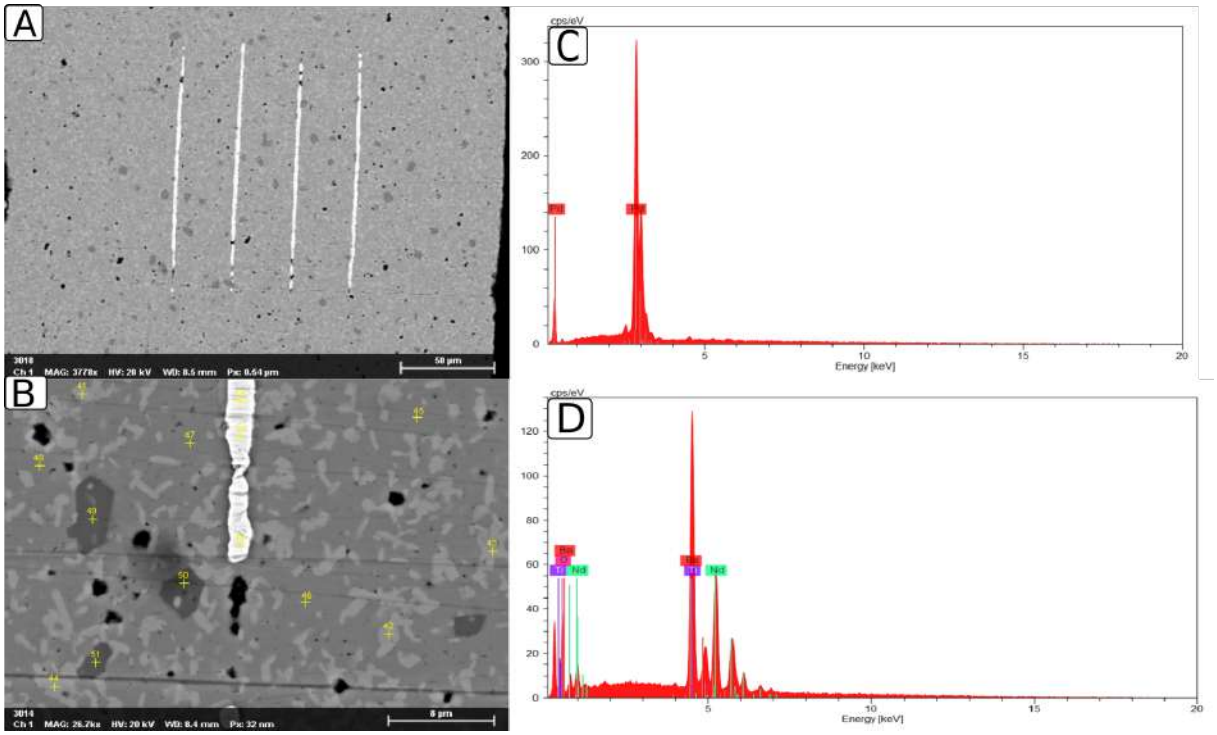

Figure 4.8: Detailed spot analysis with EDS using Bruker software on the alloy Nd-Ti-O-Ba and the metal Pd. A) BSE image of the container mapped by Mineralogic as Nd-Ti. B) Detailed BSE image focussing on both the matrix as the bright structures. C) Spectrum of EDS spot analyis on the bright structure giving Pd as results. D) Detailed spot analysis on the matrix based on the image of slice B showing the elements Nd-Ti-Ba-O. All patches with different colors in the matrix gave the same results.

Complexes of Ni and Ba-Ti

Spread out over several places in the PCB rectangle shaped boxes are being attached to the copper plates or found isolated. All containers, typically in marked by the classification in a light and dark brown/green tints, exists out of a complex structure. Sometimes it follows a more whirling shaped patron and in other cases it follows a more horizontal patron. Over the three slices 12 of these structures were found. They are typically surrounded by Sn and covered by thin frames of Cu and Ni.

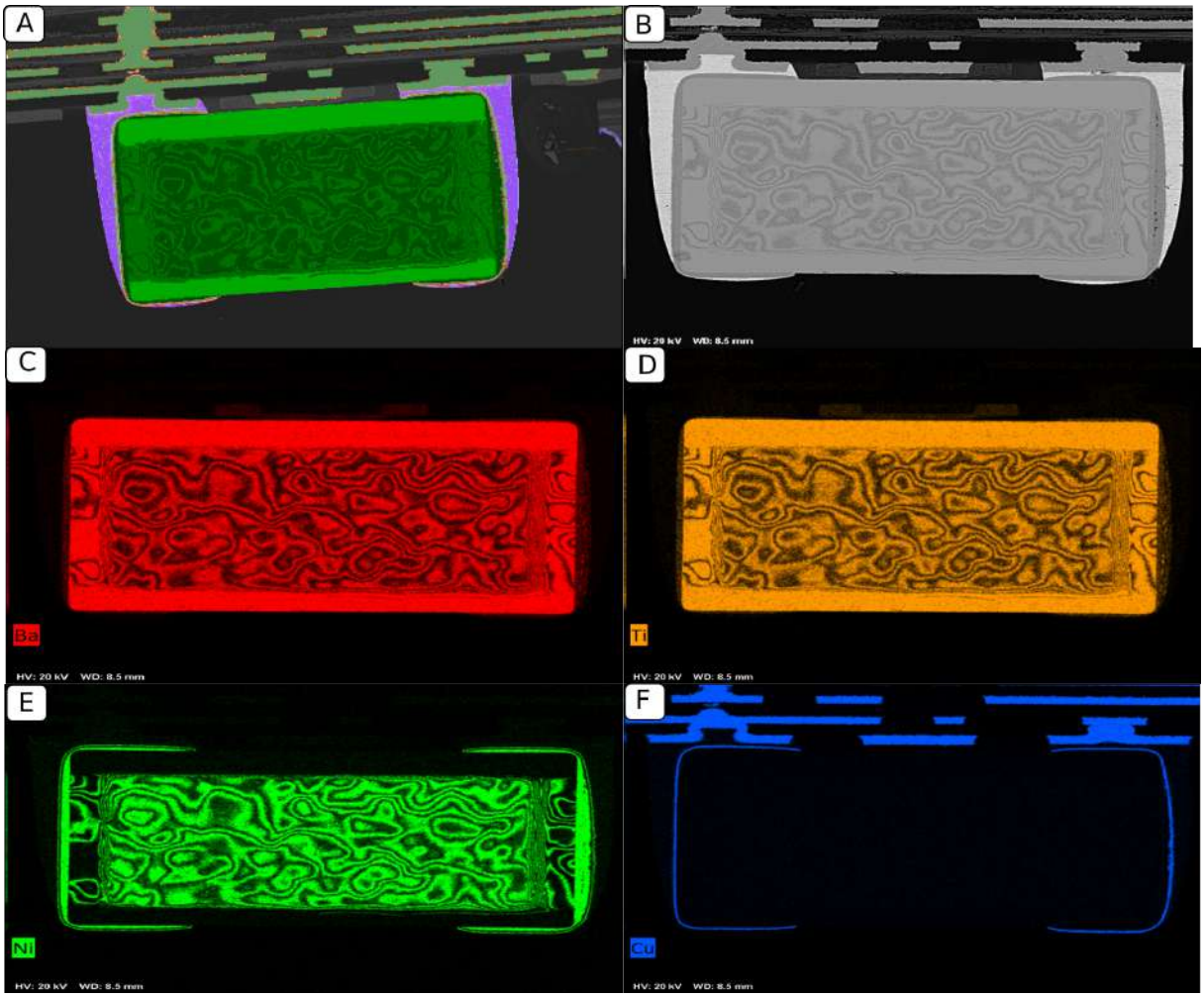

Figure 4.9: Detailed EDS mapping using Bruker software on Ni and Ba-Ti alloy. A) Mineralogic detailed mapping of one of theses containers defined by a wrong classification: Ni-Ba-Ti vs Ba-Ni-Ti surrounded by Sn (blue), Cu (orange) and Ni (Green) B) BSE images of that structure. C) EDS mapping indicating the presence of Ba in red. D) Ti shown in orange/light brown E) Ni shown in yellow. F) Cu shown in blue.

In a first analysis by Mineralogic, these structures were captured by specifying the alloy Ni-Ba-Ti on concentration difference of Ni and Ba. It was chosen that the alloy Ni-Ba-Ti was marked in a dark green and the alloy Ba-Ni-Ti in light brown/green. Hence, when

the concentration Ni was higher than Ba a pixel was grouped under the name Ni-Ba-Ti. The other way around for Ba-Ni-Ti defined by a higher concentration of Ba to Ni. Using spot and mapping analysis with EDS in Mineralogic the classification was proved right (figure 4.9 A). However, using Bruker with a very detailed approach the composition in these structures became more clear. At first, eds spot analysis was done around 1 μm to see the difference between Ba-Ni-Ti and Ni-Ba-Ti. The results show that when choosing a spot well within Ni-Ba-Ti, this was analyzed as pure Ni but analysis at the edges with Ba-Ni-Ti it gives back a mixture. A spot analysis well within Ba-Ni-Ti was analyzed as Ba-Ti. It also have to be expressed that these analysis were done with 20 Kev, while the mapping analysis in mineralogic was done at 30 Kev.

It is most likely that pure Ni was sputtered or coated on top of the alloy Ba-Ti. The result gives a very thin layer of Ni on top of Ba-Ti, with an hazy boundary. When analyzing in a lower resolution and with a large energy beam (30 Kev) this results in a too large interaction surface and volume resulting in measuring the elements Ni, Ba and Ti at the same time. A detailed mapping analysis conducted in Bruker makes the situation more clear. The result is given in figure 4.9. It shows how Ni colors the areas where Ba and Ti are not detected and vice-versa. It also shows in figure 4.9 F and E a small frame of Ni and Cu surrounding the structure. 4.9A shows in blue how Sn covers the structures and forms the transition between the copper plates and the copper components.

Fe based alloys

Fe is quite abundant in the PCB and is present in a relatively high amount of different alloys. A table with all the different components and its average composition is given in table 4.1. The average composition is a statistical result from all pixels being placed in the same group defined to a particular alloy. This means that for pixels the wt % of each elements can change but as entrapped within certain ranges are all defined to the same alloy. The average composition gives one value with a standard deviation of 20 %.

Fe-Cr-Ni is an alloy found in parts of the capsules surrounding the PCB. The alloy is not attached to the copper plates but is rather present as metallic components surrounding the PCB. Fe-Cr-Si happened to be the composition of a holder encapsulating copper wires, as seen in slice 4. The alloy Fe-Ni-Co is observed only at one particular place (Slice 3). It has been the only place where Co was found within the phone. The alloys Fe-Ni-Zn and

Fe alloy	Fe %	Cr %	Si %	Ni %	Co %	Zn %	O %
Fe - Cr - Ni	73	20	/	7	/	/	
Fe - Cr - Si	89	8	3	/	/	/	
Fe - Ni - Co	54	/	/	29	17	/	
Fe - Ni - Zn	57			14.31		13	13
Fe - Zn	56					26.5	13.5
Fe	100						

Table 4.1: All Fe alloys detected within PCB and their average chemical compositions.

Fe-Zn are present within the same structure/container. Within the Fe-Ni-Zn alloys small lenses shaped structures are mapped parallel above each other in two different columns. These lenses exists out of pure Ag. Within this structures there are small parallel lines crossing the internal components and enclosing the Ag lenses. These lines exist out of Fe-Zn. These are neatly mapped in the right hand side of slice 4 (see appendix). When looking at the BSE in detail the same structures are visible, with the lines being a bit darker than the rest of the matrix. Pure Fe is only found as sole component of a screw visible in slice 2.

Ta - Mo - W

Ta is found in two locations within the PCB. In slice 2 it is found in the right corner well isolated from other metallic parts in the PCB. Ta was enclosed entirely by ceramics. Close, although not in touch a small W wire was detected of just a few μm. Also, this wire was completely isolated from other metals by ceramics. However, the structures of the ceramics was more compacted and fine grained in comparison with the ceramics surrounding Ta. The Ta block is around 8 mm long and 1.5 mm wide.

In slice 4 (figure 4.10) Ta is present in two structures similar as described above. They are located next to each other. They have about the same size (8 x 1.5 mm) and are, as in the other case, surrounded by ceramics. In contrast to the other sections there is close contact with other metals at the two outer ends of the base of the Ta block. In both cases gold is attached as a sort of link to other metals. Directly attached to the gold is W, present as thin wires. They connect the bulb like structures of Mo with Au. Again a wire made out of W is used to connect these parts of Mo with Sn.

The image (figure 4.10) was obtained after running an analysis setting up a field analysis in Mineralogic at a resolution of 2 μm on the left hand side of slice 4. It does indeed provides more detailed results. However, analyzing a full slice at 2 μm could easily result in analyzing time of more than 100 hours.

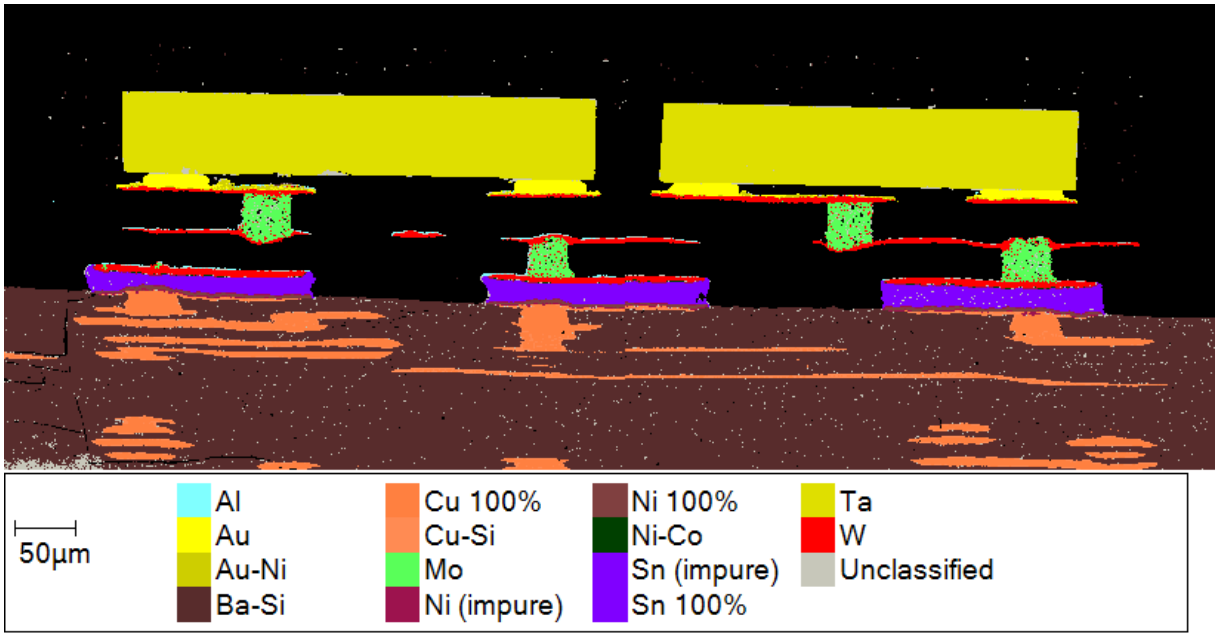

Figure 4.10: Detailed EDS mapping using Mineralogic on a small section out of slice 4.

The element O was detected in some of the pixels within the Ta boxes. There could be several reasons for its occurrence. It could have been that when building the phone both Ta and O is used. This is less likely as many of the other pixels are detected as pure Ta. Another explanation could be that an oxidation process occurred caused by time, decay of the phone or during preparation (e.g. during polishing) of the samples.

Capsules, ceramics and aluminum

Ceramics are found between copper plates, around and often en-capsule other components of the PCB. The composition of the ceramics changes but shows how three elements regularly are coming back: Si, Al and O. Additional to this composition one element with a weight distribution of around 10 % is part of this. This could be either Ca, Mg or Ba. Aside these ceramics also pure Si is present within the phone. Si is often existing in square shaped phases surrounding parts of critical or precious metals as gold for example.

The PCB is mainly surrounded by Al or the alloy Cu-Zn-Ni. Based on the slices Al can take up to 12-13 % of the wt% of all components analyzed. This is even more for Cu-Zn-Ni which lies around 22-23 %. 29 to 34 % of the Cu is present within Cu-Zn-Ni in the sections slicing full PCB parts. All Zn can be found with these capsules and around 70 % of all Ni is there as well.

4.3 Camera and surrounding PCB

Slice 5 (figure 4.11) provides data on two different components of the phone: the camera and the PCB. The latter is not directly attached to the camera but is more solidly built around. The PCB shows very similar components and structures as discussed here above. However, certain new components and elements were detected. Also the camera contains element not yet detected. The different components are presented in figure 4.12.

4.3.1 Precious metals

Au is observed in various parts of the the printed circuit boards. Right of the camera there are Cu square blocks on a certain distance from each other and all by two parallel from each. These blocks are coated by Cu and phases of Au can be found between these blocks. More to the right Au is again found coated on top of Ni and Cu. Below the camera 17 gold circles are detected trapped in ceramics, most likely a cross section through gold wires. The precious metal has also been found as a thin layer around a Fe-Cr alloy component in the left hand side of the slice. In this side of the slice there is a block made out of Ga-Ar. On top of this block a layer of gold is detected trapped in Si. The layer has an irregular thickness with an oval shaped gold component just next to it.

A very thin layer of gold is positioned on top of some copper plates. There is no continuity nor patron in the detection of these coatings. There is a very small thin layer of Ni between Cu and Au. Detailed map and spot eds analysis with Bruker helped to understand how there are actually two different phases. Where gold is found on top of these copper plates Pd is detected. In these cases an alloy of Au - Pd is present, with around 45 % Au and 55 % Pd (figure 4.13).

Ag is detected as lenses within a Fe-Zn-Ni alloy. In slice 6, Ag is found as a coating around the camera. Aside being present as in alloy with Au, Pd is found in two other different phases. First, as a pure metal within a Nd-Ti-Ba-O alloy similar as discussed in the section on PCB. These structures has been found two times within slice 5. Second, Pd is found in alloy with Ag at the edges of these containers. In these cases, Pd is present as an alloy with the following composition: 60 % Pd and 40 % Ag.

4.3.2 Fe-Nd-Pr alloy

In the middle of the slice between two parts of the PCB the camera is situated. Here two large bars existing out Fe-Nd-Pr can be found with an average composition of 70 % Fe, 22 % Nd and 6 % Pr. In the overview images they have a green color and are surrounded

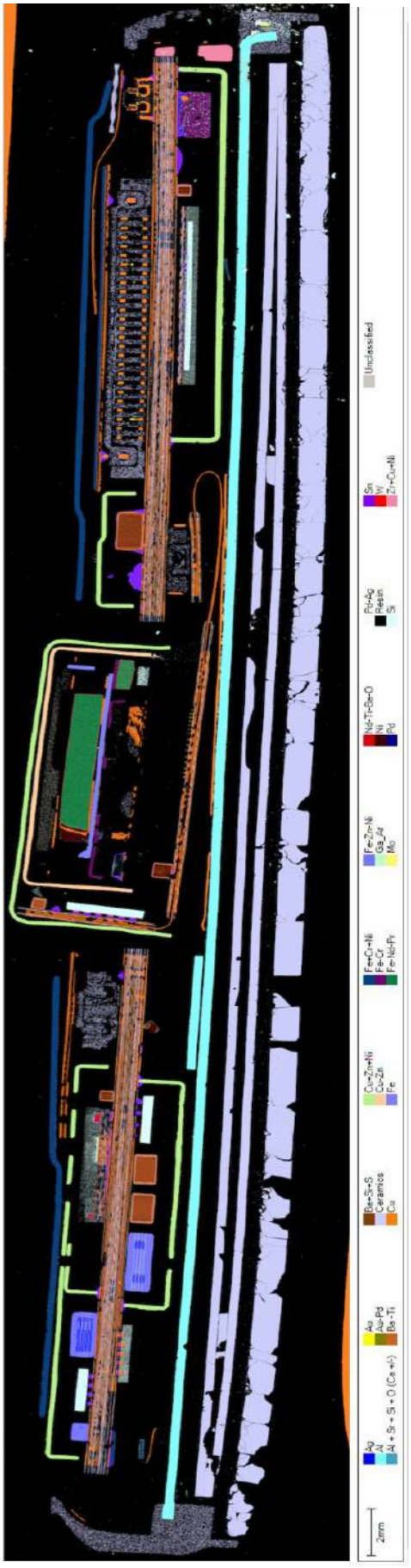

Figure 4.11: Overview image of slice 5 capturing the camera and the surrounding PCB. Light microscopy image of this section can be found in appendix.

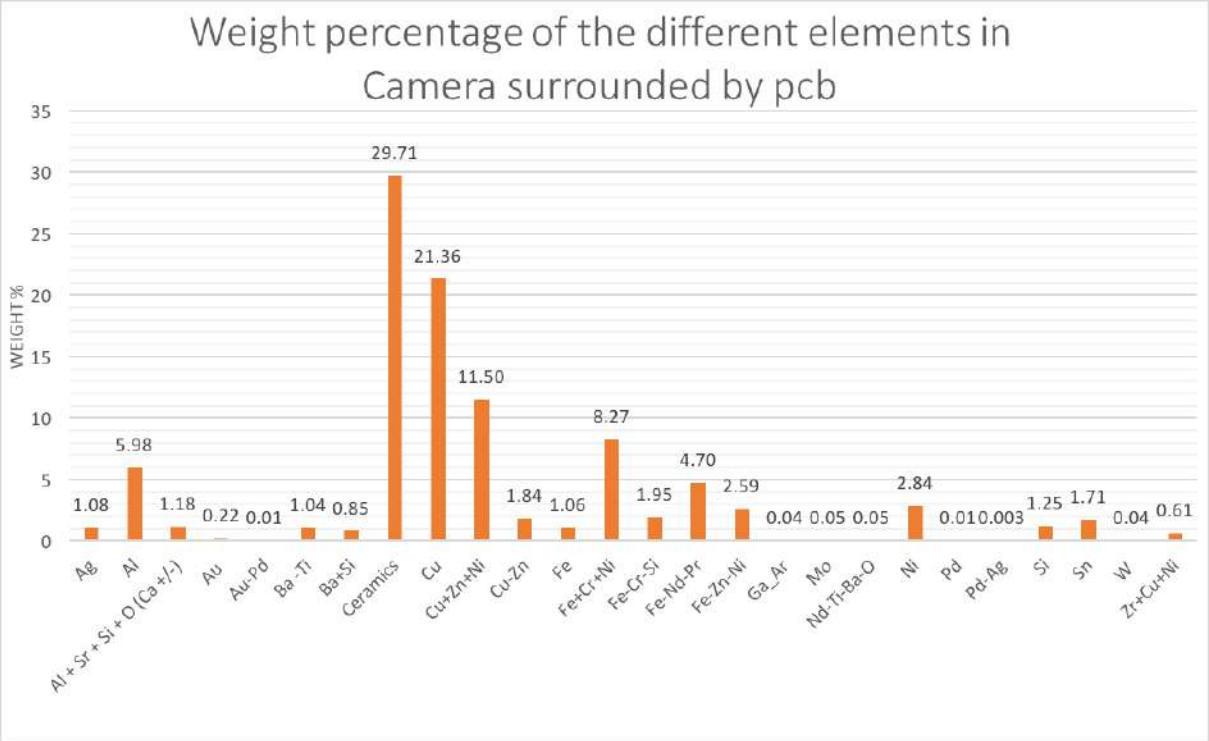

Figure 4.12: Average chemical composition (in weight %) of the camera and PCB surrounding the camera based on slice 5.

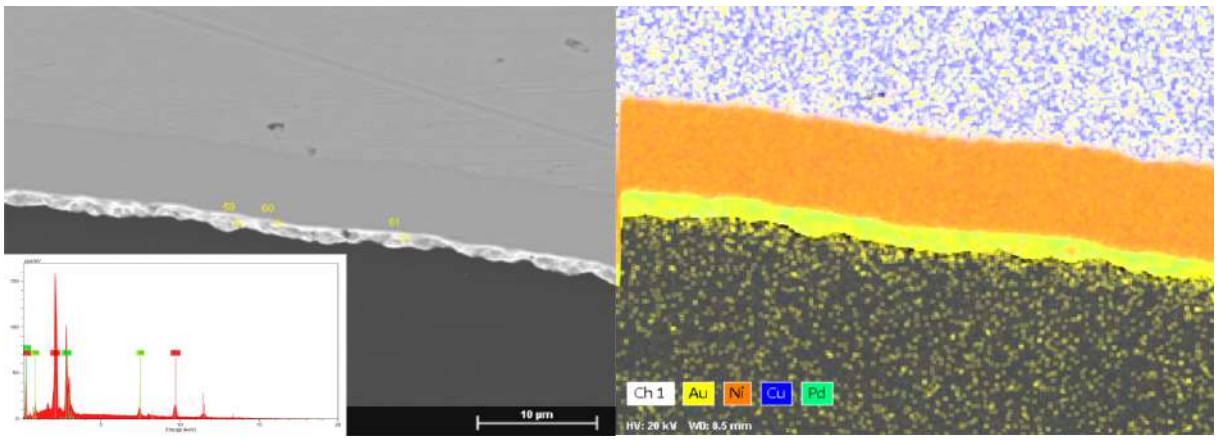

Figure 4.13: Detailed map and spot analysis with EDS using Bruker Software differentiating the phases Au, Pd and Ni.

by Ni and Cu. Between the two bars there are two other bar shaped phases consisting out of respectively Fe and Fe-Cr.

Although the whole phase is characterized as Fe, Nd and Pr this composition is not always detected. The Latter, Pr, is only in few cases analyzed with detailed spot analysis at 20 Kev. However as the magnets are defined as a continuous and homogeneous entity under BSE it is assumed that these magnets have the same composition: Fe-Nd-Pr. The

fact that the EDS can not detect always Pr is the result of a wide range of rare earths spectra falling very closely together. Hence, the software has problems defining the right element to the present spectra and often classifies these under the same name, which is Nd in this case. It is advised to use 20 Kev during analysis as this reduces the background noise. There is however another reason not to lower the Kev too much. These Fe-Nd-Pr have a strong magnetization effect deforming the images acquired from the BSE if the intensity of the beam is too low.

4.3.3 Critical metals

In the left hand side of the slice there is a part of the PCB, capsuled by Cu-Zn-Ni alloy, containing a variety of critical and precious metals. As mentioned before there is Ag in a Fe-Zn/Fe-Zn-Ni matrix hanging below the copper plates. On top of the copper plates there is a box made out of Si. Within this box there is a large Sn thick bar. After copper plates are following each other. In difference with the regular copper plates, these are fairly thicker and are more connected with each other. After 6 of these plates there is Ni bar marking the end of the sequence of copper plates. On top, there are three different components. in the left and right corner there is a small container consisting out of Nd-Ba-Ti-O with Pd inside. In the upper left corner this box is simply consisting out of the Nd-Ba-Ti-O alloy with Pd inside. It does not show any direct interface with Ni or other metals close by. In the upper right corner this alloy is entrapped within a more complex structure, more similar to the Ba-Ti and Ni alloy based structures spread all over the PCB. In this case Pd is again capsuled within the Nd-Ba-Ti-O alloy but also forms a thin line as capsule around the structure together with an alloy of Pd-Ag and Sn. Here Sn has a clear interaction surface with Ni and Cu. In the middle of the Si box there is a small elongated rectangle shaped component in a pale yellowish color. This bar is classified as Ga-Ar, respectively 55 and 45 wt %. The length of the box is around 800 - 900 μm and has a width of 50 μm. At the bottom a thin layer of Sn and Au separates these metals from the Cu plates. On top of the Ga-Ar bar Au is present.

In the right-hand side of the slice there is a large whitish beam placed under the copper plates. Close by a zone of both Al and W is detected during automated microscopy. A more detailed image using Bruker is made (figure 4.14). The image shows how detailed this section is on small scale. At the interface there are at least 3 different components lying on top of each other. There are Al blocks on top of a larger Si bar. The spectrum analysis combines the two elements as the penetration depth of the electron beam is high enough to both receive information of both components. On top there are small parallel lines with a darker color under BSE. They contain Ti. However it is hard to tell how

much interference there is with underlying materials. On top of these parallel line there are small rectangle shaped components with a space between each. They have a bright color with BSE mapping and the spectra results indicate the presence of W. Overall, interface with other elements makes it hard to distinguish the correct chemical composition and provide quantitative data.

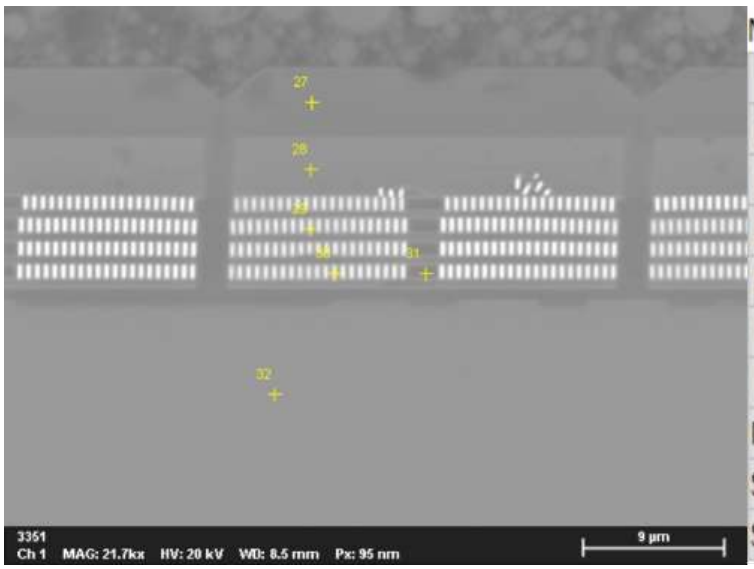

Normalized mass concentration [%]

Spectrum	O	Al	Si	Ti	W
27	45.51	3.41	51.08		
28		92.20	7.80		
29	17.42	16.99	10.90	5.85	48.84
30	20.80	11.38	10.20	4.62	52.99
32			100.00		
31	35.42	18.89	39.96	5.73	
Mean	**29.79**	**28.57**	**36.66**	**5.40**	**50.92**
Sigma	**13.08**	**36.07**	**35.85**	**0.67**	**2.93**
SigmaMean	**5.34**	**14.73**	**14.64**	**0.27**	**1.20**

Figure 4.14: Detailed spot analysis on W rich components and the surrounding elements in slice 5.

The screen in this sample is classified as ceramics and exists out of Si-Al-O-Ba. No other elements could be detected.

4.4 Speaker and bottom of the phone

The bottom of the phone is studied in slice 8 (see appendix). The different components are shown in figure 4.15. The internal structures do show some comparison with the PCB parts but are in general terms different. The most iconic component of these parts of the phone is a large rectangle shaped Fe-Nd-Pr metal bar in the left hand side of the slice. The composition is similar as to the parts of the camera. Also here the metal is enclosed by Fe. Fe it self is covered by a thin layer of Cu and Ni.

The slice is consisting out of many copper plates but in contrast to the PCB the position of these plates is rather irregular and often interrupted by bars of Fe-Cr, Al and Sn bullet shaped phases. Similar to slice 5, very thin layers of Au and Ni can be found on top or below the copper plates. In none of these case Pd is detected, in contrast with was found in slice 5. Gold is found irregular through the section as bullet shaped components,

most likely representing a section through gold wires. There is never any interaction with other metals.

Particular a lot of gold is present in the upper right corner on top of copper plates. Close to these gold components a small rectangle shaped component is found consisting out of Ga-Ar. The composition is the same as in slice 5. Also here there is a irregular shaped gold layer on top. Interesting here is that Bruker detects a very small wire of Pt (less than 1 μm thick) at the contact of gold and Ga-Ar.

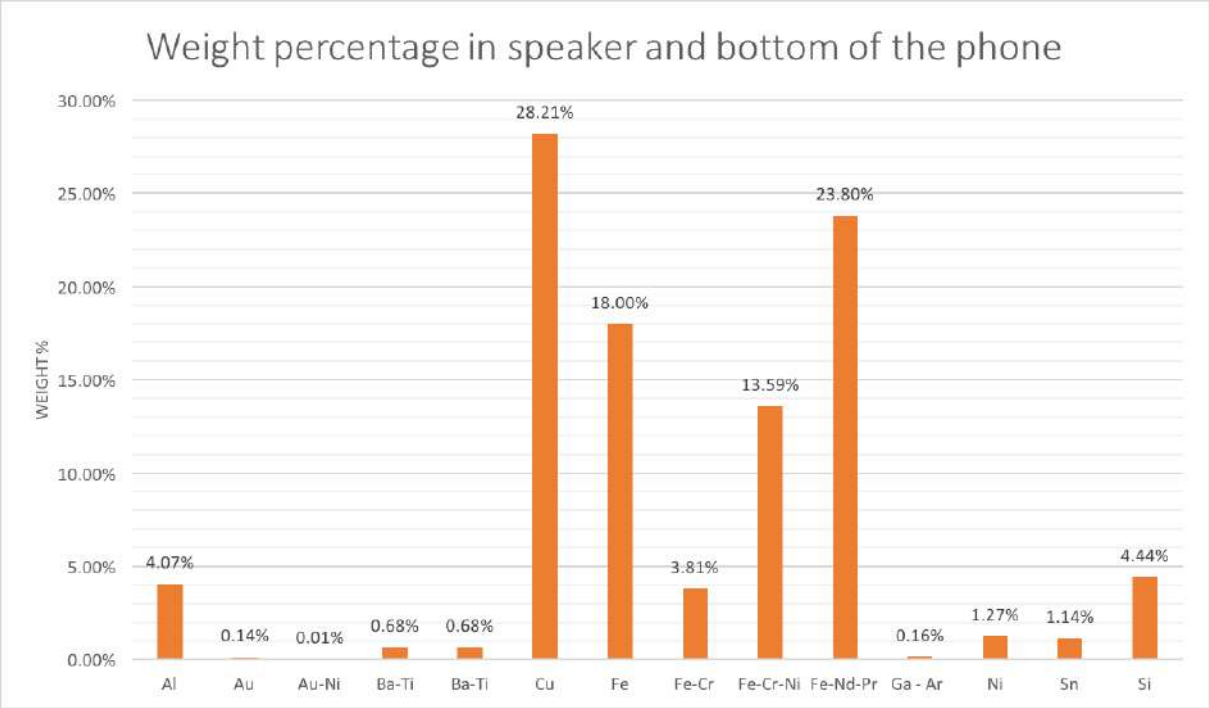

Figure 4.15: Average chemical composition (in weight %) in the bottom of the phone around the speakers.

Slice 7 does not provide any additional information.

4.5 The edges of the phone

The top and bottom of the phone are represented in slice 1 and 9 (results in appendix). The top (Slice 1) is mainly consisting out of resin or plastics and large homogeneous components: Al, Ceramics, Zn, Fe-Cr-Ni and Si. Cu is present as thin plates or wires shaped components. When Cu is in close contact with other metals as for example the alloy Fe-Cr-Ni the metals Sn and Ni are present as a connection between these two metals. Au is found only once in the upper part of the slice.

Of the bottom of the phone (slice 9) only a small area has been analyzed due to threshold values delimiting non-bright zones. What can be seen are Cu wires often in association with Ni. The alloy Fe-Cr-Ni is present as well. The most interesting component is a box consisting out Au, Cu, Sn, Ni, Si and ceramics. The whole frame work is mainly consisting out of ceramics with some copper and Nickel in between. Sn bullets are connecting Cu bars. Au is found in the middle as a thin beam and two golden bullets. The golden beams are on top of a Si made rectangle brought in connection with a thin layer of Ni.

4.6 μ-XRF results

In comparison with the radius of EDS Analysis the μ-XRF covers a much larger area when conducting a spot analysis. The diameter of a spot analysis with μ-XRF is around 40 μm. In comparison, EDS has a spot analysis with a diameter of 1 μm. This results in much finer and accurate resolution for the EDS. This is an issue for the phone components. In slice 3 there is a small box containing the alloy Nd-Ti-Ba-O and small wires of Pd. Examining with μ-XRF causes that the radius of the beam is too large to solely focus on one component (figure 4.16). This delimits the use of μ-XRF for sole investigation of certain components and receiving quantitative data. Many of the different metallic parts in the phone are smaller than 20 μm with close contact of other metallic parts.

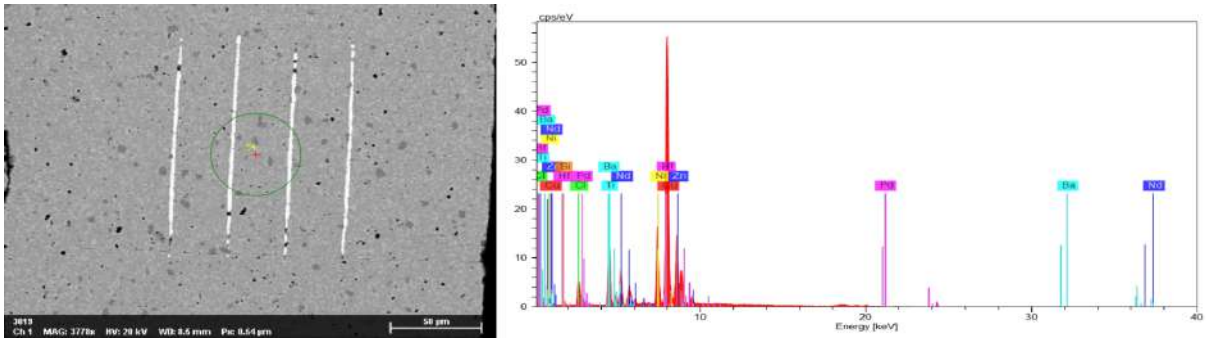

Figure 4.16: μ-XRF spot analysis on Nd-Ti-Ba-O with results given in a spectrum plot.

A similar situation occurs on vertical scale. The penetration dept is quite large with values between 60-100 μm. This cause interference with not targeted components in heterogeneous material. A smartphone is very heterogeneous and can have complete different composition within μm range. Hence, when the electron beam penetrates the surface of the targeted component it is often most likely that the beam will hit components beneath. As a results spectra are obtained containing a high variety of different elements, including non desired elements. Again the alloy Nd-Ti-Ba-O can serve as example. It is known from above description that parts of the PCB are encapsuled by a metal alloy made out

of Cu-Zn-Ni. When firing the Micro-XRF on the alloy Nd-Ti-Ba-O the elements Cu, Zn and Ni also show up in the spectrum results. Thus, it is assumed that the electron beam is penetrating through the Nd-Ti-Ba-O alloy hitting the surface of the capsule surrounding that part of the PCB.

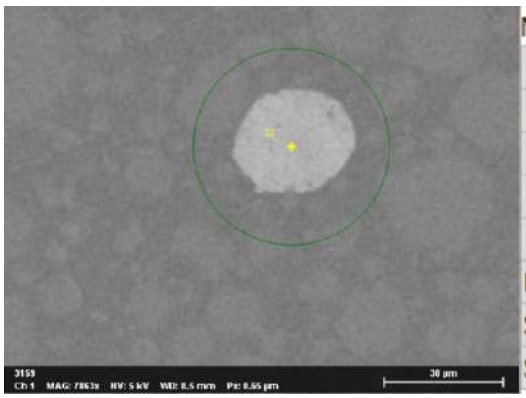

Normalized mass concentration [%]

Spectrum	Si	Au
28	89.25	10.75
30	99.13	0.87
31	94.61	5.39
32	94.24	5.76
Mean	**94.31**	**5.69**
Sigma	**4.04**	**4.04**
SigmaMean	2.02	2.02

Figure 4.17: Left: μ-XRF spot analysis on Au particle in slice 8, Right: Quantative data from several gold particles in its neighborhood, analysed with μ-XRF.

When the surface of the targets is extremely thin the obtained data from this surface could be lost due to all the information gained from the material below. That is to say that the peaks received from the surface are so small they disappear in the background noise of the obtained spectra of all the material under neat. An example is given in figure 4.17. It is known that gold particles are often within a Si rich substance. When analyzing these gold particles the spectra received does not include detectable peaks for gold as the peaks of Si are too dominant.

The Micro-XRF was mainly used to target compositions in order to confirm the different elements or to detect new elements not able to detect with the EDS, as for example REEE. Most of analysis were given unusable results as from above described reasons. Only in one particular case new results were found. In slice 8 the large Fe-Nd-Pr magnet was analyzed. Although it was known from slice 5, using EDS, that these components also consists Pr, it was not detected with EDS in slice 8. Using Micro-XRF Pr was detected with the same quantitative data as found by EDS in slice 5.

Chapter 5

Crushed smartphone sections

The crushed particles show a wide variety of different shapes and colors in the polish sections. Glass particles are making up most of the material inside, mostly as small glass splinters filling up voids between other components. For the BSE and EDS detector only the particles that are at the upper surface of the polish section will be analyzed. This results that of only a little fractions of a larger component is analyzed. An analogy can be made with the small top of an ice berg exceeding the surface of the water.

When shredding the phone the outcome was very heterogeneous. Plastic parts, having a more ductile character, end up still having a large fraction (> 1cm). Also metals embedded within plastic parts, like fractions of PCB, maintain a large part of their original structure. On the contrary loose metallic parts or glass are often reduced to below mm size particles. Hence, This fraction is easily spread as dust and lost.

5.1 Light microscopy

Light microscopy is a fast and easy method to follow up the results of shredding. Ideally, all components of the mobile phone were analyzed and classified during the analysis of the whole mobile phones, aka the slices. Thus, all components should be more or less be identified by their appearance under the light microscope based on their visual appearance. An example of an overview image is given in figure 5.1.

A lot of copper parts can easily be identified based on their color. But also, often recognizable structures as copper plates or wires could easily be spotted. It has to be said that these components are fractures and only exist out of a small fraction of their original structure. What also could be noticed is that the typical container-liked structure consisting out of Ba-Ti with Ni, Fe-Zn with Ag, Nd-Ti-Ba-O with Pd are easily detected.

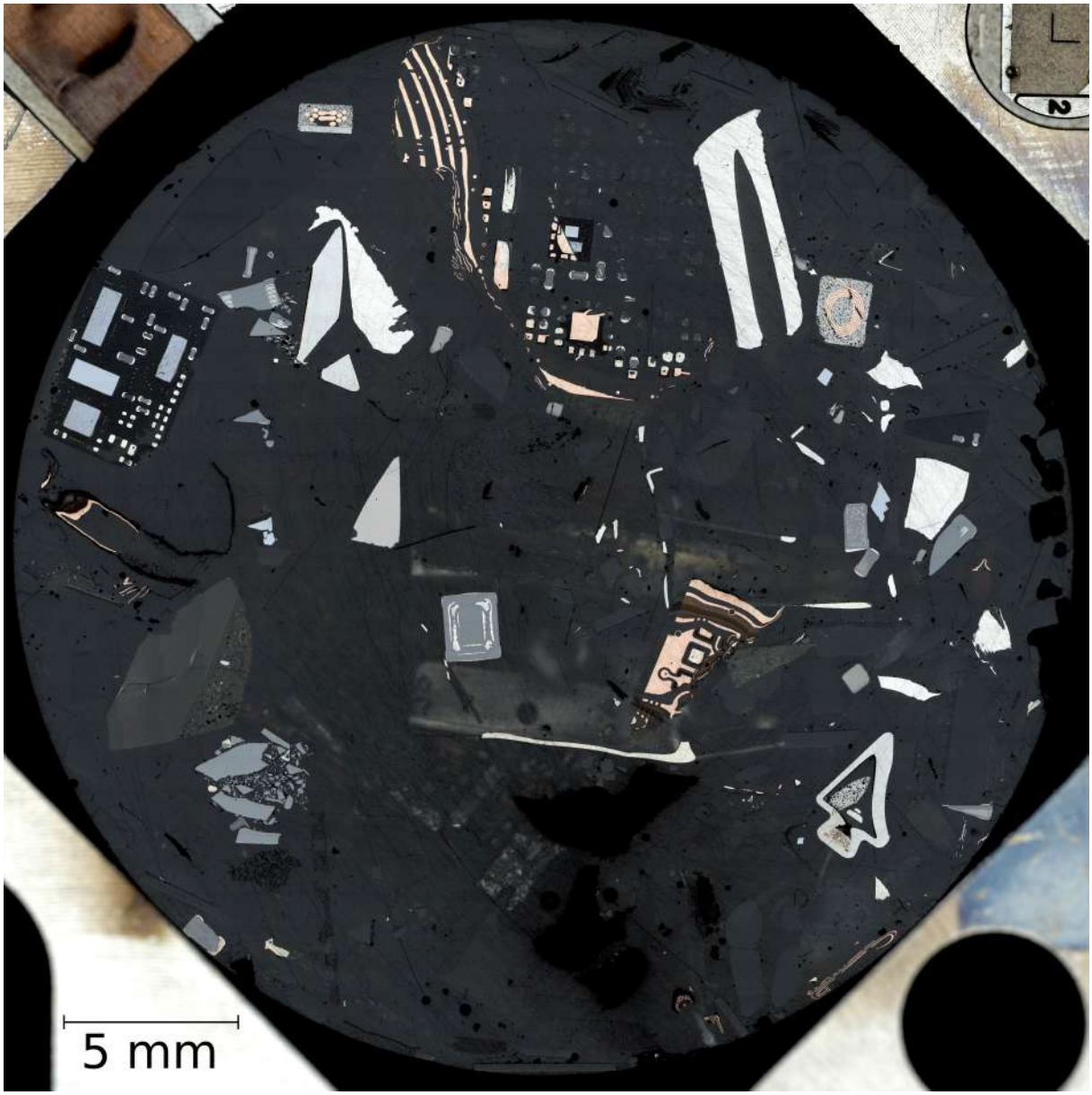

Figure 5.1: Overview image of crushed mobile phone particels under light microscopy (section 2).

Often the whole structure remained intact or just small corners or parts are gone. This makes it easy to retrace elements as Pd, Ag, Nd, Ni, Ba and Ti.

Au could be found relatively fast in the light microscopical images. However, there is a certain regularity to spot the precious metal. Au is always present in Si-rich boxes. Picture 5.2 is a good example how gold is entrapped in a Si rich matrix (having typical a darker color with a coarse structure). In some cases gold is found in association with one of these containers. This is similar to the situation of Ga-Ar where gold was found on top. Also, in this scenario both the Au as the box-like structures are embedded in this

Si-rich (or ceramic) matrix.

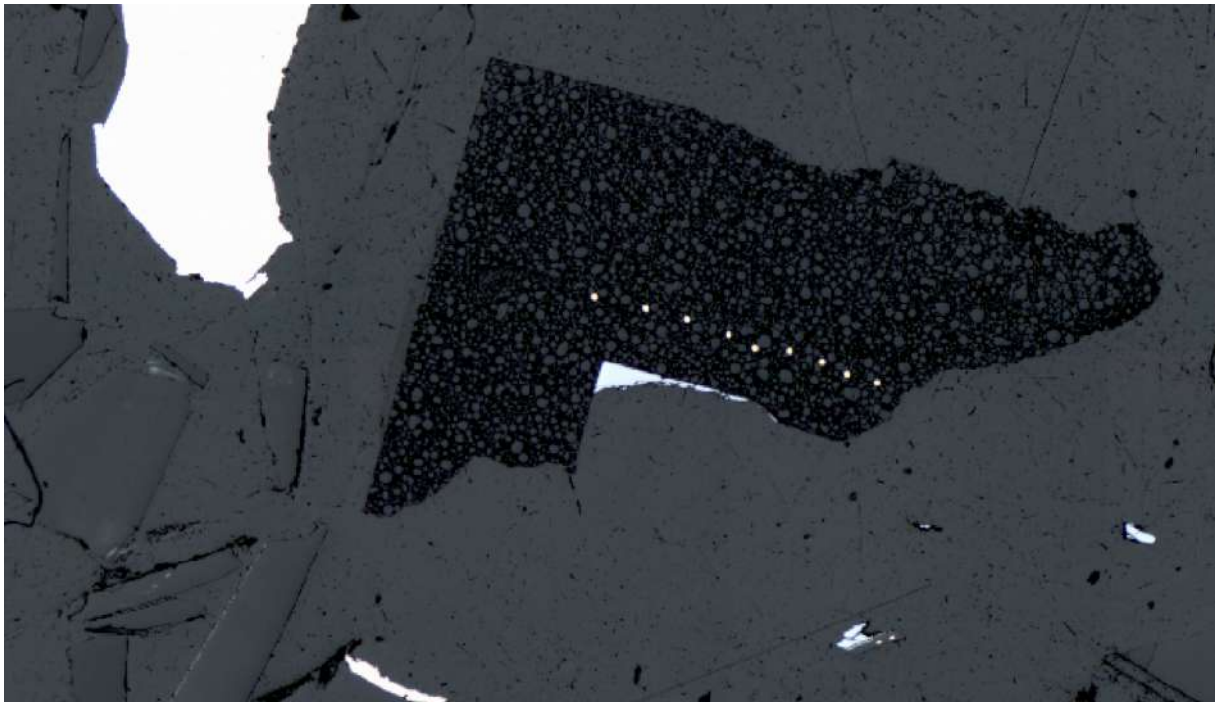

Figure 5.2: Gold particles embedded in a matrix consisting out of Si.

5.2 BSE images

BSE images were acquired with a brightness around 22 % and a contrast of 31 % to capture as much detail as possible of the different components. From the BSE it became clear how very bright particles as metals are in contrast with others, e.g. parts of screen, ceramics, silica etc . . .. This is used to set up a high threshold value in order to avoid analyzing non-metals. The main reason here is to reduce the mapping time of the section, as these are already mapped in previous analysis.

5.3 EDS mapping

A macro in Mineralogic was run to map the whole section. The final classification system obtained from the analysis of the slices was incorporated. Results showed that less that 5 % of the material analyzed was not classified. This is promising in that way that the classification can be used again and almost no new material is detected. The overview images were generated with a resolution of 10 μm. There are two reason not to choose

for a higher resolution. First, the material is already analyzed at 5 μm. Thus, the goal here is more to evaluate how the material behaved after fracturing and how Mineralogic captures these changes. Second, based on previous argument the time span is shorted which is an important parameter in this discussion.

Two polish section of about 3 cm diameter were fully analyzed using the grid analyzing method with Mineralogic. The composition map of section two is shown in figure **??**. The results of section 1 can be found in appendix. A relatively high threshold value was chosen to focus only on the metallic fraction. In both cases, the largest weight fraction detected was pure copper. In the first section 55 % of the material analyzed existed out of pure copper (figure 5.3). In the second section this was 28 % (figure 5.4). Cu is mainly used in copper plates in the PCB. In the first section, Cu could also be find back in Zr-Cu-Ni and Cu-Zn-Ni taking up respectively 11 and 9 % of the material analyzed. Ni is also quite abundant. It is for respectively, 11 and 5 % present in slice 1 and 2. Ni is present as a pure metal and in alloy as Zr-Cu-Ni and Fe-Zn-Ni. Ni is found mainly back as parts of the container structures alternating with Ba-Ti and as thin layers on top of the copper plates. Ba-Ti is highly present in the first section. In that sens most of the Ni is badly liberated with 80 % being trapped in Ba-Ti. In the second section Fe is the second most abundant metal with 24 wt %.

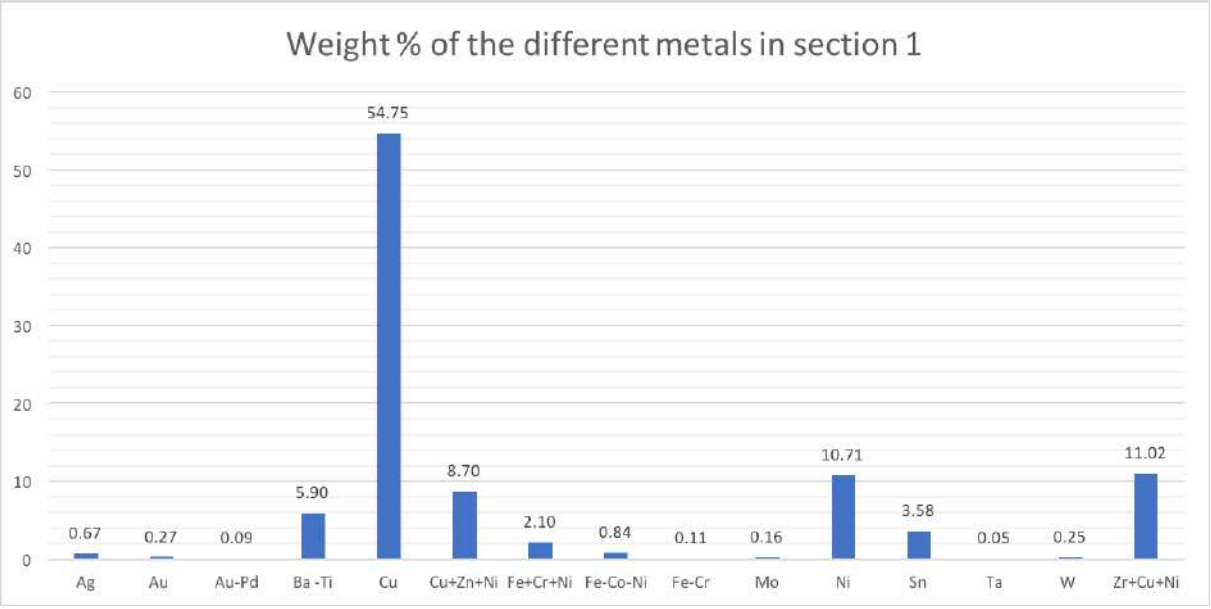

Figure 5.3: Weight percentage of all metals in slice 1.

The precious metal Gold was detected in two forms. Au is in native form and present as alloy in Au-Pd. In both cases Au is distributed for 80 % in pure metal and for 20 % in

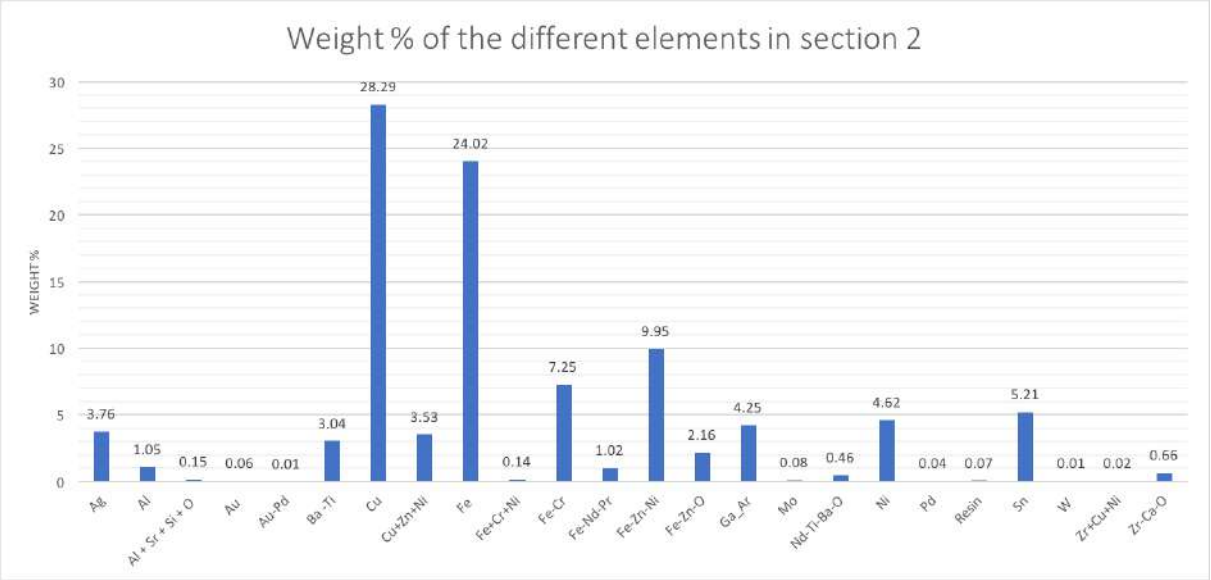

Figure 5.4: Weight percentage of all metals in slice 2 .

alloy. Au is mainly found as round shaped components within a silica matrix or ceramics. In other cases it is found as a thin layer on top of copper plates, with a rare occasions in alloy with pd. In section 2 Au is found as round particles on top of a Ga-Ar plate. Also, here some gold particles exists out of Au-Pd. A summary is given in figure 5.5.
Ag (0.67 % wt) is in all cases disclosed with a matrix of Fe-Ni-(Zn), similar as what is analyzed in slices 3 and 5. In the other section, Ag is present for 4 wt %. Here around 31 % of the silver is associated with Fe-Ni-(Zn). Another 20 % is equally divided between Au-Pd and Nd-Ti-Ba-O. The remaining fraction of Ag is begin associated with Ga-Ar, where it behaves like a cover surrounding the alloy.

In the first section the elements W and Co were observed close to each other. Co exists in the alloy Fe-Co-Ni. Around the alloy small amounts of Au, Ag and Ni were noticed. It was the only location were W was identified. W remained relatively in its original structure. Again, thin tungsten wires, as in slice 2 and 4, were encountered. In section 2 several large surfaces of Ga-Ar were distinguished. In their approximate, vertical and horizontal orientated boxes are placed. These have a composition of mainly Nd-Ti-Ba-O. In some cases this can vary with Zr-Ca-O. These structures reminds of structures in slice 5. Here, also a Ga-Ar was present lying next to a horizontal and vertical shaped box containing Nd-Ti-Ba-O. 65 % of the surface of Ga-Ar is liberated from other other metals. Light microscopy and BSE images makes clear how a large part of this is still surrounded by ceramics. Fe-Nd-Pr is found present surrounded by Fe beams. They are positioned in that way that the Fe beams are surrounding the magnets, embrace the piece of Fe-Nd-Pr.

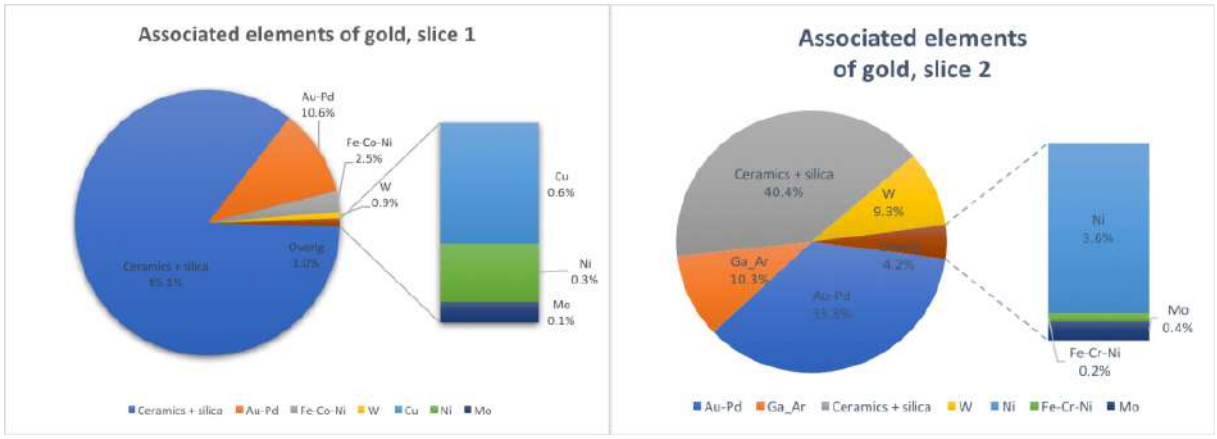

Figure 5.5: Associated elements of gold from two different slices.

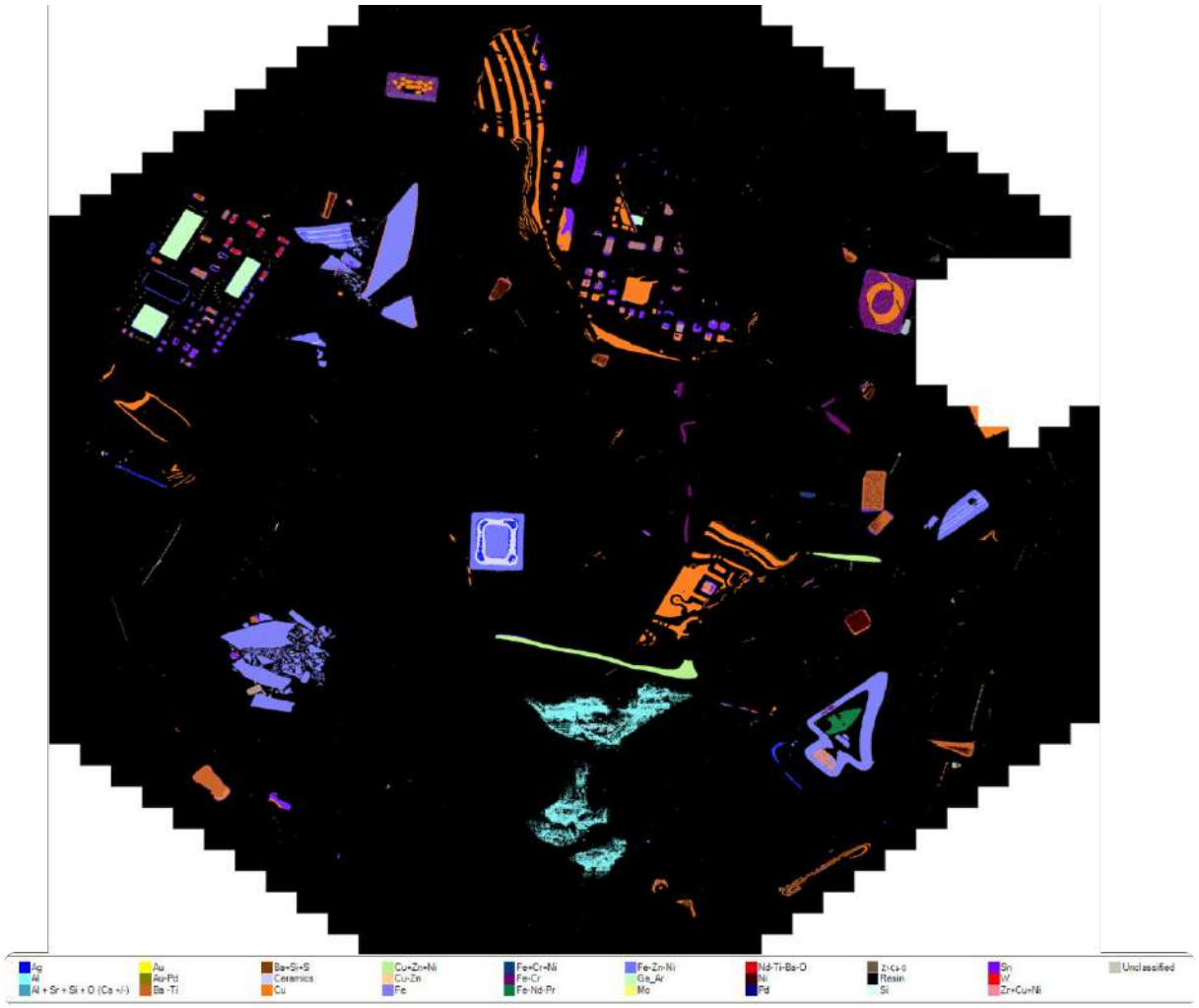

Figure 5.6: Overal image after EDS mapping through Mineralogic of a section of crushed smartphone parts.

Chapter 6

Molten smartphone sections

Out of the molten phone two different polish sections were made. One containing a fine ground powder and another made out of sections through large chunks of molten pieces. In first instance the goal of these section would have been to spot vertical trends in elemental distribution. Light microscopy soon shown there is actually no difference between the ground particles and the profiles through the molten clumps. Instead, the metal concentrates inside these are surrounded by molted ceramics spread in an irregular patron.
The overall goal would be to examine how Mineralogic reacts on molten WEEE parts and how the compositions defined before changes through the melting process.

6.1 Adapting the workflow

At first, light microscopical images were taken. These tiled overview image show the whole polished section. These image are then used to mark spots of interest and the coordinates of that spot are set as supplementary information to that image. Correlative microscopical tools from ZEISS made it possible to save these positions and use them in acquired BSE images. Basically, the position of the corners of the sample holder are passed to the SEM. As a results the marked spots in the light microscopical image can be requested, after which the system will automatically set the sample holder in the right position in the SEM to obtain BSE images of that spot. It is a very handy system to quickly locate zones of interest from much slower and less clear BSE images.
It was chosen to analyze these marked spots independently with Bruker. This would allow the user to have better understanding how the the material behaves and how to built a classification system. Additional a grid analysis was conducted but only in search of precious metals. Hence, the brightness and contrast of the images were set in such way only the brightest particles as Au were trapped in the BSE images and selected by the

EDS.

6.2 Metal concentrates

The main goal of these analysis was to see how the different metal and alloys maintain their chemical composition. What can be seen is that complex mixtures are formed with a lot of different metals inside. The main observation is that metals cluster together and then in their preferred composition crystallize. An example is given is in figure 6.1.

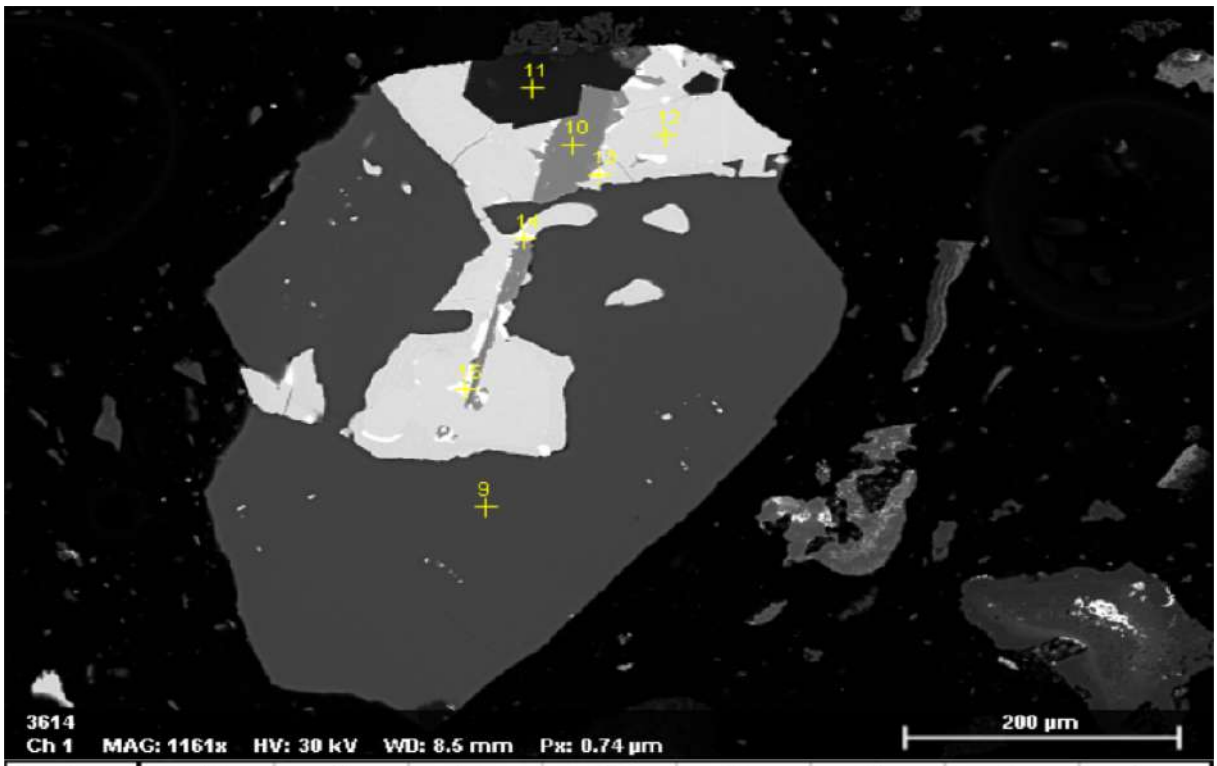

Spectrum	Al	Si	Mn	Fe	Cu	Zn	Ag	Sn
9		100						
10	0.8	52.4	4.7	42.2				
11	2.2	92.4			3.1			
12	1.7	13.9			84.4			
13	1.0	4.0		0.5	3.6	0.6	66.2	24.2
14	1.1	1.2		0.7	3.1	0.5	68.1	25.3
15	0.9	2.9		0.3	4.0	0.5	66.8	24.7

Figure 6.1: Clustering of different melt fractions and recrystallization.

It shows how four different compositions are tangled into each other. The BSE image already helped to identify these based on grey level differences. EDS spot or map analysis helps to identify their composition. The darkest surface is completely existing out of Si. On top of that there is a lighter surface detected as mainly copper with some Si and Al. Crossing right through the middle an mixture of Fe and Si is present in a needle shaped

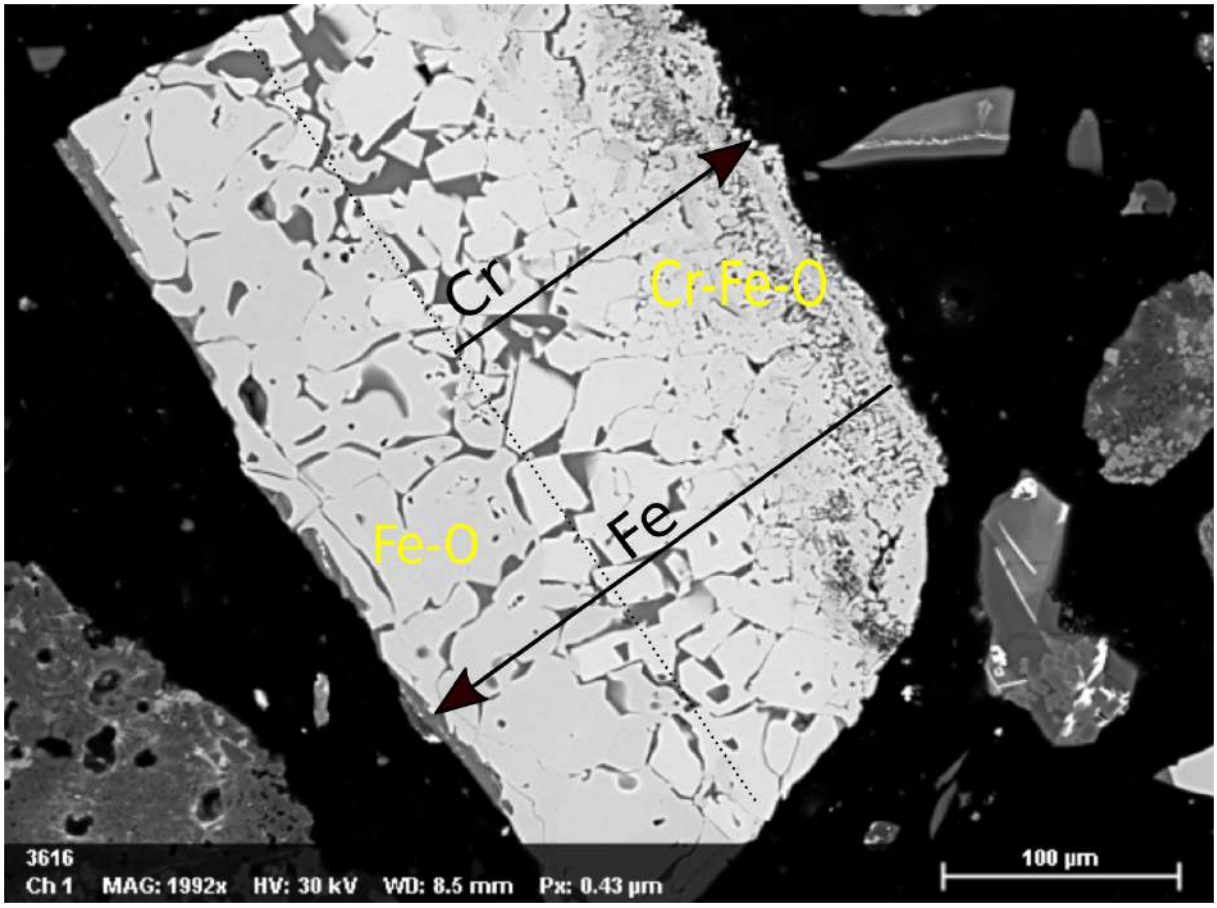

Figure 6.2: Vertical trends in the concentration of Fe and Cr.

phase. The elements Mn and Al were part of this mixture but are in minor quantities. On top there is a large light surface identified by Bruker as Cu with some Si and Al. Within this surface and often close to the iron rich needle small bright spots are visible. Results for these spots showed that these are enriched in Ag and Sn including minor elements (Ag, Si, Fe, Zn and Cu). Based on these finding a small paragenesis can be made. it looked liked Fe crystallized first follow by Si. Afterwards, the copper and later the Ag rich components followed.
These 4 mixtures with dominantly Fe, Cu, Si and Ag are regularly coming back through the samples.

In some concentrates some linear trends can be observed. This means that clear boundaries are visible or there is a clear transition from elemental quantities. A good example is illustrated in figure 6.2. It shows how in the left-hand side the images consists out of large crystals in a darker grey color. Towards the right upper corner the crystals become smaller in a lighter grey color. What could be observed is that the darker large crystals are Fe oxides. With an Fe % of 72 this looks like the mineral magnetite. Halfway that line Cr becomes part of the chemical composition. How smaller the crystals become how

more Cr is present. The amount Fe decreases along that same line.

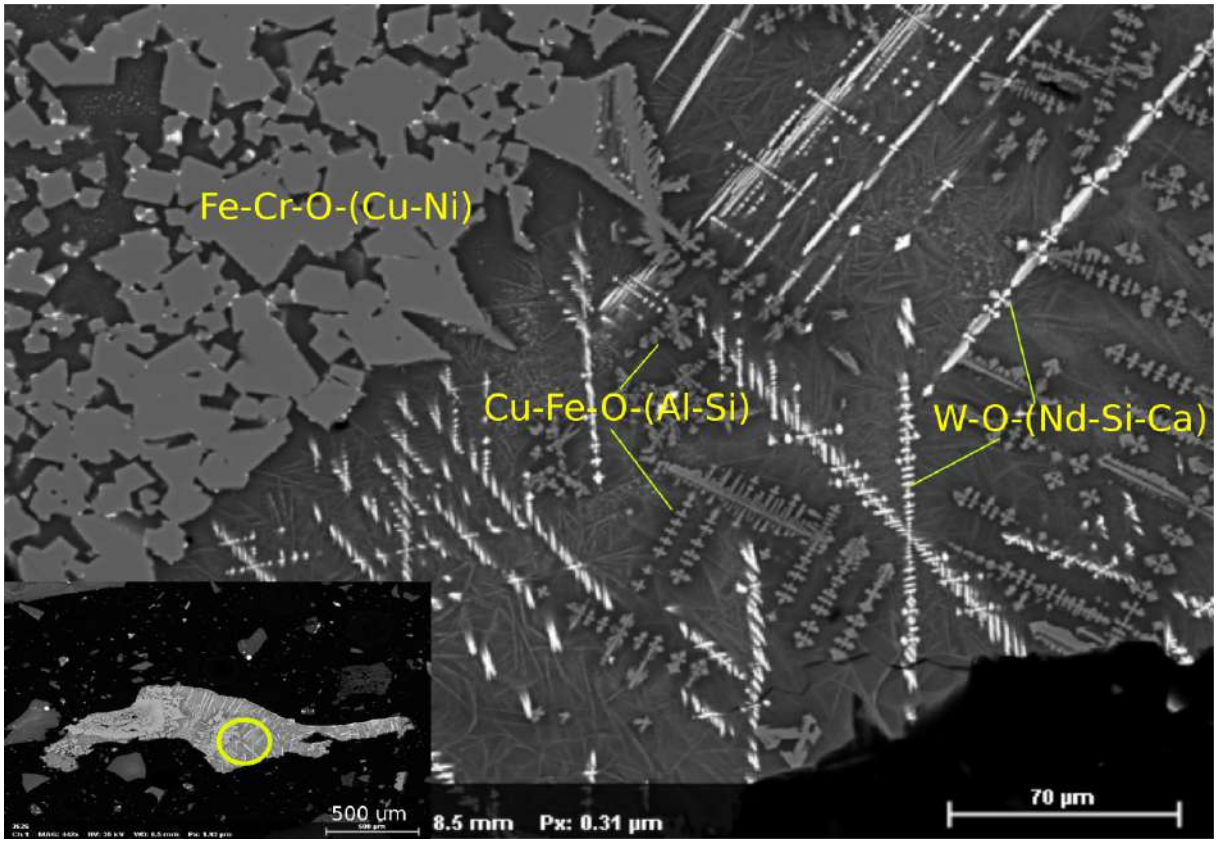

Figure 6.3: Crystallized W particles along with the elements Cu, Fe, Nd, Si, Ca and O.

Another type of crystallization after melting is shown in figure 6.3. In the left corner large crystals are present with a more cubic shape. They are typically consisting for 80 % out Fe-Cr-O. The remaining 20 % exist out of Cu (15%) and Ni (5 %). Aside very fine and well crystallized particles are visible. They have a linear shape crossing each other. Bases on the brightness difference under BSE two different forms can be spotted. The brighter crystals consists dominantly out of W (50 %) and oxygen (30 %). The minor elements are Nd, Si and Ca (all around 5 %). The darker crystallized particles are consisting dominantly out of Cu (33 %), Fe (28 %) and O (26 %). The remaining components are Al and Si.

Figure 6.4 represents a schematic overview of all elements detected and with which elements they form new chemical compositions. The chemical compositions in the different phases are completely different then before melting, with often far more complex composition. Also, not all elements have been found. In Contrary, the element Mn was detected, which has not been identified before.

What could be observed is that the elements Al and Si were present in all phases. Cu is omnipresent through the whole sample existing in most of the other metal concentrates. Typical associations with large amounts of Cu are found with Ni, Ag, Sn, Fe and Zr but also the metals, Cr, Mn, Zn, Ti, Mg, Cr and Co are found together with Cu. Another regular element that is coming back is Fe. Typical compositions are Ni, Mn, Cr, Cu and O. Aside, another group of elements are relatively independently from the others. They are mainly orientated around W with as other elements: Nd, O, Ca and Na.

	Al	Si	Cr	Fe	Ni	Cu	Mn	Zn	Ag	Sn	O	Nd	W	Ca	Zr	Ti	Co	Mg	Na
Al		x	x	x	x	x	x	x	x	x	x	x	x	x	x	x	x	x	x
Si	x		x	x	x	x	x	x	x	x	x	x	x	x	x	x	x	x	x
Cr	x	x		x	x	x					x						x		
Fe	x	x	x		x	x	x	x	x	x	x	x	x	x		x			
Ni	x	x	x	x		x		x	x		x				x		x	x	
Cu	x	x	x	x	x		x	x	x	x	x				x	x	x	x	
Mn	x	x		x		x												x	
Zn	x	x		x	x	x			x	x								x	
Ag	x	x		x	x	x		x		x									
Sn	x	x		x		x		x	x							x			
O	x	x		x	x	x			x			x	x	x					
Nd	x	x		x									x	x					x
W	x	x		x								x		x					x
Ca	x	x		x		x						x	x						x
Zr	x	x			x	x				x									
Ti	x	x			x	x				x									
Co	x	x	x	x	x	x													
Mg	x	x			x	x	x	x											
Na	x	x		x		x						x	x	x					

Figure 6.4: Schematic overview of the different compositions found.

6.3 Precious metals

In search for precious metal a grid analysis was conducted. To avoid long analysis time and to solely focus on precious metals the brightness and contrast were set higher. By doing this only very bright elements are visible. Hence, elements with a large atomic number as Au, Ag, Pd but also W and Sn

The largest part of the components identified existed dominantly out of oxidized W. The second most present element was Sn. Ag is mainly found in composition with Sn. The ratio between the two metals (Ag - Sn) is around 3 to 1. Other elements found together with Sn are Nd, O, Si and Ca. There are large fractions of pure Ag present with a size larger than 50 μm. Aside, Ag is also present in small spots next to, but not in the same composition, with Cu. A similar scenario was already described in figure 6.1. Au has been found once. It was present in a large round shape with a diameter of around

50 μm, being larger than any concentration of Au detected before. 10 % of that phase consists out of Cu, the rest is Au. The Au rich phase is quite isolated from the rest but a group of Sn enriched particles surrounds the precious metal (figure 6.5.

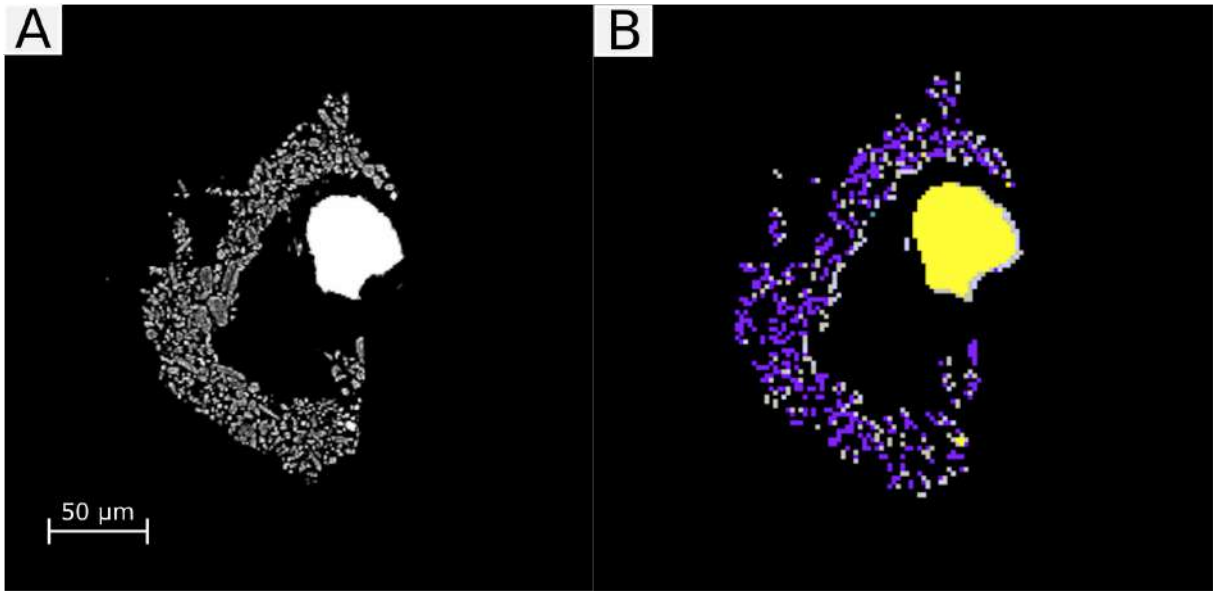

Figure 6.5: A) BSE image of very bright particle. B) Gold particle (yellow) surrounded by Sn (Blue).

Chapter 7

Discussion

The results give an interesting and unique view on smartphones. No other scientifically studies (published) have provided yet such information on the inside of smartphones. And although the results look promising on first sight there are still several issues in obtaining and treating this data. This chapter will start with critically discus the results. After, a final disclosure will be made by filtering the most useful information and discussing their potential attribution to the recycling industry. In the second part the limits of Mineralogic and automated microscopy in characterizing WEEE are discussed. Some suggestions for improvements are made.

7.1 The use of automated microscopy in WEEE

7.1.1 Detecting different compositions under the microscope

All elements in smartphones discussed in chapter 2 (table 2.3) have been found during analysis, with exception of Be, Cd, Hg, Rh and Sb. It has to be stated that the concentration of elements as Hg, Cd, Rh and Sb are extremely low (Holgersson et al., 2016; Oguchi et al., 2011b). Thus, capturing these elements might have been a very difficult task with the microscope. During sample preparation essential material could have be lost, including these elements. Another reason is that during the manufacturing of this type of smartphone (Nokia Lumia 925) these elements were simply not used. This is a likely scenario as the design and use of material differs for each type of smartphone (Holgersson et al., 2016; Oguchi et al., 2011b).

The results described in literature are always the result of bulk chemical data. Setting up such an analysis requires that a certain set elements must be chosen prior to the experiment itself. As seen in table 2.3 often elements are lacking as each research focused on a set of elements defined by what is important to reach their goals. On contrary, elemental

mapping with EDS does not require such methods and easily captures all elements (with exception of the light elements) present. Hence, the elements Mo, Co, Nd, Pr, Ta, W and Zr were not analyzed in the smartphone bulk chemistry data of Holgersson et al. (2016), although they proved to be relatively abundant in the smartphone using the SEM.
Much of the elements detected were found within alloys. These could exist out of 2, 3 or 4 elements. In contrast to identifying minerals by Mineralogic defining alloys is a new concept. It is a rather complex business to link the found alloys with a relevant description in literature. There are several million different alloys existing. Most information on them are kept in privatized databases or are made by the manufacturer itself of the smartphone (or its components). If this latter is the case than information could be hold back by the respective company. Still, there are few possibilities to check the viability of an alloy. For instance, the alloy can be checked on its existence if the chemical composition is thermodynamic stable. Website as: http://guides.lib.umich.edu/?b=s, https://www.nist.gov/ and https://materials.springer.com/ can provide information to clarify more on the existence of different alloys. Another way is to find patents showing the existence of these alloys. In search of the correct alloys it is often not the question if the assembly found is correct but rather if there are no missing elements. In the case of Nd-Ti-Ba-O, if no extra effort was done by using Bruker software, aside Nd-Ti no other elements would have been linked to the alloy.

In table 7.1 an effort is made to link all found chemical composition to their potential use in a smartphones. Basically all alloys could be linked to specific research, a patent or a textbooks on alloy and material. Hence, all alloys found during the analysis are justified more or less on their existence. However, most of this information is for electronics in general and thus it can not be said that these characteristics can be applied specific on smartphones. In some of the references, as Au-Pd, Ga-Ar and Fe-Nd-Pr, there is a clear mention and link of use in mobile phones. A case of which it is almost sure an element is missing is Fe-Nd-Pr. Here the element B is missing (Croat et al., 1984), but this has rather to do with the detection limits of the SEM on lighter elements.

In case of pure metals in some cases pixels were analyzed containing both the metal and oxygen. We found this was the case for Fe, Ta, Au and Mo. Not all pixels gave a spectrum containing oxygen. Therefore it is not a continuous patron. It is hard to tell if this phenoms is due to the use of oxygen rich material or post manufacturing process. This could refer to oxidation process during use of the device or oxidation caused by polishing the metals.

Alloy	Properties	Reference
Al-Sr-Si-O	Light metal casting with improved mechanical properties	(Timpel et al., 2012)
Ba-Ti	Ferroelectric glassceramics	(Chen, J., Zhang, Y., Deng, C., Dai, X., & Li, 2009)
Ba-Si	Semiconductors	(Kishino et al., 2007)
Cu-Zn-Ni	Bearing assembly, ballast, casting, step soldering, and radiation shielding	(Ilyenko and EffenbergS., 2007)
Cu-Zn	Bearing assembly, ballast, casting, step soldering, and radiation shielding	(Ilyenko and EffenbergS., 2007)
Cu-Zr-Ni	Metallic glass	(patent) (Gore et al., 1998)
Fe-Zn-Ni	Corrosive resistance	(Tang et al., 2001)
Fe-Zn	Corrosive resistance	(Tang et al., 2001)
Fe-Cr	Stainless steel	(Ustinovshikov et al., 1996)
Fe-Cr-Ni	Stainless steel	(Umeda and Okane, 2001)
Fe-Ni-Co	Magnetic properties	(Fukamichi, 1994)
Nd-Ti-Ba-O	Dielectric properties	(Choi et al., 2000)
Au-Pd	Increase of melting point, hardness, strength and elasticity	(Predel, 1994)
Ga-Ar	Semiconducting	(Blakemore, 1982)
Fe-Nd-Pr	Permanent magnets	(Croat et al., 1984)

Table 7.1: List of all alloys identified, their properties and references.

7.1.2 Behavior of metals in a smartphone

Au is the most valuable and targeted metal when recycling smartphones (Chancerel et al., 2015b). This is mainly due its high value in comparison to the other metals and its abundance in the phone. However, only a small fraction of this gold is being recovered (Buchert et al., 2012; Chancerel et al., 2015b; Chancerel and Rotter, 2009; Hagelüken and Meskers, 2008). A large part of this is being lost during pre-processing stages (Chancerel, 2009; Chancerel et al., 2009). An issue linked to bad liberation (Reuter et al., 2013).

So far literature does not mention a more geometallurgical approach, as by using electron and automated microscopy, on solving this problem. In this study, an attempt is made to characterize a full smartphone and characterize all elements inside. It gives an idea on where the different metals are situated, which shape they have and to what extent they are surrounded by other other metals or ceramics and plastics. Aside visual information also statistical data was provided for each slice: bulk data of the material analyzed, assay data describing all the elements distributed within different phases, association data on

the metals found in close contact and liberation data. However, these statistical data have to be dealt with caution. There are some hold backs to make strong arguments based on the provided statistical data by Mineralogic.

The main problem with dealing with the statistical data is that the samples are very heterogeneous. They can not represent a larger samples than them self. In the case of the parallel section through the phone the interior components and structures could change within 1 mm. Or even in case of a 'random picked' quantity of shredded material it is impossible to analyze and study these as a representative sample of a larger quantity. However, the data can give a strong impression on how the elements are distributed and give a better understanding on how the material behaves. But, it is not possible to compare different sections with each other or generalize the information. For example, Au can have a high weight % in one slice but little in other. The slices actually can have the same amount of gold but the quantities of other material differ.

Au is often found within a matrix of silica. Often gold particles here are round or spherical. These are most likely sections through gold wires hold in place in a Si rich substance. In a few cases Au has been found in association with other metals. A clear example is the association with Ga-Ar. In another scenario gold has the function of being a connector between the metals W, Mo and Ta
Aside, Au is being detected as a very thin layer on top of copper plates, preceded by a thin layer of Ni. Here,it can be Au is in alloy with Ni and/or Pd. As these layers are so thin and sporadically it is hard to discuss how the exact relationship between these three elements is over the whole phone. To summarize, targeting gold in processing steps one should look at silica rich zones, Ga-Ar rich parts, metallic rich zones with Ta, Mo or W and copper plates and parts coated with Ni and Au. In a limited extent Au is be found in association with Fe-alloys.
Studies as Holgersson et al. (2016) and Chancerel et al. (2011) and basically most of the industry (Hagelüken and Meskers, 2008) focus on the extraction of PCB for the recovery of Au. Most studies often provide only information on the PCB as it is seen as the most richest zone rather than the whole phone itself. However, this studies proves otherwise. It is true there are some very rich zones of Au in the PCB but there are some non neglectable zones in the other parts of the phone as well. Especially in the bottom of the phone and around the speakers gold was present abundantly as a pure metal in a Si matrix, a coating on top of copper plates or in association with Ga-Ar.

The other two precious metals Ag and Pd show certain regular patrons. Ag has been found quite abundantly all over the different slices. Also here, it is thus a misinterpreta-

tion to assume that only in the PCB Ag is present abundantly. Within the PCB it was shown that a lot of Ag is linked with Fe-Zn-Ni. Here, Ag is placed within a box containing out of Fe-Zn and Fe-Zn-Ni. Often with these kind of boxes Ag forms a surrounding frame pressed between Ni and Sn. Hence, often Ag is both shown in association with Fe-Zn-Ni as Sn and Ni. It has be noticed that Ag covers a large part of the Camera. Pd is detected in two particular locations. First, Pd appears as wire shaped parts within Nd-Ti-Ba-O. Second, the metal is in in alloy with Au coated on Cu and Ni. When looking at the distribution Pd is mainly present within a matrix of Nd-Ti-Ba-O, less than 10 % being present as in alloy with Au.

The following critically defined elements ((European Commision, 2010) were detected under the electron microscope: Ta, Ga, W, Mo, Cr, Co and Nd. Ta, Nd and Ga were found in rectangle or square shaped bodies. These components were situated above the copper plates. Although they are quite isolated from other metals they were emplaced or surrounded by a Si or ceramic material. In case of Ta and Ga, the metals Au, W and Mo were often found in close approximation. They both have the roll of capacitor and transmitter and are being connected through other parts of the phone by these materials. W components are often wire shaped. In other cases they seemed to function as a bridge between different metal, causing to being wrapped up between different metals. Nd was also found as part of large magnets (Fe-Nd-Pr).
Cr and Co were both found in alloy with iron. Especially Cr was abundantly present in large structures capsuling parts of PCB or other highly enriched metal parts. Co has been found only once in a small beam in presence of Mo.

A summary of all the metals, their compositions, location, average weight and associated metals can be found in the appendix.

7.1.3 Quantitative comparison

To compare the obtained results with chemical data from literature is a blunt move. One has to consider that each mobile phone manufactured has different features. Hence, differences in elemental composition are possible. Therefore comparing the microscopical results of just one specific type of phone (Nokia Lumia 925) with bulk data of different phones is not optimal.

A more accurate comparison can be made with bulk chemical data of the type of phone

itself. These data has been provided by research conducted at the University of Liège. These data are yet to be published but could be used for this research (Pers. Comm., Lambert F - Ulg, 2018). The results are shown in the upper graphs of figure 7.1. The data represents the bulk chemical data of the phone. Additional to these graphs a summarized overview is given of these elements under the microscope. A more subjective approach is done to compare more or less these data. Each element is divided in a class (very high - rarely) based on occurrence and size through the phone.

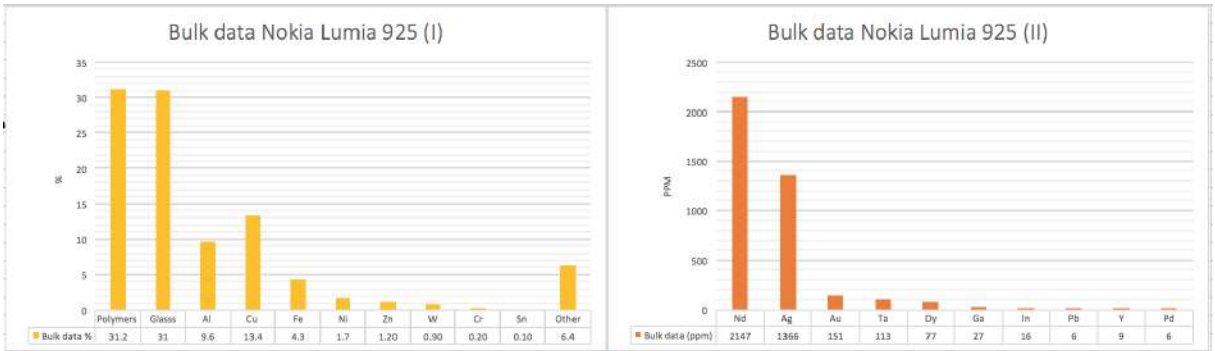

Material	Occurence	Summary	Material	Occurence	Summary
Polymers	Very High	All parts of the phone, often metals are embedded within	Nd	Medium/Low	In magnets with Fe around the camera and speaker and in the alloy Nd-Ti-Ba-O in the PCB
Glasss	Very High	Screen of the phone existing out of Al, Si, O, Na, Ba and Ca	Ag	Medium/Low	Spread over the phone with high concentration in the pcb in
Al	Very High	All parts of th phone (casings, in ceramics, . . .)	Au	Low	Found regulary through the phone in small sizes often isolated
Cu	High	Coppper plates, framing, all parts of the phone, High concentration in PCB	Ta	Low	Found 3 times as a section through a box with Ar in the pcb
Fe	High	all parts of the phone, often in alloy with other elements	Dy	/	Not detected
Ni	High	Mainly in the pcb found together with Cu, Sn and Ba-Ti	Ga	Low	Found 2 times as a section through a box with Ar both in the pcb
Zn	Medium	all parts of the phone, mainly in alloy with Cu and Fe	In	/	Not detected
W	Very low	only in small bits and small wire, regulary found close to Ta	Pb	Rarely	only once in association with gold
Cr	Medium	Find regurarly in alloy with Fe	Y	/	Not detected
Sn	Medium	only in small pits and small wire, less than Au	Pd	Very low	Often detected within Nd-Ti-Ba-O and Au-Pd

Figure 7.1: Overview of the bulk chemical data of Nokia Lumia 925 (Pers. Comm., Lambert F - Ulg, 2018) and a summeer version of the microscopical results.

The data shows that elements as Cu, Al and Fe are the most abundant metals in the phone. A more or less same interpretation was made out of the microscopical data. It has to be stated that these elements are often 'hidden' as part of an alloy. Ni and Zn, respectively the fourth and fifth most abundant metal in the chemical data, does on first insight not implicate such high occurrence under the microscope. However, both elements are parts of alloys with Fe and Cu, used in quite a lot of material in the phone. A similar observation can be mode for Cr, mainly found in alloy with Fe. As discussed, Sn is an abundant metal always detected in a pure state in close proximity to the copper plates. W in the chemical data, with almost 1 %, is highly abundant in comparison to other elements. In contrast, similar conclusion can not be conducted from microscopical data. Here, W was seen rarely and in very small components. An explanation could be that during preparing the slices large parts of W were trapped in parts of the phone in between and thus not detectable under the microscope. Previous studies (Holgersson et al., 2016) never included W in their data on the PCB. It might be an indication that W is not

in high concentration in PCB but should be searched for in other areas. As mentioned before the vibrating motor, making it able to have the trill function on your phone, has not be included in the slices. As W is a major component of this motor this could explain the missing quantities of W (Constantinides, 2012; Nickel, 2010) .

Nd and Ag both show compatible results between the chemical bulk data and the microscopical results. Nd is found in two types of alloy with high concentration in the speakers, camera and PCB. Ag is more or less omnipresent with high concentration in association with Fe-Ni-(Zn) in the PCB. Also gold can be found through the whole phone. Different to Ag, Au components are much smaller and more isolated from other metals. The chemical data for Ag and Au is low in comparison to the values given by (Buchert et al., 2012), respectively 3500 and 340 ppm. This could be explained by the use of components during the manufacturing of this specific phone, being more economic on the use of precious metals. Another guess could be that different parts of the phones were forgotten during analysis for gold. It is often suggested in literature that gold is mainly present in the PCB. However, the results of microscopy do imply that gold can be in all parts of the phone.

Ta and Ga were found just a few times. However they take up a relatively large surface as a section through a box solely containing Ta or Ga-Ar. Dy was measured in the chemical bulk data but was not detected by EDS. Assumable a similar story can be told as with W. After all, Dy is a major component of the vibrating motor in a smartphone (Constantinides, 2012; Nickel, 2010). The elements Y and Pt have values below 10 ppm. The analytically error is probably large below this values to make a strong conclusion on these elements. Yttrium was not detected under the microscope. Pt was detected although just once and in a very small size. Surprisingly Pd is reported in such low quantities (below 10 ppm). From the microscope Pd is found regularly back in a Nd-Ti-Ba-0 matrix and in alloy with gold. This surely implies a larger quantity than 6 ppm. Pb was only found once in very small extent in association with gold. Hence, comparable with the chemical data. Indium was not detected in the microscope. It was suggested (Pers. Comm.,Lambert F - Ulg, 2018) to be part of the screen. This was not found with EDS and μ-XRF.

A large group of elements do not show up in the chemical data. Also vice versa some elements are not detected as mentioned above. A summary is made in table 7.2. Strangely elements as Ti, Ba, Mo, Zr and Sr were not detected. This could hardly be caused by analytic error. There presence in the slices is quite high in comparison to elements as Pd and Pb, which were detected although being reported in low quantities. A reason, already

implied, is the selectivity of bulk chemical analysis. In contrast to the EDS all elements to be measured most be chosen prior to the analysis. As a results a certain amount of elements is just not analyzed.

Bulk data	Microscope	Occurrence	Summary
Dy	Ti	Medium - Low	In alloy with Ba, often in close contact with Ni
Y	Sr	Very low	In alloy with Al and O
In	Mo	Very low	Pure metal often in small bits pressed between several metals
	Zr	Low	Found in alloy with Cu and Ni
	Ba	Medium - Low	In alloy with Ti, often in close contact with Ni
	Co	rarely	Found once in alloy with Fe and Ni

Table 7.2: Missing elements in bulk chemical data compared to the results of microscopy and vice versa.

7.1.4 Liberation, association and elemental deportment data

Mineralogic provides aside visual data also statistical data on liberation, association and assay data. The latter can be expressed in elemental deportment data. That is to say to which extent the elements are distributed along their native form and alloys. This information is for a part incorporated in this work. It could also be noticed that the content on this matter is somehow limited. This is mainly because the results are ambiguous and biased.

An example on elemental deportment is given in figure 7.2. It represent the element deportment for Cu, Ni and Fe in PCB. This data might give interesting information but is hard to use because of the heterogeneity of the samples and the type of components. The data is generated from three intersections through the PCB. It was already mentioned how internal composition can change within a few mm. Therefore, this information can give a better understanding but it can not provide essential information on the distribution of Cu or other metals spread over the phone. Aside, this data is based on the specific gravity of the defined classes. Normally this is defined from known minerals with a well-known specific gravity constant. This is not the case for e-waste. Here, the specific gravity constant is a calculated approximation for the found alloys. Therefore, it can be argued that the final results are biased. Another argument to leave out these results out the discussion is that this information are not considered of importance. The most valuable metals are all found in native form and the metals found in alloy are maybe more interesting to recycle as an alloy instead of the pure metal.

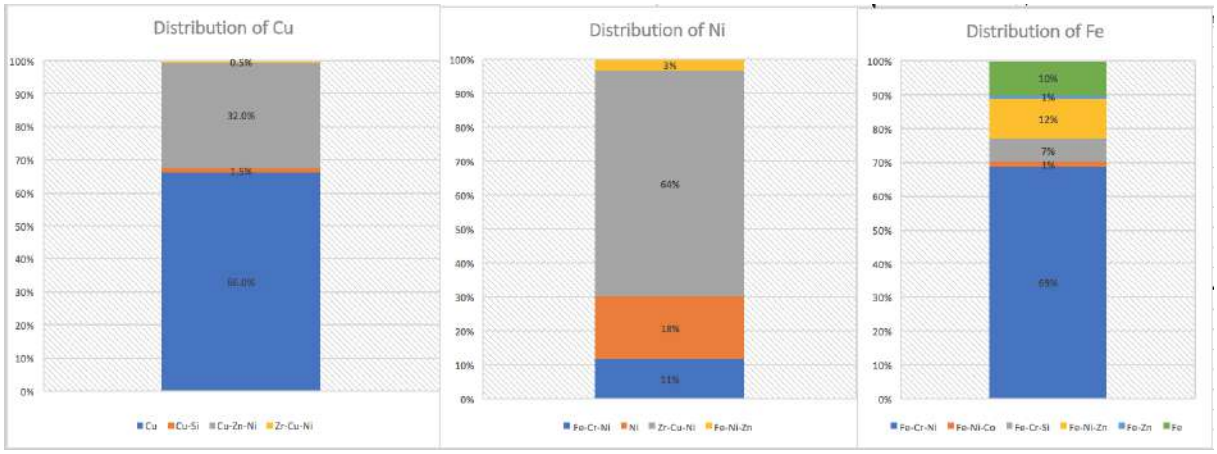

Figure 7.2: Deportment data of Fe, Cu and Ni in the PCB based on section 2,3 and 4.

Liberation data in crushed particles is shortly discussed. However the issue in this matter is that due to heterogeneity entire different results can be obtained for different sections. Also 3D aspects should not be forgotten in these samples as often components can vary rapidly in size and occurrence in different perspectives. It is also of importance to remind that the brightness and contrast settings do not always capture all aspects as ceramics and plastics. As such surfaces considered liberated are actually being trapped withing ceramics or plastics. For this, it is important to look at BSE images. In refinery processes where acids or other chemical solutions are used to liberated precious metals it is interesting to look how much of the surface of the targeted metal or alloy is liberated. It should be emphasized that the heterogeneity of the sample and hidden surface can give false impressions.
The most valid information to use is association data. It gives a better understanding to which metals are often attached to other metals or how metals are trapped within ceramics.

7.1.5 Following up: crushing and melting

Following the material up after shredding and melting with microscopy can give some interesting insights. With the aid of Bruker software the different samples could be easily analyzed. The shredded samples helped to understand how the different metals behave after shredding. A large proportion of them is found in their original state with surrounding metals or ceramics. As for example Pd in a container of Nd-Ti-Ba-O or Au in matrix of Si. On the other hand, often very small bits of metals were found indicating that they crumbled from their original structure. It could imply that a large part of them are actually ending in the dust fraction.

The results for the molten phone are harder to interpreted. The original composition and metal combination are almost completely vanished and new element combinations have been found. It shows how certain metal cluster together after melting and/or reclassification. A good example is Au which seems to be attracted Au from different parts of the phone into one concentrate with Cu. Another example is the combination of Sn with Ag.

Based on all analyzes an attempt is done to suggest some preliminary suggestions for recycling. These are theoretical suggestions solely based on the results from automated and correlative microscopy.

7.1.6 Preliminary suggestions for recycling

Gold Au is ferquently available within a silica matrix. Pre-processing steps should emphasize this behavior. Once the silica is shredded in smaller bit gold might get easily lost and if it still detectable in the microscope it is often still entrapped within the Si substance. Aside, pre-processing steps could be designed to target gallium, and so directly try to include gold as there presence is linked to each other. Also, copper plates being shredded should not purely seen as a source for Cu. Often they are coated with a layer of gold and nickel. Probably the most important suggestion that can be concluded from the microscope is the omnipresent of gold. Au is concentrated within PCB, but still large fraction of gold can be found in other part of the phone like around the speaker and camera. Based on melting results it seems that Au clusters together with Cu.

Silver and Palladium Ag and Pd are two most valuable metals after Au (Chancerel et al., 2015a). In contrast to Au these two metals are often encapsulated by other metals. In case of Silver this is often Fe-Ni-(Zn) and for Palladium it is the alloy Nd-Ba-Ti-(O). These containers, often situated on top of the copper plates in the PCB, could be seen as a target during pre-processing. During shredding these boxes are separated from the PCB and often heavily damaged. However, they more or less keep the same configuration and the precious metal is not liberated. This could result that the metal gets easily discarded to fraction not further treated for those metals. It has to be said that, as seen for Nd-Ti-Ba-O containers, they could still be attached to parts of the PCB without losing their set-up. In that case picked up PCB could include a large part of Pd, ready to be recovered at a smelter for instance. If these boxed would get teared apart from the PCB, there is a high change they would get lost or send to another fraction. A last note, there is a significant amount of silver attached to the camera, which could be seen as a target.

Tantalum and Gallium A similar conclusion can be made for Ta and Ga. Both are highly concentrated in specific containers used as capacitors and semi-conductors. They were nicely mapped under the microscope and showed how they were quite isolated from other components. Being placed on top of the PCB they are considered to undergo the same fate after shredding as the other box shaped components. Either they get lost (dust) or they end up broken in very small fractions more difficult to recover in a pre-processing plant. Another option is that they get stuck on the PCB after which it might be recovered during a smelting process. Both elements were not found in molten smartphone sections.

The visual image of Ta and Ga boxes on the PCB can help to locate these metals. During the pre-processing steps they could be segregated and collected separately. A study by (Piotrowicz and Pietrzyk, 2016) shows more how tantalum easily can be recovered after collecting and separating all the tantalum capacitors. Recollecting Ga-Ar as a whole might be sufficient enough for re-use. Recycling potential for Ga-Ar, also found in led and solar panels, is described in (Yun-Ying et al., 2017). Ga-Ar is surrounded by Au and therefore indirectly increasing its importance of being targeted.

Tungsten and Molybdenum Targeting W and Mo might be a hard and difficult job during pre-processing steps. Both metals are in a very low amount present. They are simply too small, too irregular in their presence to focus on. However, the vibrating motor might containing a large amount of W, something which could be true from analyzing the molten material. Here quite a lot of material contained W. W was found not to concentrate together with Cu. This might lead to problems during smelting processes were Cu is mainly used a lead metal to collect other metals.

Neodymium and magnets There are two options for targeting Nd: Fe-Nd-Pr magnets and Nd-Ti-Ba-O capacitors. The latter is less abundant than the magnets. However the magnets are easily be shredded as could be observed. They end up shredded with a lot of Fe around, most likely caused by its magnetic susceptibility. Hence, the magnets could end up with scrap iron and steel. Nd-Ti-Ba-O could be recycled if not teared from the PCB. It could be an extra motivation knowing Pd can be found inside. Also here it needs to be noted Nd and Cu do not interact during smelting. Thus, this might be problematic in end refinery steps.

A focus should made on the speaker and the camera of the phone as there are places of high concentration of Fe-Nd-Pr in the phone. In overall, the problem with Nd is that there is high concurrence from material with much larger magnets as wind turbines (Volker, 2016).

Iron Iron is abundantly present in the phone, although mostly within alloys. This might already suggest not to target solely the metal Fe but the alloy in itself for re-use. After shredding the material ends up in different fraction and sizes. Melting the material can make the situation even worse as Fe ends up many different concentrates, with even more different metals than the original alloys.

Copper, Nickel and Tin A similar conclusion can be made for Cu and Ni, where it would be best to focus on copper plates within the PCB (with on top Sn and Ni) or re-use of the alloy Cu-Zn-Ni. During melting the elements Cu, Sn and Ni are found often together.

7.1.7 Rebuilding the phone

Another suggestion of using this data is in helping to rebuild the phone of the future. It might be a very hard and complex matter to recycle smartphones today but this should not be the case in the future. It would be good to convince policy makers and manufactures of smartphones to take in account the recycling steps already during the first steps of designing the phone. That is to say changing the location and accessibility of the different components to improve and ease the processing steps to recycle these metals efficiently. Similar suggestions were already discussed in Chancerel and Rotter (2009). An adequate knowledge on the composition of the EEE, the location of the different metals and their mutual relationships was seen as important for product design for a more efficient pre-processing. Mainly the lack of information was seen as a problem to have a decent information flow between the manufacturer and the operators of pre-processing facilities. The European Commission (European Commision, 2010) already set out a stronger policy for manufacturers to take into account the LCA (life cycle analysis) of a product.

To achieve such goals there is collaboration needed from the two sides. On one side the manufactures and on the other side the recycling companies. The use of Mineralogic in this story would serve as a medium to help defining the difficulties and issues recycling companies have. Both visual as statistical data from Mineralogic can provide a base to express the needs for a better recycling system to manufactures (figure 7.3).

Clustering of material A first suggestion based on the results obtained in this project is to cluster the metals of interests. Critical metals as Ta and Ga are relatively highly concentrated in certain locations. However these locations are spread out over the phone. Regrouping these metals in to certain zones would make it for recycling companies more

attractive to redesign their processing route aiming for these zones.

Increasing accessibility Another issue is the accessibility to certain metals. Au for example is often found embedded in Si rich matrix. During shredding these particles are spread easily. Similar for Ag which is often entrapped in matrix of Fe-Ni-Zn or Pd within Nd-Ti-Ba-O. Often precious or critical metals are found in containers attached to the copper plates. Making them accessible and easy to separate from the PCB could improve the recycling of these metals or the reuse of the containers in future electronics.

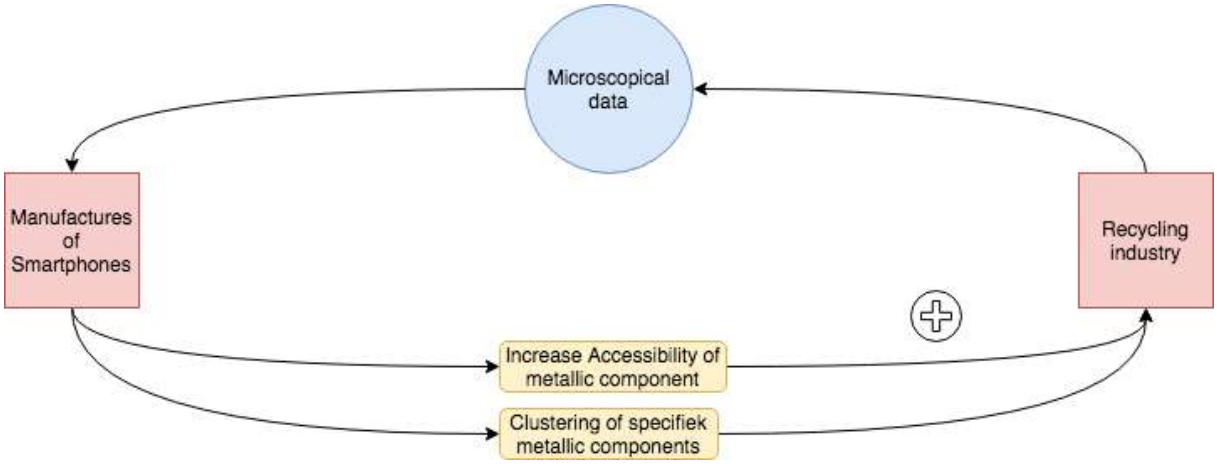

Figure 7.3: Schematic overview on linking microscopical data with building a sustainable smartphone.

7.2 Adapting Mineralogic to WEEE

In this research most of the data was acquired from the SIGMA SEM equipped with the software Mineralogic provided by ZEISS. The device and software were in first instance designed to bring solutions to issues in mining and industrial products. Hence, the software is customized to easily identify minerals, elements, particles and provide statistical data on these. Working with man-made electronic material is a relatively new challenge. As a result the software is not entirely adapted to provide the right and efficient solutions to deal with these kind of samples. Although, it has to be said that the flexibility of the systems provides a decent base. In this section all the issues in characterizing electronic waste are discussed. Suggestions are given in order to improve the system for a better analysis on WEEE.

7.2.1 Preparation of samples

Studying the internal composition of a smartphone without loss of information has been found a difficult and challenging task. It was chosen to slice the phone parallel to its base to receive the most information of the phone without losing information on the internal structure and composition. The main problem with acquiring data this way is that all the components between two slice is lost and no information on the vertical axis was yield. Additionally, slicing the phone already means a loss of 2-3 mm as cause of the thickness of the saw. This is quite problematic in studying a representative sample, as information is missing, especially due to the heterogeneity on μm scale. A good example is the vibrating motor containing elements as W and Dy which was not at all found back in the samples. The vibration motor placed left of the camera and known to exist out out of several rare earths (Constantinides, 2012; Nickel, 2010) was not included. Aside, preparing the sample is time consuming and costly. Almost a week was necessary to obtain the final samples ready for use. It is hard to reduce this time-span as the hardening of the resin takes a full day and automated sawing to achieve exact parallel sections took up a day as well. This results in a high workload and a specific use of special devices and material.

Shredding the sample is not any better in acquiring a homogeneous sample. A lot of material gets lost in the process (dust) and due to the heterogeneity of the sample it is almost impossible to prepare polish section with crushed particles representing the whole phone.

7.2.2 Issues in Mineralogic dealing with WEEE

- **Impure pixels:**

  In case of electronics the borders between two phases are often abrupt and sharp. A good example is Cu and Ni lying as two layers on top of each other. This is a scenario often seen at the top of the the copper plates within the PCB. The problem here in Mineralogic is the determined resolution grid. In most of the cases this was 5 or 10 μm. As a result the border between the two phases can be wrongly classified as a Cu-Ni alloy, while this is not the case at all. This not only lead to difficulties in classifying and coloring the images but also makes it harder to interpret statistical data. The problem is schematically presented in figure 7.4. Increasing the resolution would give a better solution to this problem but will increase the analyzing time exponentially. Another example is Ni sputtered on top of Ba-Ti, where the resolution was in first instance to high to make a difference.

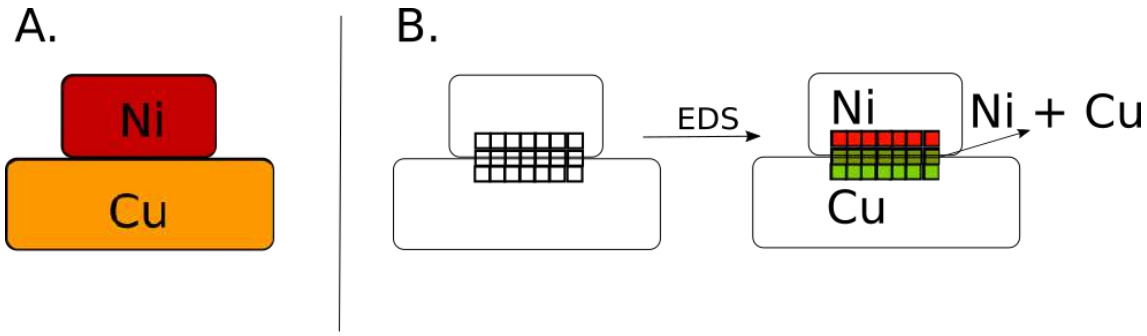

Figure 7.4: Left: The real situation. Centrum: A grid is drawn over the sample. Right: An EDS analysis is conducted.

- **Undetected elements:**

  For each pixel analyzed with EDS during automated mapping a quantitative result is given based on a X-ray spectrum. Hence, after mapping, Mineralogic directly makes up a quantitative result from the spectra for each analysis. This might result in a wrong outcome with missing elements. The whole sample has been analyzed with a intensity of 30 keV, leading to more background noise. This can cause that elements are automatically filtered out as part of the background noise. In the case of rare earth elements the intensity peaks corresponding tot the specific element lies in very close proximity of other rare earth elements. Therefore, Mineralogic might automatically refer several rare earth elements under the same peak to just one element.

  To avoid this scenario very specific analysis were done with Bruker, where the spectra could be verified by person. Also, by reducing the intensity form 30 to 20 keV

hidden elements normally falling in the background noise are now more easily identified. Specific examples are Nd-Ti that afters specific analysis was finally identified as Nd-Ti-Ba-O or Fe-Nd which actually was hiding the element Fe-Nd-Pr.

In solving this matter the use of μ-XRF was thought to bring a more accurate solution. However, as discussed the issues becomes even more complex and was considered to not bring any extra value to this research.

- **Slow and inefficient mapping strategy:**

  Mapping a smartphone through a grid analysis is time-consuming. Two reasons can be pointed out. First, the actual sample is large. With a size of 6x1 cm a large surface most be examined. Secondly, a lot of important information is present in a very small area: metals, alloys and ceramics. Most of the components of the phone have a large surface as touch panels, screen, copper plates, capsules etc . . . . However, conducting a grid analysis all pixels of 5 μm size within these components are analyzed as just one analysis could be enough since they are all homogeneous phases. To avoid longer analysis than 50 hours large components as screens, touch panels and covers were avoided being analyzed once they were examined in a previous slice or the resolution was set higher (10 μm).

- **False alloys and/or impressions:**

  Another issue faced during mapping analysis is that pixels are classified under a metal or alloy that is actually not existing. This is a similar scenario to the issues with impure pixels and undetected elements. The primary conclusion here is that some features of the phone are too detailed to be mapped with the resolution set. An example is Ni sputtered on top of Ba-Ti. Grid analysis could not identify these details but rather mixes all elements in that area under one solution. Also on vertical scale this can be the case. This means that the intensity is too high (30 kev) penetrating several different layers of metals superimposed on each other. As a result one can identify this as a complex alloy. However a detailed Bruker and BSE analysis helps to understand the situation better. The latter is a time-consuming exercise.

7.2.3 Improving the system

A 'thought' study has been done in order to tackle these problems. The following three aspects are considered to be the most important to improve: efficiency, time and accuracy. In order to do so, some improvements are suggested.

Segmentation

In an MLA analysis the BSE images are segmented in to different phases. The centroid method based on a single x-ray acquisition defines the composition of that phase (Sandmann, 2015). So in case that four different phases would be detected in the BSE image four analysis would be conducted instead of multiple analysis in a grid analysis. To goal would be to achieve a similar set-up to increase the efficiency of automated microscopy on electronic waste. However, WEEE are too complex too apply such a plain approach. On one hand the amount of different metals and alloys makes it very hard to distinguish these different phases. On the other hand a single centroid analysis might not be enough to guarantee a correct representation of that phase.

In order to obtain a right segmentation it is suggested to combine both the information of light microscopy and BSE images. That is to say a segmentation based on both the color and grey level images. This can be approached in two different ways. In the first way the two images would successively be used to segment. At first the color images would be segmented based on color differences. This is a technique already used for multispectral images. Pirard et al. (2008) already showed how minerals based on optical microscopy images could be automatically recognized within multispectral images. It was already laid out how these techniques could lower the cost of the sensing technology, the flexibility of the operating mode and the speed of operation (Pirard et al. (2008)). The light microscopical image would after be superimposed on top of the BSE image and all phases defined before are now transferred to the BSE images. A second segmentation would then take based on the BSE image, which contains more details. This would result in newly defined phases on top of the original ones.

In the second approach the BSE image and the Light microscopical image would be superimposed on top of each other. A segmentation would be made on the new image. An example of how such segmentation could work is defined in Multispec. Multispec (Biehl and Landgrebe, 2002) is designed for hyper spectral images and satellite images. However, it is a useful tool to demonstrate this theoretical set-up. The results (figure 7.5) shows how nine different classes could be defined purely bases on the color differences from the superimposed images. There are still some issues but the color images defines the copper plates, the Sn in between, Pd in a Nd-Ti-Ba-O alloy, etc. . .

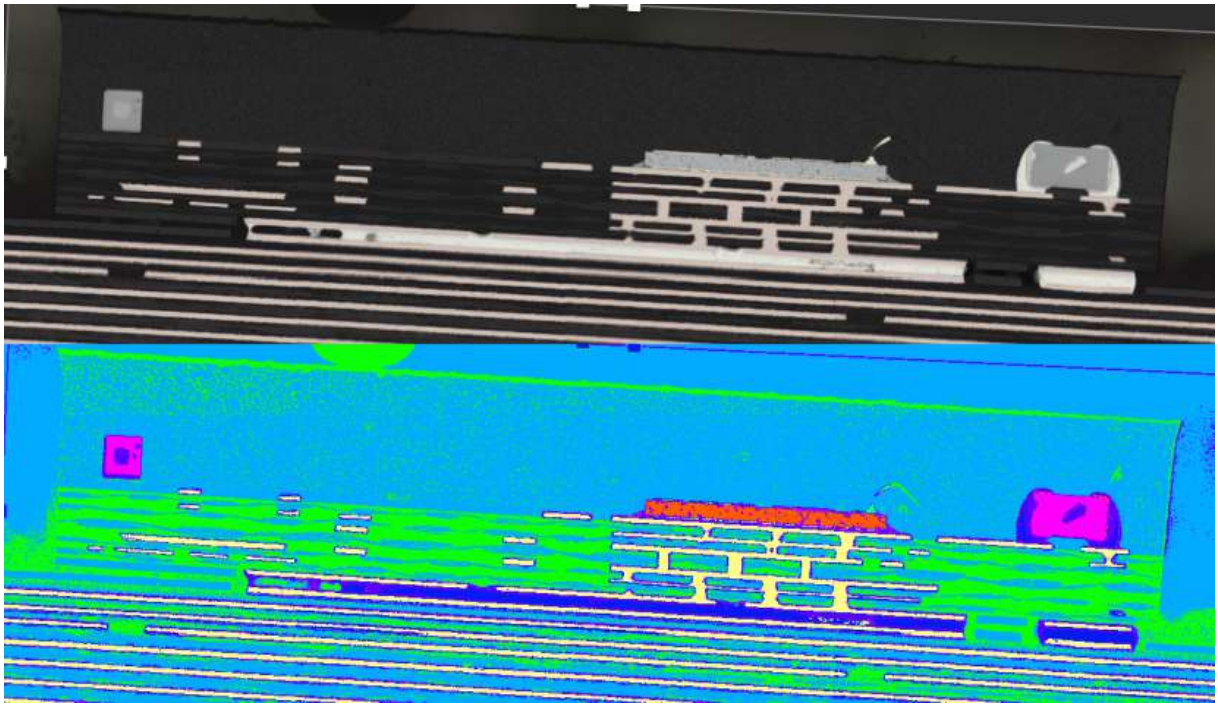

Figure 7.5: Segmentation of the superimposed image of light microscopy and BSE by use of Multispec.

EDS analysis

After the different phases are defined an EDS analysis shall be conducted. Ideally a single centroid spot analysis would be enough to attribute a specific chemical composition to the defined phases. This would avoid the edge problems were pixels were defined as impure as there is now a clear boundary based on the phase discrimination. Still, a large risk is taken to not have any secure knowledge on the rest of that phase surface. Hence, the risk of missing information is high. For example, coating of Au and Ni might not be easily detected in color and BSE images. A single x-ray acquisition would not take into account these aspects. Therefor it is suggested to conduct a cross spot analysis as illustrated in figure 7.6. In this case if there is transition to another elemental composition a boundary line will be drawn based on the contact zones detected. This method still leaves some zones untouched and in question but the risk is decreased substantially in contrast with the centroid analysis. Also, the question needs to be asked to which extent it is necessary to understand the details of each composition. A good example is Ni on top of Ba-Ti. With or without detailed analysis it has become clear how these three elements are entangled with each other at certain locations. Aside, as the amount of EDS point analysis is reduced the resolution for each analysis could increase. And if necessary, the additional use of Bruker can be a handy aid to point specific composition to a certain phase.

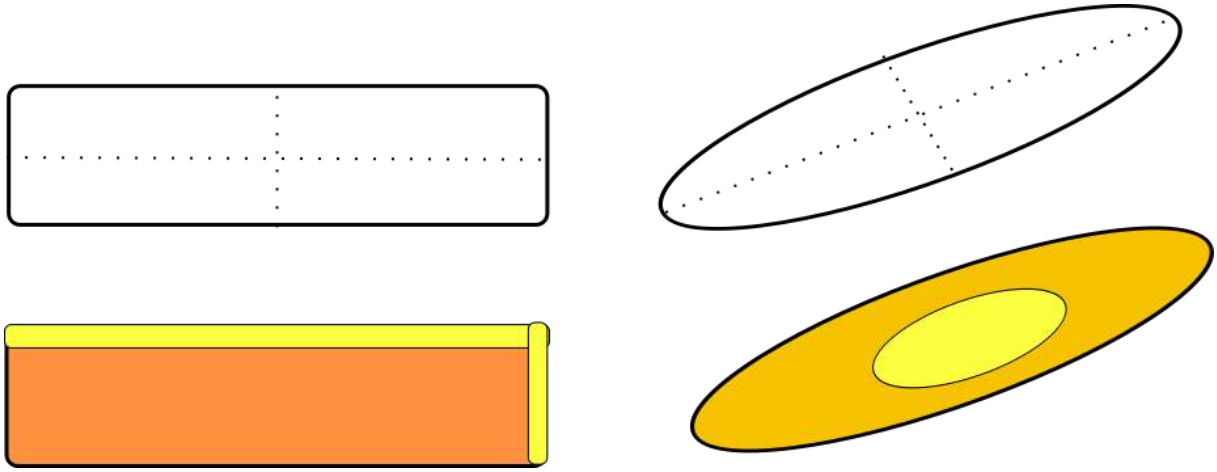

Figure 7.6: Cross - line EDS spot analysis based on the segmented phases.

In this model the use of the classification system would be used the exact same way. That is to say that phases can be defined by the results form the spot analysis in that phase. Based on these results the optimal boundary will drawn.

An overview of the newly defined flow sheet is schematically proposed in figure 7.7.

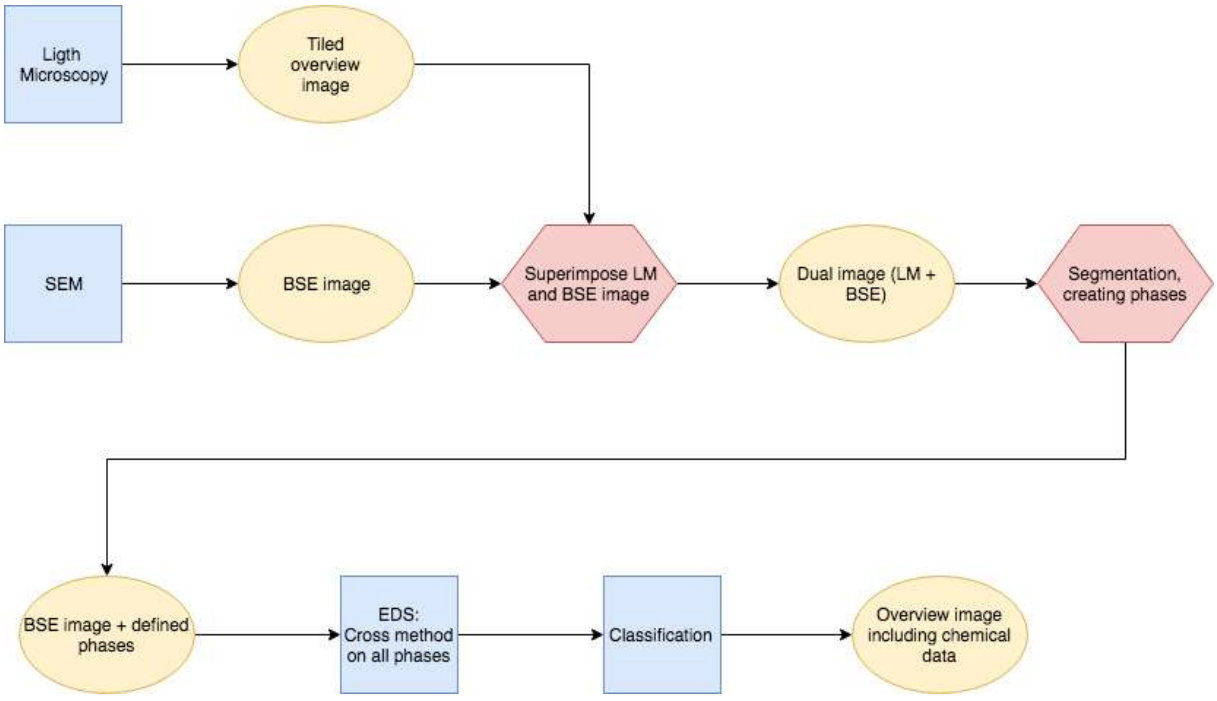

Figure 7.7: Schematic overview of the proposed workflow.

7.2.4 Further suggestions

A major issue in this work is providing a representative sample of the smartphone for the SEM. As be said, it is very time-consuming exercise where certain choices had to be made. For further research it can be suggested to study section perpendicular to the ones now studies. This could help to have better understanding on the 3D elemental composition of that phone. Rontgen images and CT scan could provides an overall 3D images of all interior components. Providing chemical data on both the X- and Y-axis this can give valuable information to combine the two methods. Ideally a 3D images could be acquired where for all components a elemental composition can be assigned using the SEM.

Another option aside from μ-XRF would be to apply wavelength dispersive spectrometry (WDS) on this kind of material. WDS is considered to give better results in comparison to EDS. WDS provides a better solution to overlapping peaks and signal-to-noise ratio. The technique is however more expensive, time consuming and less user friendly. It is therefore less used in SEM technology(Newbury and Ritchie, 2013; Thermo, 2008).

Chapter 8

Automated microscopy in E-waste characterization: an economic evaluation

In contrast to physical lab experiments, simulations and pilot plants, there is no direct implications for improvements in grades or recovery using automated microscopy. That is to say microscopy can be a first step in addressing the problem leading to suggestions for a better recovery process. However, there is no guarantee this will lead to success. Thus, it is not evident to express the value of (automated) microscopy in numbers. Assumptions can be made but there is a certain risk bound to it.

Another way of looking at the economical validation of Mineralogic is by looking at the risk of the investment cost. When new processing units or a plant in general needs to be built this is coupled directly with high investment costs. By using Mineralogic a more profound knowledge could be gained to make more assured decision on which process units and circuits should be based to achieve the desirable grade and recovery.

8.1 SWOT analysis

A SWOT analysis provides a structural answer on how to asses economically the use of Mineralogic in the recycling industry. SWOT stands for Strengths, Weaknesses, Opportunities and Threats. It highlights the most important aspects of Mineralogic in a logical and structural representation. An overview of a SWOT analysis on the use of Mineralogic in recycling is given in table 8.1.

Strengths	Weaknesses
• Flexible systems, user friendly • Broad chemical analysis supported by Bruker software • Correlative microscopy (link with OM)	• Slow analysis and sample preparation • No recognized scientifically research or proof from success • Little recognition
Opportunities	**Threats**
• research in WEEE is an upcoming market • Mining industry trying to combine WEEE and ore • Growing market forced by stronger regularization	• High investment costs without guarantee on success

Table 8.1: SWOT analysis.

Based on this work it can be suggested that Mineralogic provides a flexible system that is overall easy to handle. An all included chemical analysis can easily be conducted on specific spots and if desired an automated analysis can easily set-up without to much prior knowledge of the software and SEM. With the use of the flexible classification system provided by Mineralogic e-waste sample do not proved to be of difficulty. In addition, ZEISS provides the option to correlate light microscopy and SEM.
The largest weakness at the moment is that research in this matter is not yet recognized and in a pioneering phase. This makes it hard to provide a critically assessment on the use of Mineralogic in WEEE. Nor is there proof that the use of Mineralogic can lead to direct new success in industry and research. It also has to be said that the analysis time can be large and sample preparation is rather challenging and time consuming to create representative samples.

It is believed that there are several strong opportunities for exporting Mineralogic to the world of recycling. There is upcoming trend in research for WEEE and this will only grow in the next years. Based on this project it is believed that Mineralogic can be a very useful tool in this matter. Also the industrial market is growing towards a more circular

economy, driven by the scarcity of primary research and a stronger regularization in developed countries. Aside, the mining industry itself will want to adjust there techniques and knowledge to combine treating both waste as ore to which Mineralogic can proof to be a key.
As stated before, at the moment little research is done in combining microscopy with e-waste. Hence, there is little assurance on the success of the use of Mineralogic. As the SEM and software bears high investment costs the risk at the moment is high.

8.2 Market and competitors

Automated mineralogy systems are sold world wide for different purposes. They mainly end up in mining companies, commercial services, universities, research centers and in a smaller extent in the oil and gas sector. Worldwide there are three main players in this sector: Mineralogic by Zeiss and MLA and Quemscam by FEI. As discussed above Mineralogic provides a fast and efficient system that can easily deal with non-geological samples. This might be less the case for Mla and Quemscan that more starts from a perspective of dealing with rocks and minerals, with a less flexible classification system. This can cause that dealing with such new material might result in tonnes of more analysis times for obtaining the same results. ZEISS is already leading the market on Automated Microscopy. So, If there would be any interest in using the methods and means of electron microscopy ZEISS has already a more optimal starting position.

To be able to sell the Mineralogic systems for its use in WEEE a profound market study will be necessary. If one looks at the market distribution today most of the systems (50 %) are sold in purpose of academical research (figure 8.1). The other half is divided in mining (20 %) and industries (30 %) (Pers Comun, 2018, ZEISS). Based on these numbers a couple of conclusion can be drawn. With half of the systems sold to academics there is large base and trust in the use of Mineralogic. To maintain and increase the potential in

Figure 8.1: Market distribution of ZEISS Mineralogic systems (Pers. Comm.)

this market solving recycling problems with Mineralogic can be a key. In developed parts of the world there is upcoming regulations striving towards an circular economy. This is especially the case for EU countries and Japan, who lack natural resources. This will automatically lead to more funds and research opportunities in the recycling of electronics.

Countries as USA and Canada both have a certain amount of natural resources. This could be one of the reasons why the regularization on recycling is very limited. The result is that in these countries WEEE ends up in landfills and is only in limited extend recycled (Balde et al., 2017). Although, it has to be said that Canada is coming with stricter laws resulting in upcoming industry and research. This could imply that already existing processing plants and refineries defined for primary ore will be adjusted to address WEEE as well and other scrap metal enriched in precious and critical metals. Something already accomplished by the mining company Mitsubishi in Japan. Other market opportunities can be found in highly populated countries as India and China. Both countries have a rise in population but also in economical growth. This leads that currently a lot of WEEE is being produced. In China for example every year 70 million smartphones are disposed (Yin et al., 2014). Especially China is doing upcoming research towards a better recycling of these waste streams.

To summarize there is certainly a possible market in which ZEISS can benefit from. Especially in EU and Japan there might be interests right now. But also upcoming market as Canada, China and India will want to focus more and more on WEEE. Still, it will not be easy to penetrate these market as there is none to little awareness on the use of Automated Microscopy in WEEE. Scientific publication, public presentations at conferences and white papers might alter this.

8.3 Value of using Mineralogic

An attempt was made to express the value of Mineralogic for recycling in numbers. This is based on the simple assumption that with the help of Mineralogic the overall recovery increases. The following parameters were used in the calculations: recovery, metal prices and machine costs. One can divide the recycling steps in three parts: Collection rate, pre-processing and refinery. Based on (Buchert et al., 2012) a general recovery for these three steps is around 12 %, which is the multiplication of the recovery for these three steps (table 8.2). A Machine costs of 800,000 /euro was assumed including training and employee costs. For this assessment it was assumed that the 'ore available' contained 1 million smartphones. Based on an average weight per phone of 110g the total weight of the ore 110 t.

Data:		*Machine costs*	*800, 000 €*
EOL smartphones	1,000,000	Collection rate	50 %
Average weight/ phone	110 g	Recovery pre-processing	25 %
		Recovery refinery	95 %
Total weight	*110 t*	*Total recovery*	*12 %*

Table 8.2: Data and assumptions used in the calculations based on Buchert et al. (2012).

It is assumed that Mineralogic will not attribute to a better collection rate. Images of Mineralogic could be used in public awareness campaigns but such reasoning is not taken into account. At the moment the refinery recovery levels are already high and therefore it assumed that also in these steps Mineralogic will not attribute in first instance to a better recovery. Three scenario's are assumed in which Mineralogic indirectly improves the recovery. These are all built starting from the standard scenario in which only four elements are recovered at 12 %: Cu, Ag, Au and Pd.

- *Scenario 1* The recovery of the pre-processing steps increases with 5 %. Thus the overall recovery is 17 %.
- *Scenario 2* The recovery of the pre-processing steps increases with 10 %. Thus the overall recovery is 21 %.
- *Scenario 3* The overall recovery doesn't increase but it is possible to extract the other critical metals.

These three scenario are rather hypothetical. It shows more or less where most value of metals in a smartphone can be found and how an increase of recovery can lead to an extensional profit margin. These scenario's are optimistic but shows a large improvement (5-10 %) in the pre-processing steps only results in smaller total recovery values (2-5 %). And even those small difference can have large influence in total value of metals. This is mainly due to the high Au content. An average amount of value for the precious metals in a smartphone (figures compiled data from 7.1 and 2.3) is illustrated in figure 8.2. The metal values for the other critical metals in comparison to the primary 4 metals is shown in figure 8.3.

It shows how the value of gold is dominantly determining the value of old smartphones. With increasing recovery the value of gold becomes even more determined. This mainly as a result of the high Au price nowadays. For instance, Cu which is highly present in a smartphone hardly increases in value with increasing recovery. Making it able to recover

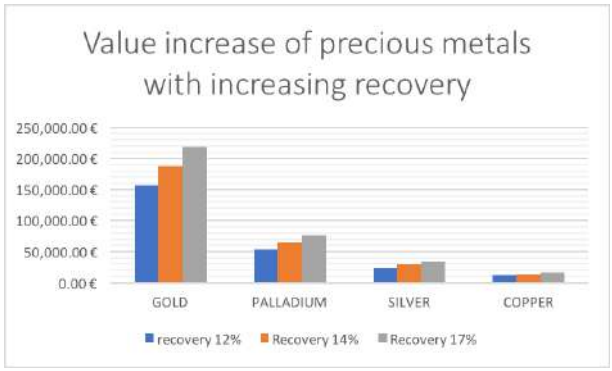

Figure 8.2: Scenario 1 and 2

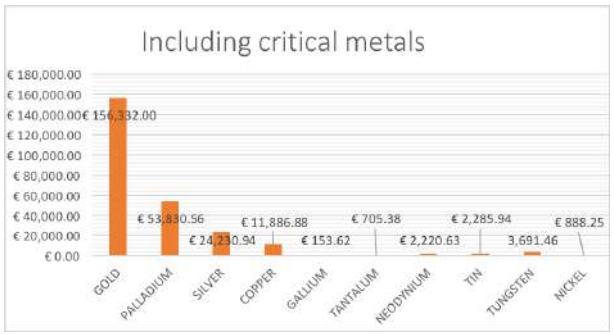

Figure 8.3: Scenario 3

other critical metals is less favorable effort. It can be observed that their value is far below the value of Au, Pd, Cu and Ag.

Table 8.3 gives the total value of metals for the three scenario's, the value increase with 20 and 40 % for the first two scenario's. It can be observed that scenario 3 is of little improvements while focusing on the primary four metals (and particular gold) is far more interesting. This is inline with the studies of Chancerel et al. (2015a). The extra values are still a fraction of the total machine costs providing the necessary information. However only a small group of smartphones are targeted (China 70 million waste mobile phones every year) . Smartphones are often just a fraction of the different e-waste stream treated. Therefore, this simulation might give some insight before a similar exercise can be made a much larger scale.

Recovery	Value of metals	Value increase
12 %	*246,280 €*	
14 %	295,536 €	20 %
17 %	344,792 €	40 %
12 % + additional metals	256,225 €	4 %

Table 8.3: Final outcome of the economic analysis.

8.4 Risk analysis

Another way how Mineralogic could be of aid, is by lowering the risk on an investment. This something explained by Yin et al. (2014) where he based himself on finding the value of intangibles in Business by Hubbard (2010). In this idea one tries to look at the risk for a possible investment. In case of recycling this could mean that an investors look at new opportunities to increase the turn-over. This would imply a new mechanical or chemical separation devices, a new processing facility or new refinery options. The risk of such an

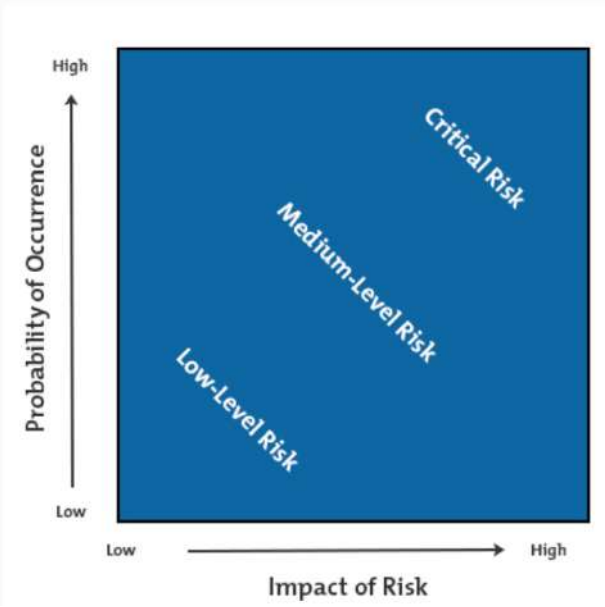

Figure 8.4: Schematic overview on the value of risk.

investment is often high as the investment costs are high and there is often no guarantee of direct and 100 % success. To help lowering this risk automated microscopy could be of use.

Mineralogic would be used in that way to increase the knowledge on the material being targeted by the new facility. Concretely this means that by gaining enough information from Mineralogic the risk of failure would decrease. One could after do the exact same exercise as in the section above. This would mean to estimate to which extent Mineralogical can help to lower the risk. After, this value can be compared with the risk value, which is the *probability of an event times the cost of an event* (figure 8.4). If the value gained by lowering the risk is higher then the purchasing costs of the device or use of the machine in other research centers one could decide if the use of Mineralogic would be worth to take into account in the risk analysis.

8.5 Recommendations

Recycling is a growing market and if more awareness and proof of the efficiency AM can be created there are possibilities for ZEISS. Au and the other precious metals are still the most important parameter when discussing the value of recycling out of smartphones. Thus, taking the value of Au into account can be considered of importance when promoting the system.

It is recommended to start more concrete research to test the findings of automated

microscopy. If so, more concrete numbers can help to express the value of AM in WEEE. Also, marketing strategies are necessary to create awareness on the possibilities of examining e-waste with ZEISS technology. This could imply white papers, presentations at conferences and peer-review publications. To have a better understanding of the market one should following the interests of industry, academy, governmental institutions.

Chapter 9

Conclusion

This study verified the use of automated and correlative microscopy on wast electronic and electronic equipment, more specific on a discarded smartphone. This was achieved by using light microscopy and ZEISS SEM, handled by their software system Mineralogic and the incorporated hardware and software from Bruker.

A smartphone (Nokia Lumia 925) was sliced, shredded and melted. Results shows how metals are distributed within the phone and how they behave after processing steps as shredding and melting. In first instance, composition maps of the interior of the phone were fabricated. The precious metals Au and Ag could easily be located and linked through specific places in the phone. The behavior of critical metals as Ga and Ta were better understood. It was shown how these are concentrated around ceramics and certain metals in specific parts of the phone. The information from Mineralogic helped to understand how easy the material could get lost during shredding. Certain patrons could be observed which might help to improve the recycling of smartphones. For instance Au on top of Ga-Ar or Pd within a matrix of Nd-Ti-Ba-O. Additionally, Mineralogic made it possible to quickly identify and classify all components as a pure metal or as an alloy. However, it has to be emphasized that the heterogeneity in the sample, the specific smartphone mode and the limits in the sample preparation makes it hard to present the study as a representative work for smartphones or WEEE in general.

Mineralogic by ZEISS provides a solid and flexible system allowing easily to generate classified images and statistics on this sort of material. However, the system is not fully optimized for this kind of material. The detail of composition of the sample on such small scale can cause that results from automated microscopy by Mineralogic lack nuances to fully understand the exact compositions and their internal relationships. Bruker software was used to solve these issues as well to assure no false impressions were obtained from element mapping. μ-XRF was another technique used to better understand the different

compositions but its results were ambiguous and of no extra value to this project.
The grid analysis used for element mapping was considered inefficient and time consuming. It was proposed to apply a segmentation on both light microscopy and BSE images to differentiate all phases. After, a detailed cross spot x-ray analysis on these phases would be considered to provide enough information to define and classify the defined phases.

A good characterization of WEEE (and in particular a smartphone) is mainly determined by a decent sample presentation. Something that is hard to achieve dealing with such material. Aside horizontal cross section it is suggest to conduct similar studies on vertical sections. If this could be achieved, it would be interested to combine chemical composition data from the SEM with whole sample 3D images from a CT scan.

With countries and industries striving more and more towards a circular economy the possibilities of Mineralogic might be of great use. This study showed that a deeper understanding of electronic waste can be achieved by automated microscopy. As such, it could be of service in academics, research centers, private institutes and mining companies opening them self towards recycling. To strive towards such accomplishments where ZEISS technology becomes of use in recycling more research will be needed to conduct and a large effort will have to be done to create a larger awareness on the possibilities of the technology of ZEISS.
This study has been a pioneering step in the use of automated and correlative microscopy in the recycling of waste electronics. In continuation of this work specific case studies would be recommended to explore if the information gained by automated microscopy can be of use to improve recycling steps. Aside it is suggested to use the acquired information to form a bridge between the recycler and the manufacturer.

Bibliography

Anindya, A., Swinbourne, D., Reuter, M., and Matusewicz, R. (2011). Indium distribution during smelting of WEEE with copper scrap. *Proceedings - European Metallurgical Conference, EMC 2011*, 1(August 2016):3–14.

Ayres, C. J. (2013). The international trade in conflict minerals: coltan. *Critical Perspectives on International Business,*, 8:178–193.

Balde, K., Wang, F., Huisman, J., and Kuehr, R. (2017). *The Global E-waste Monitor. United Nations University.* IAS-SCYCLE, Bonn, Germany.

Baum, W. (2014). Ore characterization, process mineralogy and lab automation a roadmap for future mining. *Minerals Engineering*, 60:69–73.

Baxter, J. and Gram-hanssen, I. (2016). Resources , Conservation and Recycling Environmental message framing : Enhancing consumer recycling of mobile phones. *"Resources, Conservation & Recycling"*, 109:96–101.

Berk, R. E. (2009). Automated SEM/EDS analysis of airbag residue. I: Particle identification. *Journal of Forensic Sciences*, 54(1):60–68.

Biehl, L. and Landgrebe, D. (2002). MultiSpeca tool for multispectralhyperspectral image data analysis. *Computers & Geosciences*, 28.10:1153–1159.

Blakemore, J. S. (1982). Semiconducting and other major properties of gallium arsenide. *Journal of Applied Physics*, 53(10):123–181.

Boghe, D. (2001). Electronic scrap: a growing resource. *Metal bulletin montly*, pages 21–24.

Brusselaers, J., Mark, F. E., Tange, L., and A (2006). Using Metal-Rich WEEE Plastics as Feedstock/Fuel Substitute for an Integrated Metals Smelter. *Technical report Umicore*, (November).

Buchert, M., Manhart, A., Bleher, D., and Pingel, D. (2012). Recycling critical raw materials from waste electronic equipment Commissioned by the North Rhine- Westphalia State Agency for Nature , Environment and Consumer Protection Authors :. *Oeko-Institut e.V*, 49:79.

Carl Zeiss AG (2014). ZEISS Mineralogic Mining - ZEISS Launches Mineral Analysis Solution for Mining Industry.

Castro, M., RemmersWaal, J., Brezeta, J., Schaikb, Van, A., and Reuters, M. (2005). A simulation model of the comminutionliberation of recycling streams. *International Journal of Mineral Processing*, 75(3-4):255–281.

Chancerel, P. (2009). Assessing the management of small waste electrical and electronic equipment through substance flow analysis. *La Revue de Metallurgie*, (April):29–30.

Chancerel, P., Bolland, T., and Rotter, V. S. (2011). Status of pre-processing of waste electrical and electronic equipment in Germany and its influence on the recovery of gold. *Waste Management and Research*, 29(3):309–317.

Chancerel, P., Marwede, M., Nissen, N. F., and Lang, K. D. (2015a). Estimating the quantities of critical metals embedded in ICT and consumer equipment. *Resources, Conservation and Recycling*, 98:9–18.

Chancerel, P., Marwede, M., Nissen, N. F., and Lang, K.-d. (2015b). Resources , Conservation and Recycling Estimating the quantities of critical metals embedded in ICT and consumer equipment. *"Resources, Conservation & Recycling"*, 98:9–18.

Chancerel, P., Meskers, C., Hagelüken, C., and Rotter, V. S. (2008). E-scrap: metals too precious to ignore. *Recycling international*, pages 42–45.

Chancerel, P., Meskers, C. E. M., Hagel??ken, C., and Rotter, V. S. (2009). Assessment of precious metal flows during preprocessing of waste electrical and electronic equipment. *Journal of Industrial Ecology*, 13(5):791–810.

Chancerel, P. and Rotter, V. S. (2009). Stop wasting gold - How a better mining of end-of-life electronic products would save precious resources. *R'09 World Congress*, (May).

Chancerel, P., Rotter, V. S., Ueberschaar, M., Marwede, M., Nissen, N. F., and Lang, K.-d. (2013). Data availability and the need for research to localize, quantify and recycle critical metals in information technology, telecommunication and consumer equipment. *Waste Manage*, 31:3–16.

Chen, J., Zhang, Y., Deng, C., Dai, X., & Li, L. (2009). Effect of the Ba/Ti ratio on the microstructures and dielectric properties of barium titanatebased glassceramics. *Journal of the American Ceramic Society*, 92(6):1350–1353.

Choi, J., Kim, J. H., Lee, B. T., and Moon, J. H. (2000). Microwave dielectric properties of BaNdTiO system doped with metal oxides. *Materials Letters*, 44(1):29–34.

Constantinides, S. (2012). The demand for rare earth materials in permanent magnets. In *51st Annual Conference of Metallurgists*.

Croat, J. J., Herbst, J. F., Lee, R. W., and Pinkerton, F. E. (1984). PrFe and NdFebased materials: A new class of highperformance permanent magnets. *Journal of Applied Physics*, 55(6):2078–2082.

Cucchiella, F., Adamo, I. D., Koh, S. C. L., and Rosa, P. (2016). A pro fi tability assessment of European recycling processes treating printed circuit boards from waste electrical and electronic equipments. 64:749–760.

Cucchiella, F., D'Adamo, I., Lenny Koh, S., and Rosa, P. (2015). Recycling of WEEEs: an econmic assessment of present and future e-waste streams. Renew. Sustai. *Energy Rev.*, 51:263–272.

Cui, J. and Forssberg (2003). Mechanical recycling of waste electric and electronic equipment: a review. J. *Hazard Material*, 99:243–263.

Egerton, R. (2005). *Physical principles of electron microscopy : an introduction to TEM, SEM, and AEM*. Springer.

Ernst, T., Popp, R., Wolf, M., and Van Eldik, R. (2003). Analysis of eco-relevant elements and noblemet- als in printed wiring boards using AAS, ICP-AES and EDXRF. Analytical and Bioanalytical Chemistry 375(6): 805814. *Analytical and Bioanalytical Chemistry*, 375 (6):805–814.

European Commision (2010). EC. Report on Critical Raw Materials for the EU. Report of the Ad hoc working Group on defining critical raw materials. Technical report.

European Commision (2012). Directives 2012/19/EU of the european parlement and of the council of 4 july 2012 on Waste electronics and electronic equipment (WEEE). *Official Journal of the European union*, 2012(June):38–71.

European Commission (2017). COMMUNICATION FROM THE COMMISSION TO THE EUROPEAN PARLIAMENT, THE COUNCIL, THE EUROPEAN ECONOMIC AND SOCIAL COMMITTEE AND THE COMMITTEE OF THE REGIONS on the 2017 list of Critical Raw Materials for the E. Technical report.

Evans, C. L., Wightman, E. M., Manlapig, E. V., and Coulter, B. L. (2011). Application of process mineralogy as a tool in sustainable processing. *Minerals Engineering*, 24(12):1242–1248.

Fukamichi, K. (1994). 7.1.4.2.2 Fe-Ni-Co alloy system. In *Magnetic Alloys for Technical Applications. Soft Magnetic Alloys, Invar and Elinvar Alloys.*

Goldstein, J. (2003). *Scanning electron microscopy and x-ray microanalysis.* Kluwer Adacemic/Plenum Pulbishers.

Golev, A., Schmeda-Lopez, D., Smart, S. K., Corder, G., and McFarland, E. (2014). Where next on e-waste in Australia? *Waste Management*, 58:348–358.

Goodall, W. R. and Scales, P. J. (2007). An overview of the advantages and disadvantages of the determination of gold mineralogy by automated mineralogy. *Minerals Engineering*, 20(5):506–517.

Gore, I. G. E., Branch, N., Roman, T., Orange, E., Wayne, K., and Gore, R. A. (1998). *United States Patent (19).* Number 19.

Graham, S. D., Brough, C. P., and Cropp, A. (2015). An introduction to ZEISS Mineralogic Mining and the correlation of light microscopy with automated mineralogy: a case study using BMS and PGM analysis of samples from a PGE-bearing chromitite prospect. *Precious Metals '15*, (October 2016):10.

Gramatyka, P., Nowosielski, R., and Sakiewicz, P. (2015). Recycling of waste electrical and electronic Recycling of waste electrical and electronic equipment. *Journal of achievements in Materials and Manufacturing Engineering*, 20(January 2007):535–538.

Gu, Y. (2003). Automated Scanning Electron Microscope Based Mineral Liberation Analysis An Introduction to JKMRC/FEI Mineral Liberation Analyser. *Journal of Minerals and Materials Characterization and Engineering*, 02(01):33–41.

Hagelüken, C. (2006). Recycling of electronic scrap at Umicore's integrated metals smelter and refinery. *Erzmetall*, 59(3):152 – 161.

Hagelüken, C. and Meskers, C. E. M. (2008). Mining our computers opportunities and challenges to recover scarce and valuable metals from end-of-life electronic devices. *Proceedings of Electronics Goes Green*, pages 623–628.

Hageluken C (2006). Improving metal returns and eco-efficiency in electronics recycling. *Proceedings of the 2006 IEEE conference*, (May):218–223.

Holgersson, S., Steenari, B. M., Bjorkman, M., and Cullbrand, K. (2016). Analysis of the metal content of small-size Waste Electric and Electronic Equipment (WEEE) printed circuit boards-part 1: Internet routers, mobile phones and smartphones. *Resources, Conservation and Recycling*, pages 1–9.

Hubbard, D. (2010). *How to Measure Anything: Find the Value of Intangibles" in Business. second ed. John Wiley & Sons.*

Ilyenko, G. and EffenbergS. (2007). Cu-Ni-Zn (Copper-Nickel-Zinc). In *Non-Ferrous Metal Systems. Part 3. Landolt-Börnstein - Group IV Physical Chemistry.*

ISRI (2003). Institute of scrap recycling industries Inc. Scrap recycling: where tomorrow begins. Technical report.

Khaliq, A., Rhamdhani, M., Brooks, G., and Masood, S. (2014). Metal extraction processes for electronic waste and existing industrial routes: a review and australian perspective. *Resources, Conservation and Recycling*, 3:152–179.

Kishino, S., Imai, T., Iida, T., Nakaishi, Y., Shinada, M., Takanashi, Y., and Hamada, N. (2007). Electronic and optical properties of bulk crystals of semiconducting orthorhombic BaSi2 prepared by the vertical Bridgman method. *Journal of alloys and compounds*, 428.1-2:22–27.

Kumar, A. and Holuszko, M. (2016). Electronic waste and existing processing routes: a Canadian perspective. *Resources, Conservation and Recycling*, 5:35.

Li, J., He, X., and Zeng, X. (2017). Designing and examining e-waste recycling process: methodology and case studies. *Environmental technology*, 38:652–660.

Lotter, N. O. (2011). Modern Process Mineralogy: An integrated multi-disciplined approach to flowsheeting. *Minerals Engineering*, 24(12):1229–1237.

Lotter, N. O., Kormos, L. J., Oliveira, J., Fragomeni, D., and Whiteman, E. (2011). Modern process mineralogy: Two case studies. *Minerals Engineering*, 24(7):638–650.

Martiny, A., Campos, A. P. C., Sader, M. S., and Pinto, M. A. L. (2008). SEM/EDS analysis and characterization of gunshot residues from Brazilian lead-free ammunition. *Forensic Science International*, 177(1).

Mermillod-Blondin, R., Benzaazoua, M., Kongolo, M., de Donato, P., Bussière, B., and Marion, P. (2011). Development and Calibration of a Quantitative, Automated Mineralogical Assessment Method Based on SEM-EDS and Image Analysis: Application for Fine Tailings. *Journal of Minerals & Materials Characterization & Engineering*, 10(12):1111–1130.

Murakami, S. and Murakami-suzuki, R. (2008). Hibernating stocks of mobile phones in Japan. *Con Account 2008 Book of Abstracts*, pages 57–58.

Namias, J. (2013). The future of Electronic waste recycling in the United states: obstacles and domestic solutions. *Columbia university, New York, United states*.

Newbury, D. E. and Ritchie, N. W. M. (2013). Is scanning electron microscopy/energy dispersive X-ray spectrometry (SEM/EDS) quantitative? *Scanning*, 35(3):141–168.

Nickel, L. (2010). The growing pull of rare earth magnets. *Metal powder report*, 65.2:6–8.

Oguchi, M., Kameya, T., Yagi, S., and Urano, K. (2008). Product flow analysis of various consumer durables in Japan. *Resources, Conservation and Recycling*, 52:463–480.

Oguchi, M., Murakami, S., Sakanakura, H., Kida, A., and Kameya, T. (2011a). A preliminary catego-rization of end-of-life electrical and electronic equipment as secondary metalresources. *Waste Management*, 31:2150–2160.

Oguchi, M., Murakami, S., Sakanakura, H., Kida, A., and Kameya, T. (2011b). A preliminary categorization of end-of-life electrical and electronic equipment as secondary metal resources. *Waste Management*, 31(9-10):2150–2160.

Ogunniyi, I., Vermaak, M., and Groot, D. (2009). Chemical composition and liberation characterization of printed circuit board communition fines for beneficiation investigations. Waste Manage. 29, 21402146. Prakash,. *Waste Management*, 29:2140–2146.

Perks, R. (2015). Re-framing the nature and success of the post-conflict mineral reform agenda in rwanda. *The Extractive Industries and Society*, pages 1–11.

Petruk, W. (1976). The application of quantitative mineralogical analysis of ores to ore dressing. *CIM Bull*, 767:146–153.

Petruk, W. (1988). Automatic image analysis for mineral beneficiation. *Journal of Metals*, 40:29–31.

Piotrowicz, A. and Pietrzyk, S. (2016). Tantalum recycling from waste of electrical and electronic equipment. *Web of conference SEED*, 00074:1–4.

Pirard, E., Bernhardt, H.-j., Catalina, J.-c., Brea, C., Segundo, F., and Castroviejo, R. (2008). From Spectrophotometry to Multispectral Imaging of Ore Minerals in Visible and Near Infrared (VNIR) Microscopy. *Library*, (September):8–10.

Pownceby, M. I., MacRae, C. M., and Wilson, N. C. (2007). Mineral characterisation by EPMA mapping. *Minerals Engineering*, 20(5):444–451.

Predel, B. (1994). Au-Pd (Gold-Palladium). In *Landolt-Börnstein - Group IV Physical Chemistry - Springer, Berlin, Heidelberg*.

Reuter, M. A., Hudson, C., van Schaik, A., Haisenkanek, K., Meskers, C., and Hagelüken, C. (2013). Metal Recycling: Opportunities, Limits, Infrastructure Pane, A Report ofthe Working Group on the Global Metal Flows to the International Resource. Technical report.

Reuter, M. A., van Schaik, A., Ignatenko, O., and De Haan, G. J. (2006). Fundamental Limits for the Recycling of End-of-life Vehicles. *Minerals Engineering*, 19(5):433–449.

Reuters, M. and van Schaik, A. (2015). Product-centric simulation-based design for recycling: case of LED lamp recycling. *Journal of Sustainable Metallurgy*, 1:4–28.

Rosenkranz, J. and Lamberg, P. (2014). Sustainable Processing of Mineral Resources. *International Journal of the Society of Materials Engineering for Resources*, 20.1:7–22.

Rotter, V. S., Ueberschaar, M., Geiping, J., and Flamme, S. (2015). Potenziale zum Recycling wirtschaftsstrategischer Metalle aus Elektroaltgeräten Ergebnisse aus dem UPgrade Projekt. *Thomé-Kozmiensky KJ, Goldmann D, editors. Recycl und Rohstoffe*, 8:201.

Rule, C. and Schouwstra, R. (2011). Process mineralogy delivering significant value at Anglo Platinum concentrator operations. *Proceedings, 10th ICAM*, pages 613– 620.

Sandmann, D. (2015). *Method Development in Automated Mineralogy*. PhD thesis.

Sarath, P., Bonda, S., Mohanty, S., and Nayak, S. K. (2015). Mobile phone waste management and recycling : Views and trends. *Waste Management*, 46:536–545.

Severin, K. P. (2004). *Energy Dispersive Spectrometry of Common Rock Forming Minerals*. Kluwer Academic Publishers.

Suckling, J. and Lee, J. (2015). Redefining scope : the true environmental impact of smartphones ? *internationa journal of Life cycle assess*, 20:1181–1196.

Tan, Q., Dong, Q., Liu, L., Song, Q., Liang, Y., and Li, J. (2017). Potential recycling availability and capacity assessment on typical metals in waste mobile phones : A current research study in China. *Journal of Cleaner Production*, 148:509–517.

Tang, N. Y., Su, X., and Toguri, J. M. (2001). Experimental study and thermodynamic assessment of the Zn-Fe-Ni system. *Calphad*, 25(2):267–277.

Thermo (2008). Quantitative X-ray Mapping : WDS Performance , EDS Convenience - Technical note: 51026. *Thermo scientific*, pages 3–4.

Timpel, M., Wanderka, N., Schlesiger, R., Yamamoto, T., Lazarev, N., Isheim, D., Schmitz, G., Matsumura, S., and Banhart, J. (2012). The role of strontium in modifying aluminium-silicon alloys. *Acta Materialia*, 60(9):3920–3928.

Ueberschaar, M., Geiping, J., Zamzow, M., Flamme, S., and Susanne, V. (2017). Resources , Conservation & Recycling Assessment of element-speci fi c recycling e ffi ciency in WEEE pre-processing. 124(November 2016):25–41.

Umeda, T. and Okane, T. (2001). ADVANCED Solidi ® cation microstructures selection of Fe Cr Ni and Fe Ni alloys. 231:231–240.

UNEP (2009). Recycling From E-waste to Resources. Technical report.

UNEP (2011). International Resource Panel, 2011. Recycling Rates of Metals: A Status Report. Technical report.

Ustinovshikov, Y., Shirobokova, M., and Pushkarev, B. (1996). A structural study of the Fe-Cr system alloys. *Acta Materialia*, 44 (12):5021–5032.

van Schaik, A. and Reuters, M. (2010). Dynamic modelling of E-waste recycling system performance based on product design. *Minerals Engineering*, 23:192–210.

Victoria, P., Braulio-gonzalo, M., Juan, P., and Bovea, M. D. (2017). Consumer attitude towards the repair and the second-hand purchase of small household electrical and electronic equipment . A Spanish case study. *Journal of Cleaner Production*, 158(158):261–275.

Volker, Z. (2016). Chapter 20 - Neodymium Use and Recycling Potential. *Rare Earths Industry*, pages 305–318.

Ward, I., Merigot, K., and Mcinnes, B. (2017). Application of Quantitative Mineralogical Analysis in Archaeological Micromorphology: a Case Study from Barrow Is., Western Australia. *Journal of Archaeological Method and Theory*, pages 1–24.

Welfens, M. J., Nordmann, J., and Seibt, A. (2016). Drivers and barriers to return and recycling of mobile phones . Case studies of communication and collection campaigns. *Journal of Cleaner Production*, 132:108–121.

Yamane, L. H., de Moreas, V., Espinosa, R., and Tenorio, J. (2011). Recycling of WEEE: characterization of spent printed circuit boards from mobile phones and computers. *Waste Management*, 31:2553–2558.

Yin, J., Gao, Y., and Xu, H. (2014). Survey and analysis of consumers' behaviour of waste mobile phone recycling in China. *Journal of Cleaner Production*, 65:517–525.

Yun-Ying, H., Li-Te, Y., Wang, J.-W., Wang, C.-T., Tsai, C.-H., and Kua, Y.-m. (2017). Recycling of spent nickelcadmium battery using a thermal separation process. *Environmental progress and sustainable energy*, 37(2):645–654.

Zeng, X., Cong, R., Chen, W.-Q., and Li, J. (2016). Uncovering the recycling potential of New WEEE in China. *Environmental Science and Technology*, 50 (3):1347–1358.

Zeng, X. and Li, J. (2016). Measuring the recyclability of e-waste: an innovative method and its implications. *Journal of Cleaner Production*, 131:152–162.

List of Figures

Appendix

1) Overview table

The table consists out of all metal and alloys defined under the microscope. Their location and associated elements are given as well.

Page 119 - 124

2) Images

Images of optical microscopy from slice 3 and 5 (both shown as element map in the written text). Element mapping of slice 1, 2, 4, 6, 7, 8 and 9 and another section of crushed smartphone parts.

Page 124 - 139

	PCB			
Precious metals	**State**	**Average composition**	**Average Weight %**	**Associated metals**
Au	Au	100% Au	0.05%	Si,Ta, W, (Si, ceramics)
Ag	Ag	100% Ag	0.77%	Fe-Ni-Zn, Fe-Ni, Sn, Ni, Ba-Si
Pd	Pd	100% Pd	0.02%	Nd-Ti
Pt				

	PCB			
Critical metals	**State**	**Average composition**	**Average Weight %**	**Associated metals**
Co	Fe-Ni-Co	54% Fe, 29 % Ni, 17 % Co	0.07%	Ag, Ni
Ga				
Nd	Nd-Ti-Ba-O	50 % Nd, 25 % Ti, 23 % O & 12% Ba	0.05%	Ag
Pr				
Ta	Ta	100% Ta	0.38%	Si, Au, (Si, ceramics)
W	W	100% W	0.04%	Al, Au,Ni, Sn, Mo,
Mo	Mo	100% Mo	0.01%	W, Sn, Al, Ba-Si, (Si, ceramics)

	PCB			
Base metals	**State**	**Average composition**	**Average Weight %**	**Associated metals**
Cu	Cu	100% Cu	28.67%	Sn, Ni, Ba-Si, Cu - Si
	Cu-Si	82% Cu, 28% Si	0.96%	Cu, Ba-Si
	Cu-Zn-Ni	64% Cu, 18% Zn, 18% Ni	21.06%	
	Zr-Cu-Ni	67% Zr; 27% Cu; 6% Ni	0.42%	
Ti	Nd-Ti-Ba-O	50 % Nd, 25 % Ti, 23 % O & 12% Ba	0.05%	Pd
	Ba-Ti	75% Ba, 25% Ti	1.08%	Ni, Cu, Sn
Ni	Fe-Cr-Ni	73% Fe, 20% Cr, 7% Ni	8.10%	Fe-Cr-Si, Ni
	Ni	100% Ni	2.02%	
	Zr-Cu-Ni	67% Zr; 27% Cu; 6% Ni	0.42%	
	Fe-Ni-Zn	57% Fe, 14% Ni, 13% Ni, 13% Ni	1.94%	
Sn	Sn	100% Sn	4.40%	
Fe	Fe-Cr-Ni	73% Fe, 20% Cr, 7% Ni	8.10%	Fe-Cr-Si, Ni
	Fe-Ni-Co	54% Fe, 29 % Ni, 17 % Co	0.07%	
	Fe-Cr-Si	89% Fe, 8% Cr, 3% Si	2.85%	Fe-Cr-Ni, Ni
	Fe-Ni-Zn	57% Fe, 14% Ni, 13% Ni, 13% Ni	1.94%	Ag, Fe-Zn
	Fe-Zn	56% Fe, 26.5% Zn, 13.5% O	0.13%	Ag, Fe-Ni-Zn
	Fe	100% Fe	1.13%	
Zn	Zn	100% Zn	5.90%	
	Fe-Zn	56% Fe, 26.5% Zn, 13.5% O	0.13%	Ag, Fe-Ni-Zn
	Fe-Ni-Zn	70% Fe, 14% Zn, 13% Ni	1.94%	Ag, Fe-Zn
	Cu-Zn-Ni	64% Cu, 18% Zn, 18% Ni	21.06%	
Zr	Zr-Cu-Ni	67% Zr; 27% Cu; 6% Ni	0.42%	
Al	Al	100% Al	9.10%	
	Al-Sr-Si-O	34% O, 24% Al, 23% Si, 17% Sr	0.04%	
	Ceramics		3.82%	
Ba	Ba-Ti	75% Ba, 25% Ti	1.08%	
	Ba-Si	89% Ba, 11% Si	1.83%	

	Camera + surrounding PCB			
Precious metals	**State**	**Average composition**	**Average Weight %**	**Associated metals**
Au	Au	100% Au	0.22%	Cu, Ni, Ga-Ar, (Si, ceramics)
	Au-Pd	62%Au, 38%Pd	0.01%	Cu, Ni, Au, Ga-Ar
Ag		100 Ag%	1.08%	Fe-Zn-Ni, Ni
	Ag-Pd	66% Ag, 34% Pd	0.00%	Ag, Ni, Nd-Ti-O-Ba
Pd	Pd	100 Pd%	0.01%	Nd-Ti-O-Ba
	Au-Pd	62%Au, 38%Pd	0.10%	Cu, Ni, Au
	Ag-pd	66% Ag, 34% Pd	0.00%	
Pt	Pt	100%		
	Camera			
Critical metals	**State**	**Average composition**	**Average Weight %**	**Associated metals**
Co				
Ga	Ga - Ar	50% Ga, 50% Ar	0.04%	Au, Au-Pd, (Si, ceramics)
Nd	Fe-Nd-Pr	70% Fe, 23% Nd, 7% Pr	4.70%	Ni
	Nd-Ti-Ba-O	50 % Nd, 25 % Ti, 23 % O & 12% Ba	0.05%	Pd, Ni, Ag-Pd
Pr	Fe-Nd-Pr	70% Fe, 23% Nd, 7% Pr	4.70%	Ni
Ta	/	/		
W	W*	/	0.04%	Al, Si,
Mo	Mo	100% Mo	0.05%	Ba-Si, Cu, (Si, ceramics)
	Camera			
Base metals	**State**	**Average composition**	**Average Weight %**	**Associated metals**
Cu	Cu	100% Cu	21.36%	Ni, Sn, Au
	Cu-Zn-Ni	64% Cu, 18% Zn, 18% Ni	11.50%	
	Cu-Zn	66% Cu, 34% Zn	1.84%	Ni
	Zr+Cu+Ni	67% Zr; 27% Cu; 6% Ni	0.61%	
Ti	Nd-Ti-Ba-O	50 % Nd, 25 % Ti, 23 % O & 12% Ba	0.05%	Pd, Ni, Ag-Pd
	Ba-Ti	75% Ba, 25% Ti	1.04%	Ni
Ni	Cu+Zn+Ni	64% Cu, 18% Zn, 18% Ni	11.50%	
	Fe-Zn-Ni	71% Fe, 15% Zn, 14% Ni	25.90%	Ag
	Ni	100%	28.40%	
	Zr+Cu+Ni	67% Zr; 27% Cu; 6% Ni	0.61%	
Sn	Sn	100%	1.71%	
Fe	Fe	100% Fe	1.06%	Fe-Cr, Ni
	Fe+Cr+Ni	76% Fe 18% Cr, 6% Ni	8.27%	Fe-Cr, Fe
	Fe-Cr	89% Fe, 8% Cr, 3% Si	1.95%	Fe-Cr-Ni
	Fe-Nd-Pr	70% Fe, 23% Nd, 7% Pr	4.70%	Ni
	Fe-Zn-Ni	72% Fe, 15% Zn, 13% Ni	2.59%	Ag
Zn	Cu+Zn+Ni	64% Cu, 18% Zn, 18% Ni	11.50%	Ba-Ti, Cu,
	Cu-Zn	66% Cu, 34% Zn	1.84%	Ni
Zr	Zr+Cu+Ni	67% Zr; 27% Cu; 6% Ni		
Al	Al	100% Al	5.98%	
	Al + Sr + Si + O (Ca +/-)	34% O, 24% Al, 23% Si, 17% Sr	1.18%	Cermamics
Ba	Ba-Ti	75% Ba, 25% Ti	1.04%	Ni
	Ba-Si	89% Ba, 11% Si	0.85%	

	Speakers at the bottom phone			
Precious metals	**State**	**Average composition**	**Average Weight %**	**Associated metals**
Au	Au	100% Au	0.14%	Cu, Ni, Ga-Ar,(Si, ceramics)
	Au-Ni	64% Au, 36% Ni	0.01%	Cu, Ni, Au
Ag	/			
Pd	/			
Pt	Pt	100% Pt		Au, Ga-Ar
	Speakers and bottom phone			
Critical metals	**State**	**Average composition**	**Average Weight %**	**Associated metals**
Co				
Ga	Ga - Ar	50% Ga, 50% Ar	0.16%	Au,(Si, ceramics)
Nd	Fe-Nd-Pr	70% Fe, 23% Nd, 7% Pr	23.80%	
Pr	Fe-Nd-Pr	70% Fe, 23% Nd, 7% Pr	23.80%	
Ta	/			
W	/			
Mo	/			
	Speakers and bottom phone			
Base metals	**State**	**Average composition**	**Average Weight %**	**Associated metals**
Cu	Cu	100% Cu	28.21%	Ni, Sn, Au, Au-Ni
Ti	Ba-Ti	75% Ba, 25% Ti	0.68%	Ni
Ni	Ni	100% Ni	1.27%	Ba-Ti, Au, Cu
Sn	Sn	100% Sn	1.14%	Cu
Fe	Fe	100% Fe	18.00%	
	Fe-Cr	89% Fe, 8% Cr, 3% Si	3.81%	
	Fe-Cr-Ni	76% Fe 18% Cr, 6% Ni	13.59%	
	Fe-Nd -Pr	70% Fe, 23% Nd, 7% Pr	23.80%	
Zn	/			
Zr	/			
Al	Al	100%	4.07%	
Ba	Ba-Ti	75% Ba, 25% Ti	0.68%	Ni

	Top of the phone			
Precious metals	**State**	**Average composition**	**Average Weight %**	**Associated metals**
Au	Au	100% Au	0.04%%	(Si, ceramics)
Ag	/			
Pd	/			
Pt				

	Speakers and bottom phone			
Critical metals	**State**	**Average composition**	**Average wiegth**	**Associated Metals**
Co				
Ga				
Nd				
Pr				
Ta	/			
W	/			
Mo	/			

	Speakers and bottom phone			
Base metals	**State**	**Average composition**	**Average Weight %**	**Associated metals**
Cu	Cu	100% Cu	28.21%	Ni,Sn
Ti	Ti-O		0.12%	Ni
Ni	Ni	100% Ni	1.35%	
Sn	Sn	100% Sn	0.68%	Cu
Fe	Fe-Cr	89% Fe, 8% Cr, 3% Si	0.10%	
	Fe-Cr-Ni	76% Fe 18% Cr, 6% Ni	5.74%	
Zn	Zn-O		52.50%	
Zr	/			
Al	Al	100% Al	8.24%	
Ba	Ba-Si	89% Ba, 11% Si		

	Bottom of the phone			
Precious metals	**State**	**Average composition**	**Average Weight %**	**Associated metals**
Au	Au	100% Au	3.55%	(Si, ceramics)
Ag	/			
Pd	/			
Pt				

	Speakers and bottom phone			
Critical metals	**State**	**Average composition**	**Average Weight %**	**Associated metals**
Co				
Ga				
Nd				
Pr				
Ta	/			
W	/			
Mo	/			

	Speakers and bottom phone			
Base metals	**State**	**Average composition**	**Average Weight %**	**Associated metals**
Cu	Cu	100% Cu	27.00%	Ni, Sn
	Cu-Si	82% Cu, 28% Si		
Ti	Ba-Ti	75% Ba, 25% Ti	1.60%	Ni
Ni	Ni	100% Ni	5.30%	Ba-Ti
Sn	Sn	100% Sn	2.30%	Cu
Fe	Fe-Cr	89% Fe, 8% Cr, 3% Si	0.45%	Fe-Cr-Ni
	Fe-Cr-Ni	76% Fe 18% Cr, 6% Ni	9.17%	Fe-Cr
Zn				
Zr	/			
Al	Al	100% Al	2.14%	
Ba	Ba-Si	89% Ba, 11% Si	2.90%	
	Ba-Ti	75% Ba, 25% Ti	1.60%	Ni

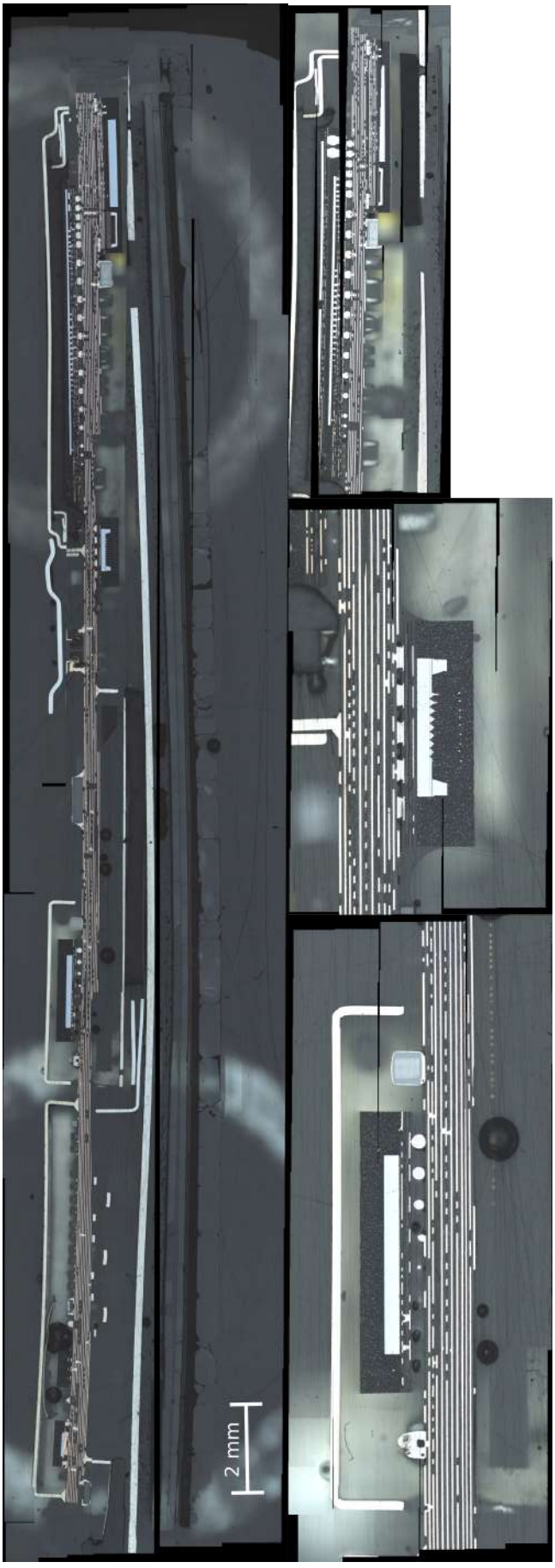

Figure 9.1: Optical microscopy image of slice 3

Figure 9.2: Optical microscopy image of slice 5

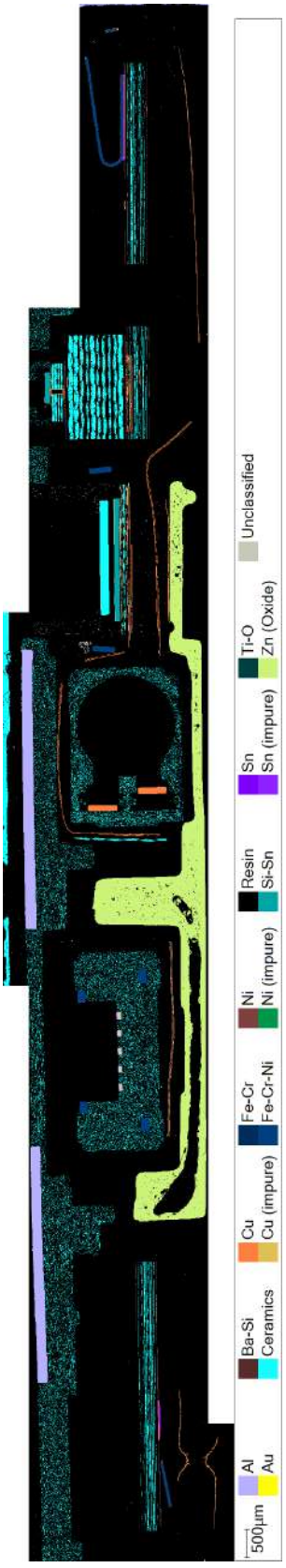

Figure 9.3: Composition map of slice 1

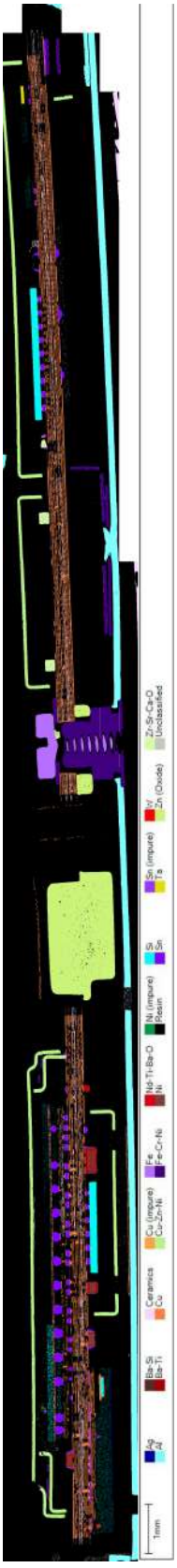

Figure 9.4: Full composition map of slice 2

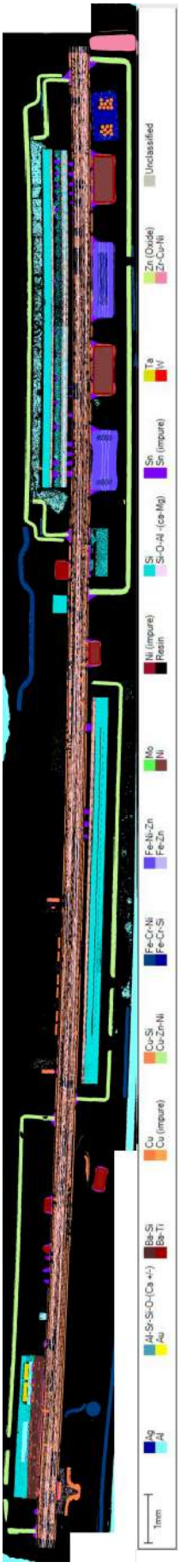

Figure 9.5: Full composition map of slice 4

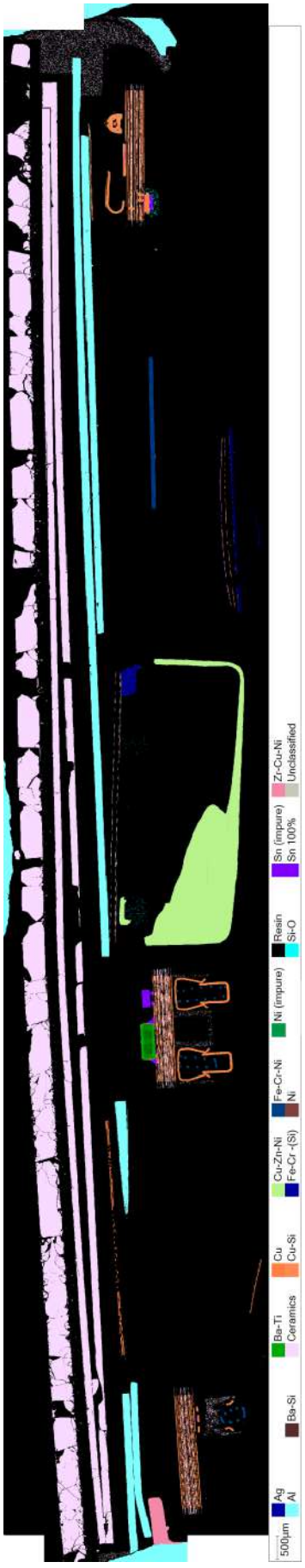

Figure 9.6: Full composition map of slice 6

Figure 9.7: Full composition map of slice 7

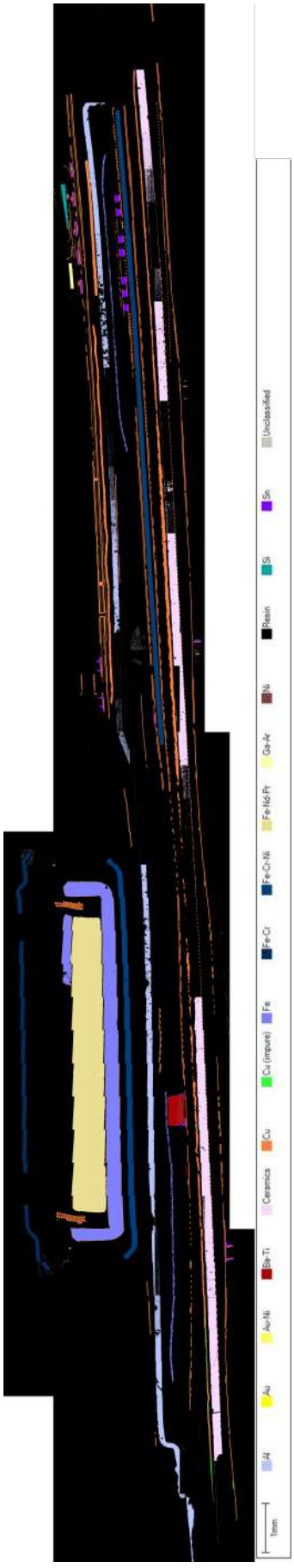

Figure 9.8: Full composition map of slice 8

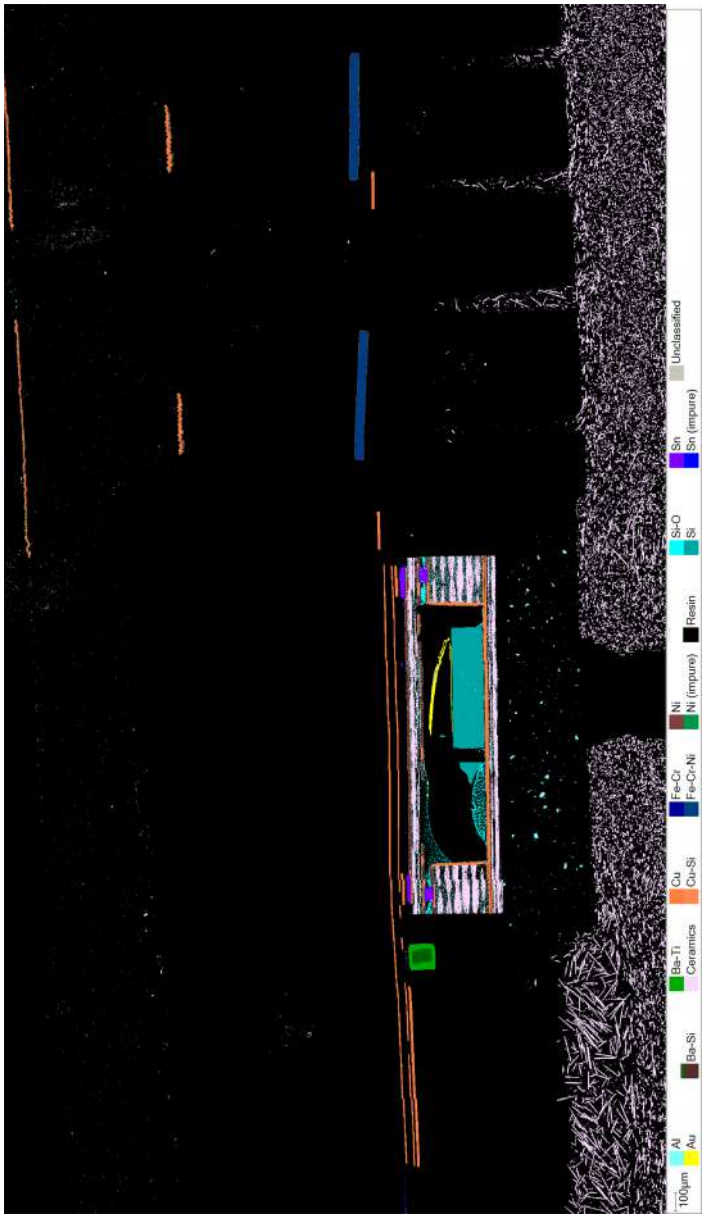

Figure 9.9: Full composition map of slice 9

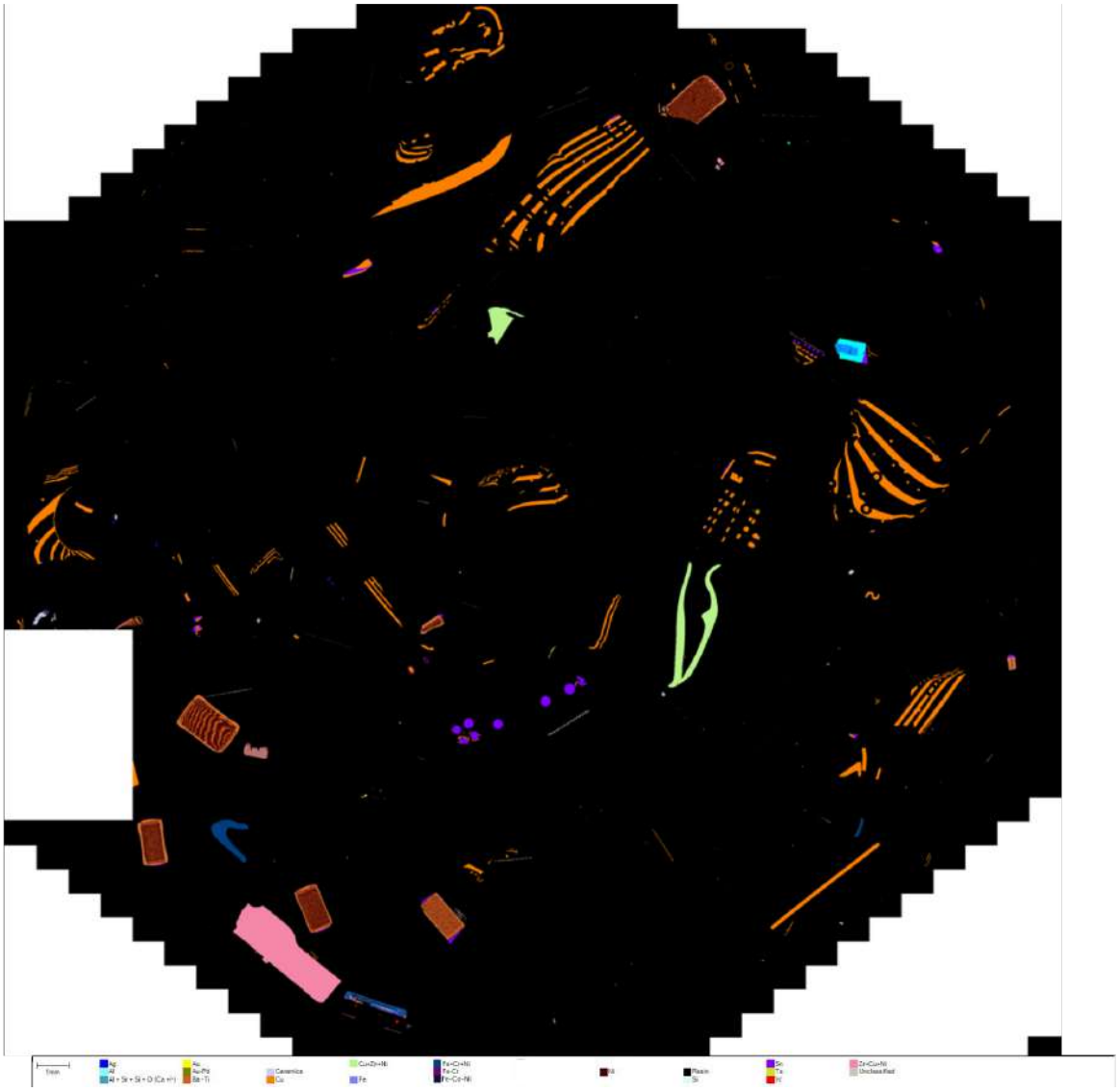

Figure 9.10: Full composition map of a section of crushed smartphone particles (II)

EMerald
Allé de la découverte, 9 B52/3
4000 LIEGE, BELGIUM
www.emerald.ulg.ac.be

EMERALD
ERASMUS MUNDUS MASTER
IN GEORESOURCES ENGINEERING